Utrecht University

Master's Thesis

Pumping test analysis performed in the Griftpark's subsurface, Utrecht, the Netherlands

Author:
Arnaud LACOSTE

Supervisors:
Suzanne FABER
Dr. Amir RAOOF

A thesis submitted in fulfilment of the requirements for the

Master's degree in Earth Surface and Water

in the

Environmental Hydrogeology group

Department of Earth Sciences

August 1st, 2022

Acknowledgements

I would like to express my deepest gratitude to my thesis supervisor Suzanne Faber for her invaluable patience and feedback. I would also like to thank Amir Raoof for introducing me to the subject and reviewing this thesis. Additionally, this thesis would not have been possible without the help of Alraune Zech and Johan van Leeuwen, who generously provided knowledge and expertise.

At last, I would like to thank my friends and family for their support during this process.

Abstract

In preparation of a tracer test, a pumping test was performed in a heterogenous and highly contaminated site. The porous media is contaminated with DNAPL that infiltrates the water table. The 1st aquifer of the site is sealed from the sides with bentonite walls and from below with an aquitard composed of several clay layers. However, this bounded aquifer is believed to have leakages through the aquitard where the clay layers are not continuous, notably in the central-east side of the site. During the pumping test, the hydraulic heads of the 1st aquifer, the aquitard, and the 2nd aquifer below the site as well as the 1st aquifer outside the bentonite walls were continuously monitored with divers. Manual measurements were also taken from several Multi-Level Sampling wells to create hydraulic head profiles with depth. The pumping test revealed that the connectivity between the 1st and 2nd aquifer is very weak in the central-east site of the site. The hydraulic separation of the 1st and 2nd aquifer in the central-east side is mainly due to a clay layer located between 54-56m below ground level. The leakages are therefore coming from another location in the aquitard or through a hole somewhere in the bentonite wall. An averaged hydraulic conductivity of the 1st aquifer was also estimated with Stallman's method based on the data collected during the pumping test. It estimated a diagonal hydraulic conductivity of 12.7m/day. A 14-layer model and two 3-layer models were also created to simulate the hydraulic head reaction of the pumping test. These models were not able to accurately match the hydraulic reaction from the site recorded during the pumping test. As such, a sensitivity analysis testing the hydraulic conductivity of the 1st aquifer, the aquitard, and the bentonite walls considering its thickness were performed to increase the understanding of their impact on groundwater flows at the site.

Contents

I. Introduction

Before the start of the industrial revolution in the end of the 19th century and even long after, the quality of groundwater in the Netherlands was never a problem. Groundwater was known to be hygienically reliable in addition to have a constant composition. In some cases, it could even be distributed without treatment (de Moel et al., 2006). However, in the late 1970s, many polluted sites began to be discovered, raising the public awareness on soil and groundwater contamination. Considering that in 1980 approximatively 60% of the of the drinking water produced in the Netherlands came from groundwater sources (VEWIN, 2017), the Dutch government realized the severity of the situation and developed its first remediation and prevention strategies for soil contamination.

Nevertheless, with the discovery of more and more polluted sites as well as the acquired knowledge on the nature and the processes involving contaminants, the Dutch government realized that remediation projects would never be concluded over several years (Rijkswaterstaat, 2014). Ongoing remediation projects all around the world with strong contaminants were nowhere near meeting the cleanup goals, even after decades of remediation efforts (Mayer & Hassanizadeh, 2005). Therefore, in the late 1990s, the Dutch authorities amended its ambitions of remediating all the serious soil contamination by 2010 and started to focus on discovering all the polluted sites and controlling the high-risk sites (Rijkswaterstaat, 2014).

One of the most polluted sites discovered in the Netherlands was found in Utrecht in the early 1980s at the site of a former manufactured gas plant. Oil, cyanide, hydrocarbons, and tar-like substances were found in the soil and groundwater over a 10 hectares area. The soil was contaminated up to 35 meters deep and the groundwater up to 50 meters (Gemeente Utrecht, 2022). This was posing a threat to the 2nd aquifer which was one of the main drinking water sources of the city. The 1st aquifer of most cities is already badly contaminated and cannot be used as a drinking water source.

Consequently, the municipality of Utrecht tried to remediate the site but, once they realized the remediation project is much more complex and expensive than they anticipated, they adapted their strategy and opted to implement an IBC methodology (“Isoleren, Beheersen en Controleren” in Dutch), also known as the stand and hold management technique. Instead of remediating the contaminated site, a containment method was installed in the mid-1990s to contain and prevent contaminants from spreading. This method enabled the municipality to monitor, reduce as much as possible the contamination risks, and give time to researchers to gain additional knowledge on the situation. This master’s thesis is a follow-up of the monitoring and remediation project of this site.

I.1. Project background

In order to fully understand the main objectives of this thesis along with the severity, complexity, and extent of the situation, a small summary of the project background has been established. It will explain the origin and location of the polluted site, the contaminants found and some of their effects on the subsurface and groundwater, the hydrogeology of the region, and a description of the containment method.

I.1.1. History

The polluted site is located near today’s heart of Utrecht city, where nowadays stands the Griftpark. However, from 1862 to 1959, the site was at the edge of the city and hosted the “Gemeentelijke Gasfabriek” (Municipal gas factory) which produced town gas for the city (Gemeente Utrecht, 2022). This town gas was produced from coal pyrolysis and other purification processes. In addition to gas

production and purification facilities, the site also hosted benzene and coal tar processing plants as well as a municipal landfill.

During the lifespan of the factory, besides gas and other components, the different facilities also produced many waste products such as hydrocarbons, polycyclic aromatic hydrocarbons (PAHs), aromatic compounds, heavy metals, etc. (Royal Haskoning DHV, 2014; Heidemij, 1990). Unfortunately, some of these waste products were spilled, dumped or purposely buried on site without knowing the consequences it would generate, leading to the infiltration and propagation of many contaminants throughout the site.

With the arrival of electricity and natural gas as a cheaper and more efficient energy source in the 1950s, less and less town gas was being used. As such, the gas factory was decommissioned in 1959 and eventually demolished in 1960. The site would remain abandoned until 1969 but, with the city growing around this abandoned space, Utrecht citizens proposed to transform this useless space into a local park. The construction started in 1979 but would then be halted in 1980 when the municipality found out that the site was severely contaminated.

After two failed attempts to remediate the site given the extent, nature and depth of the contaminants, the authorities in charge opted to implement the first IBC (Isolate, Management and Control) procedure in the country. This meant committing to a substantial economical investment for many years to come to avoid worsening the situation. Consequently, a containment method, described in more detail below, was set up and the construction of the park could resume. The Griftpark was officially opened in 1999 and further research has been initiated to find a better solution.

Figure 1: *Aerial pictures of the Griftpark in 1923 and 2010 (Wikipedia 2022; Het Utrechts Archief)*

I.1.2. Contaminants

Even though this master's research thesis will not focus on the nature and effects of the contaminants on the subsurface, a small overview of the different contaminants in the park could help understand the risks and challenges of this remediation project. In particular, understanding the transport properties of these contaminants is essential to evaluate their potential spread and threat to groundwater. Among the list of contaminants found in the Griftpark and affecting the groundwater quality of the site are hydrocarbons such as benzene and toluene, Poly Aromatic Hydrocarbons (PAHs) such as naphthalene and indene, heavy metals, cyanide and sulphuric acids.

PAH and hydrocarbons, which in this case come from spilled coal tar, are often in the form of Non-Aqueous Phase Liquids (NAPLs) and more specifically Dense NAPL (DNAPL). When trapped in the soil/aquifer matrix, NAPL substances act as a continuing source of dissolved contaminants for groundwater, preventing the restoration of aquifers for tens to hundreds of years (Newell et al., 1994). They move as a separate phase through the groundwater with extremely low dissolution rates. Therefore, given their high toxicity, a tiny volume of NAPL can pose long term threat to the

groundwater quality (Mayer & Hassanizadeh, 2005). They are also extremely difficult to completely remove from contaminated sites due to their complex behavior with the porous media. DNAPLs have the particularity of being denser than water and thus they penetrate into the water table until they reach the bottom of the aquifer. These substances pose biggest environmental threat among the contaminants found in the Griftpark given their high toxicity, longevity, volume spilled, and ability to sink into the water table.

Even though cyanides, heavy metals and sulfuric acids are not considered as the biggest threat in this case, they are still very toxic for the environment and humans. Cyanide ions can disrupt the process of cellular respiration by combining with key enzymes of the respiratory chain (Jaszczak et al., 2017). High amount of heavy metals in the environment have been linked to mutagenic effects, cancerogenic effects and increases cases of malignant tumors in humans (Staykova et al., 2005). Sulfuric acid is classified as a group I carcinogen product by the international agency of research on cancer (IARC, 1992).

I.1.3. Hydrogeology of the region

The earth subsurface is made of different formations lying on top of each other. The nature and the different properties of each formation have a huge impact on groundwater flow and mass transport (Fetter et al., 2018). Therefore, when talking about polluted sites, it is crucial to understand the hydrogeological situation of the site as well as the contaminants properties in order to contain, anticipate, and remediate their plumes. This is quite challenging given that the subsurface is mostly inaccessible. Hydrogeological properties are generally estimated from drillings and interpolation techniques, which present many analysis limitations.

For a general understanding of the hydrogeology characteristics of the Utrecht region, a cross section of the subsurface at the Griftpark is show on Figure 2. The top layer of the subsurface is made of an arrangement of sandy formations (BXz, KRz, URz, STz) and reaches a depth of approximatively 55 meters according DINOloket subsurface model of the Netherlands. This arrangement characterizes the first aquifer as it is followed by an aquitard made of clay (WAk) of approximatively 15 meters. Then, we have another arrangement of sandy formations (PZWAz) followed by a succession of clay and sandy formations (MSz, MSk) at depths between 130 and 170 meters. This third arrangement defines the second aquifer from which the region extracts groundwater for drinking water purposes (Utrecht Province, 2021). Figure 2 also shows that the Griftpark sits on top of a fault line which could have some repercussion of the position of the clay and sandy formations.

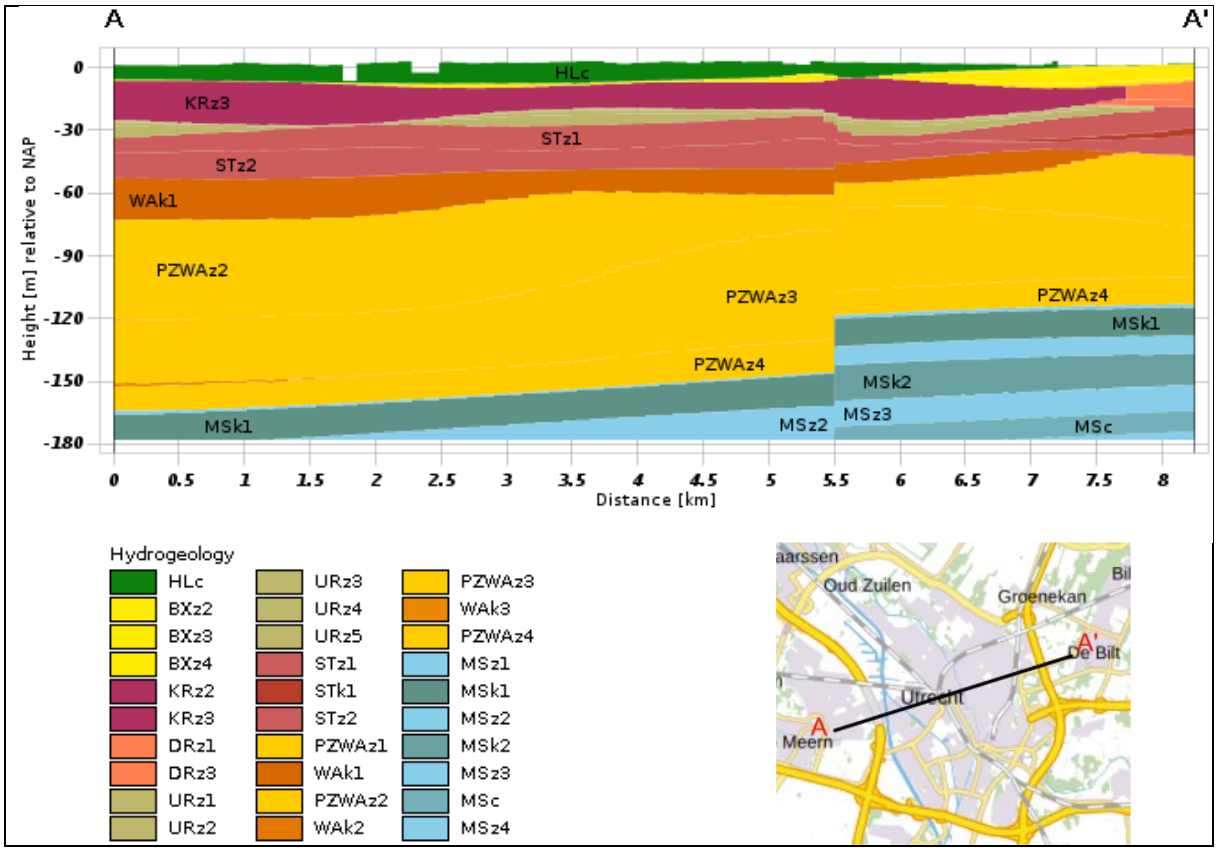

Figure 2: *Hydrogeological cross section of Utrecht subsurface (DINOloket, 2017)*

However, with the many drillings performed since the site has been discovered to be polluted, in addition to evaluating the extend of the contamination, we have also found out that the porous media is highly heterogenous. One of the major characteristic of this heterogeneity is the non-continuity of the aquitard. This aquitard is not composed of a singular clay layer which would confine the 2nd aquifer, but of several clay layers with sand in between. As a result, the first and second are connected, likely helped by the fault passing through the Griftpark. This means DNAPL and other contaminants can potentially reach the 2nd aquifer. This has complexified every analysis of the site subsurface as well as the implementation and efficiency of the containment method. Based on the sonic drills made in the 1990s, the Grondmechanica department of the University of Delft has made a map estimating the locations of the different clay layers below the Griftpark (1988). The map is displayed in Figure 3 but a bigger format is available in appendix G.

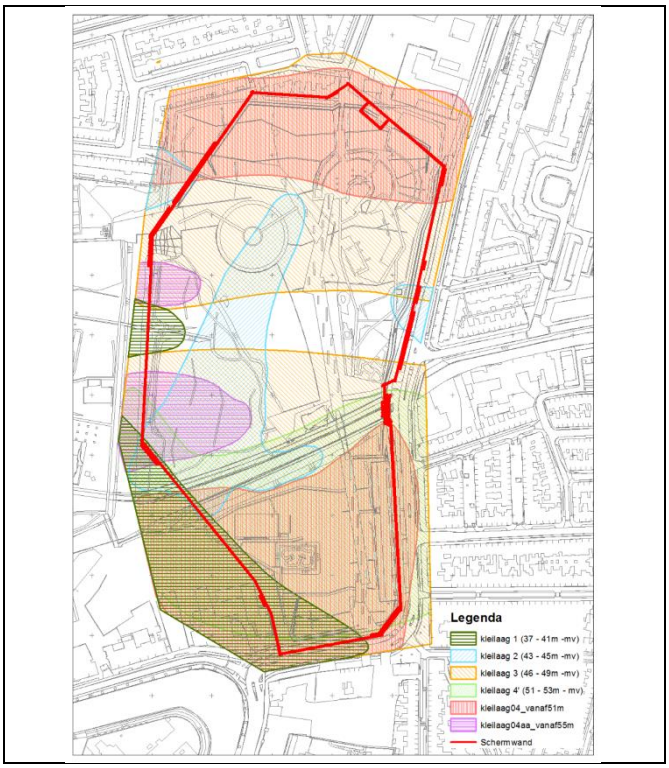

Figure 3: *Griftpark clay layer formations (Grondmechanica Delft, 1988)*

I.1.4. Containment method

The containment method developed for this specific site consists of a vertical cement-bentonite wall around the newly constructed park that, along with the clay layers of the aquitard, would contain and prevent the contaminants from spreading. These walls reach a depth of approximatively 55 meters where it connects with the clay layers. The objective is to seal the contaminated region from the 1st and second aquifer.

Given the non-continuity of the clay layers, three pumps have been installed in the Griftpark to create a seepage from the 2nd aquifer to the 1st aquifer. This prevents contaminants from infiltrating the second aquifer as well as to remove some contamination. In addition, the pumps lower the water table of the area inside the bentonite walls compared to the 1st aquifer surroundings, avoiding leakages from inside the walls to the 1st aquifer. This effect has to be taken into account because the bentonite walls, as clay layers, are still permeable materials even though their hydraulic conductivity is extremely low. A conceptual model of the Griftpark subsurface is shown on Figure 4 for a better visualization and understanding of the containment method action.

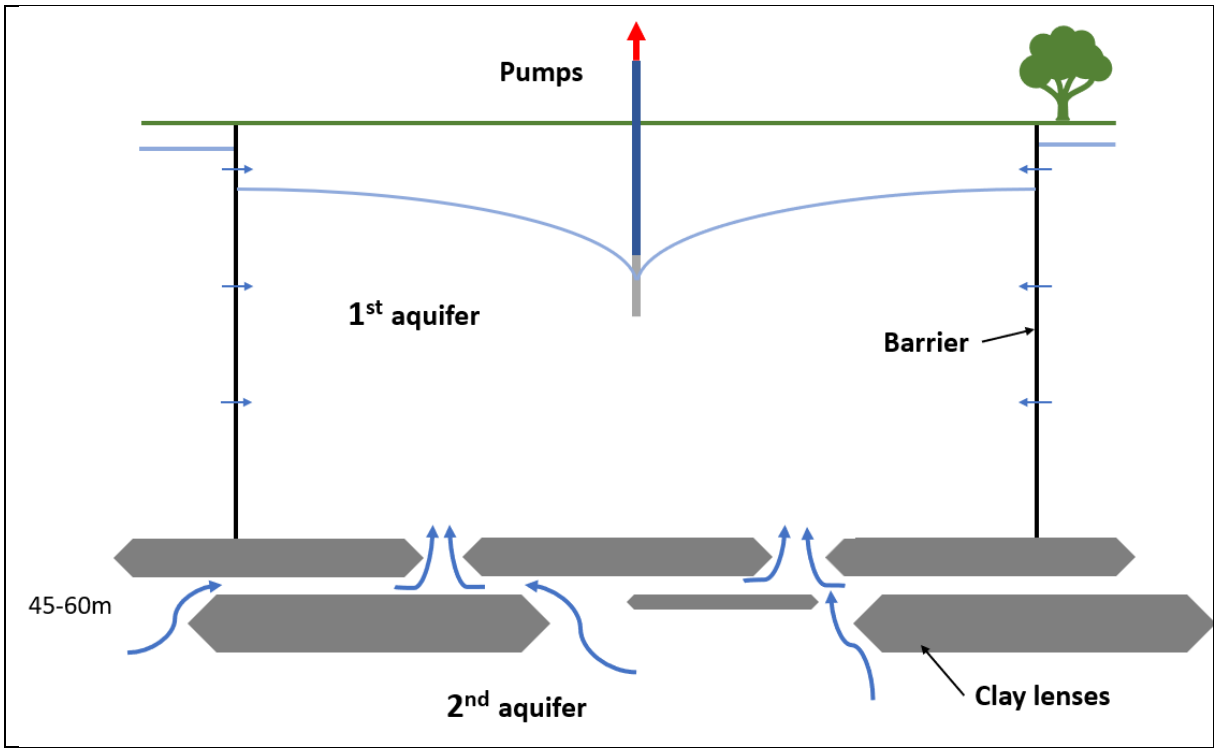

Figure 4: *Conceptual model of the Griftpark subsurface*

To monitor the contaminant spread as well as the site groundwater flow, several monitoring wells at different depth and locations have been installed in and around the Griftpark. Thanks to this monitoring system, the containment method could be shown to be effective. The location of each monitoring well, of the bentonite walls, and of the three working pumps (B20, B21, B22) can be seen in Figure 27 of Appendix A.

I.2. Aim & Research questions

As briefly introduced, the containment method developed in the Griftpark is very costly and would require to be maintained almost indefinitely to avoid aggravating the contamination risks. As a consequence, Utrecht municipality has actively been working with researchers to gain a better understanding of the situation and to try to find a better solution for the future. However, it is easier said than done in a project of such complexity. There are many uncertainties remaining on the Griftpark subsurface properties that have been complicating every study analysis and actions given the inaccessibility and heterogeneity of the subsurface. Among them, is the connection of the 1st and 2nd aquifer and the permeability of bentonite screen walls at certain locations. It has been proven that the two aquifers are connected but the mechanics, the location, and the consequences are still to be well understood. This could have some profound effects on the efficiency of the containment or remediation method put in place.

As such, it is not well understood whether the containment method is working as planned, i.e. the groundwater pumped from the site is coming from the 2nd aquifer past the clay lenses (Scenario A), or from leakages through the bentonite wall (Scenario B), or a combination of the two where the importance of each aspect need to be evaluated. Figure 5 illustrates these scenarios.

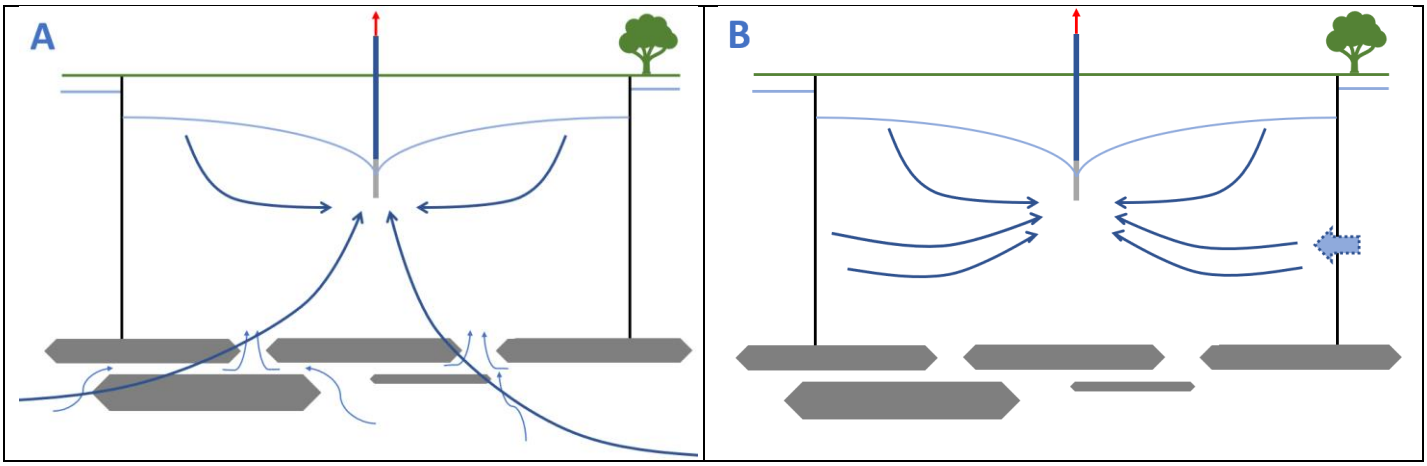

Figure 5: *Hypothesis scenarios of the pumped groundwater in the Griftpark*

In order to evaluate these two scenarios as well as to gain further knowledge on the connectivity of the two aquifers and the heterogeneity of the porous media, a vertical tracer test was originally planned in the Griftpark. It is to be noted that vertical tracer test are very different and less frequent than the usual horizontal tracer tests. Usually, groundwater mainly flows horizontally in unconfined and confined aquifers (Cohen and Cherry, 2020). Vertical tracer tests through several layers are even more unprecedent given the many challenges and uncertainties they face, especially in heterogenous porous medias. Still, they can reveal some quite insightful information and can be key for further research.

The vertical tracer test was divided into two MSc. Research given its complexity and time needed to be carried out. The first one had to focus on modeling groundwater flows in the Griftpark as well as to set up the tracer test. The second one, which this MSc. Research thesis is about, had to focus on the realization and analysis of the experiment results. The objectives of this MSc. Research thesis are:

- To evaluate the connectivity of the first and second aquifer.
- To obtain an increased understanding of the Griftpark soil's heterogeneity (layering) and its effects in groundwater flow.
- To evaluate the best way to model the Griftpark subsurface.

This study will be particularly focusing the surroundings of pump B20 in the central-eastern part of the Griftpark (Appendix A). It was believed to be the location where the 1st and 2nd aquifer are connecting given no clay layers were placed in the map made by the Grondmechanica department of the University of Delft (Figure 3). However, during the drilling of boreholes in preparation for this study, clay depositions were also found at this location (Appendix C).

I.3. Approach

Unfortunately, a vertical tracer test could not be performed in the Griftpark due to some technical difficulties with pump B20 that lasted more than 4 months, disrupting the timeline of this project. A pumping test was performed instead. This test was already planned as a pre-requisite for the tracer test but was also further developed to suit the timeline and objectives of this thesis.

As a consequence of this modification, the literature review of this MSc. Research Thesis was performed on the challenges of performing a vertical tracer test in a heterogenous aquifer rather than on pumping tests. Still, much of the information on the consequences of scale, heterogeneity, and verticality is relevant for pumping tests.

The connectivity of the 1st and 2nd aquifer will be evaluated by spatially and temporally analyzing the provoked hydraulic head changes during the pumping tests. Furthermore, thanks to the wide range of well depth, these hydraulic head results should also provide information on the Griftpark soil's heterogeneity and its effects on groundwater flow. Then, the collected data from these test will be used to estimate physical properties of the Griftpark subsurface, either analytically or numerically with 3D models. The idea of this estimation is to improve the subsurface model and our understanding of groundwater flow in the Griftpark. As there are different ways to estimate aquifer properties and model groundwater flows, different solutions will be compared with each other as well as with the collected data to determine which is the most effective method to model these flows.

II. Literature review

In porous aquifers, and especially heterogenous porous aquifers, modeling groundwater flow and solute transport requires detailed knowledge of aquifer parameters and their spatial distribution. Geophysical measurement at borehole locations can give useful insights on subsurface parameters but often yields limited results due to resolution, detection range, parametrization problems, and because it a point measurement. Tracer tests can help to effectively investigate and characterize aquifer properties based on effective parameters values such as tracer concentrations and groundwater velocity.

During this literature review I will briefly explain what tracer tests are, which types of tracers could be used in the Griftpark, and the different techniques that have been previously used. We will also look at the many challenges that come along with the execution of tracer tests at sites such as the Griftpark as well as why this vertical tracer test is quite unique. However, before that, we will look at some of the basic equations explaining the physics of groundwater flow and how to solve them in order to apply them to this tracer test experiment.

II.1. Fundamentals of groundwater flow

II.1.1. Darcy's Law

The law describing water movement through the porous media was developed by Henry Darcy in 1856. He demonstrated through an experimental study that a one-dimensional water flow through a pipe filled of sand was proportional to the cross-sectional area of the pipe, the head loss along this one, and inversely proportional to the flow length. The law was then expanded to multidirectional flow. Mathematically, it can be expressed as:

$$\vec{q} = -K\,\nabla h \qquad 2.1$$

where $\vec{q}$ is the specific discharge [L T^{-1}] vector, also called Darcy's flux, with three different components, q_x, q_y *and* q_z, one for each direction. *K* is the hydraulic conductivity [L T^{-1}] second order tensor that, when oriented along the principal axes, is composed of only three non-null components, also one for each direction. ∇h is the hydraulic head gradient [-]. This equation indicates that groundwater will flow down the hydraulic gradient and the discharge is dependent on the hydraulic conductivity of the porous media.

This law is also based on a macroscopic concept where the porous media can be replaced by a representative continuum. This means that the hydraulic properties of the subsurface are evaluated for a Representative Elementary Volume (REV).

II.1.2. Transport equations

Groundwater also transport many substances with its flow. Understanding how those substances mobilize in the subsurface is also key to project how contamination could propagate. It can also bring to light properties of the subsurface through the comparison of experiments and models. The advection-dispersion-reaction model, based on the concept of mass conservation, is often used to describe mass transport in three-dimensional saturated porous media . Its equation can be written as:

$$R\frac{\partial C}{\partial t} = -\bar{V}.\nabla C + \nabla(D_H \nabla C) + S \qquad 2.2$$

where *R* is the retardation factor, *C* is the solute concentration, *t* is the time, $\bar{V}$ is the average pore water velocity, D_H is the hydrodynamic dispersion tensor which includes mechanical dispersion and molecular diffusion, and *S* is the sink/source term accounting for the solute transformation (e.g., degradation, generation). The sorption process is included in the retardation factor.

However, this general transport equation can only be resolved with numerical techniques. Still, even with numerical techniques, there are different ways to solve this equation. MODFLOW, a computer software programmed to solve groundwater flow equation, uses for example the finite difference method (FDM) whereas FEFLOW uses the finite element method (FEM).

II.2. Tracer tests

The principle of a tracer test is to introduce an additive (e.g., particles, solutes, gases) or physical quality (e.g., temperature) into the groundwater and monitor its movement and spread. Given that the subsurface is not easily accessible, the tracer spread has to be deduced from groundwater samples collected around the tracer injection location. Aquifer properties such as groundwater velocity, effective porosity, layers connectivity, solute transport, and many more, can then be estimated from the analysis of these samples' tracer concentrations. However, they often depend on subsurface properties (e.g., physical heterogeneity) or processes (e.g., sorption, biodegradation) that affect groundwater and solute transport. Given the difficulty to measure and to spatially estimate these properties and processes given the heterogeneity of the porous media, their effect on groundwater flow and solute transport must be well understood in order to properly estimate many of the aquifer properties previously mentioned. In the next section the implications of scale and heterogeneity on tracer tests will be discussed. In the following section the different types of tracers generally used will be discussed, as well as the subsurface properties they reveal. Subsequently, different tracer test as well as the challenges that come along with vertical tracer test will be discussed.

II.2.1. Importance of scale and aquifer heterogeneity

When conducting a tracer test, it is important to consider the scale of the subsurface properties under investigation to adjust the tracer test method to it, especially in heterogeneous aquifers. Tracer tests conducted to investigate aquifer properties at local or point scale, i.e., for Representative Elementary Volumes (REVs), will not give the same information as tracer tests operated in the field. Even though the principle of tracer tests and the properties investigated at local and field scale are the same (e.g. groundwater velocity, solute transport), the implications of these properties have very different consequences at each scale. For example, it has been shown that aquifer properties can vary in space and are scale dependent (Ptak et al., 2004). Therefore, the scale of the investigation has a huge impact on the estimated property. It has been observed that dispersivity, which is one of the properties characterizing physical heterogeneity, often increases with transport distance (Gelhar, 1986; Dagan, 1989). This can be explained by that fact that at field scale, preferential pathways around low conductivity zones tend to increase the spread of solute plumes, an effect that will not be included in the mechanical dispersion at pore level.

We do not only encounter heterogeneity in the physical aspects of the subsurface but also in chemical aspects. The porous media is formed out of different geological layers, each one of them with different chemical properties. This chemical heterogeneity can be seen through the sorption properties of aquifer material (Grathwohl and Kleineidam, 1995; Ptak and Strobel, 1998) or through the enhanced spread of solutes at field scale (Burr et al., 1994; Ptak and Schmid, 1996). Another effect of the chemical

heterogeneity of the porous media which also combines with the physical heterogeneity, is the makrokinetic sorption behavior. This sorption behavior is characterized by an effective retardation factor increasing with time, even though sorption is locally at equilibrium in the porous media (Miralles-Wilhelm and Gelhar, 1996; Ptak and Kleiner, 1998). It account for the kinetic effect of groundwater flow in addition to the sorption capacity of the porous media which is of measured at equilibrium and without any flow.

Furthermore, the physical and chemical heterogeneity effects on groundwater flow or solute transport (i.e. dispersivity, sorption, etc.) do not take effect separately but rather all at once, which makes them quite difficult to account in a model. Depending on the different properties of the porous media and the scale at which they are studied, some of these effects can have greater impact on the groundwater flow and (reactive) transport processes than others. For example, Teutsch et al. (1998) showed that in case of equilibrium sorption, the most significant contribution to high effective retardation factors comes from gravel, due its high sorption capacity. However, in case of kinetic sorption, the same gravel contributes only very little to the effective retardation due to its high hydraulic conductivity as short contact time does not allow much dissolved components to diffuse into the gravel. In this case, the mean arrival times of solutes are mostly controlled by relatively medium conductivity sand which has a small sorption capacity but quickly reaches equilibrium. This shows that physical and chemical heterogenous porous media can have a very complex groundwater and solute transport behavior depending on the properties of this one. As such, knowing that the porous media of the Griftpark is highly heterogeneous, a good understanding of the effects caused by heterogeneity will be crucial to accurately estimate groundwater flows and transport properties.

When planning a tracer-based investigation to study groundwater flow or solute transport as well as when running model simulations, subsurface heterogeneities must be taken into consideration to see if they could have any impact on the study. If considered impactful, then it is necessary to review the relations between the investigation scale (characterized by the size of the investigated aquifer domain), the scale of heterogeneity (characterized by the typical size of the aquifer structural elements), and the detection scale of the investigation method. A detailed treatment of scale study is also given by Dagan (1986), Neuman (1990), Teutsch et al. (1990), Di Federico and Neuman (1998), and Zlotnik et al. (2000).

Usually, aquifer material can be considered homogeneous if the heterogeneity scale is much smaller than the investigation scale. However, it becomes relevant if the heterogeneity scale is in the order of the investigation scale. For most laboratory experiments, the media is often well mixed and thus homogeneity is assumed, unless the purpose of the study is to study the heterogeneity. For the experiments where homogeneity is assumed, deterministic approaches are then used to evaluate the measured data and estimate the aquifer parameters.

At a regional scale, in the order of kilometers, irregularities in the subsurface may tend to average out if the characteristic heterogeneity scale is substantially smaller than the scope of the research. In that case, it is acceptable to use effective parameters for the assessment of flow and transport (e.g. transmissivities from large scale pump testing, constant macrodispersivities, and effective retardation factors).

Often however, as a the Griftpark site, the investigation is on a scale in the order of ten to hundreds of meters. At this scale, which can be considered intermediate compared to laboratory experiments or large-scale studies, several characteristics of heterogeneity are displayed and cannot be neglected. As a consequence of the variable aquifer properties, strong irregular solute spread and a scale dependance of effective transport parameters can be expected. To unravel the heterogeneity structure, the detection scale of the investigation must be smaller than the heterogeneity scale. This

makes these types of investigation much more complex and expensive than investigations at small or large-scales where homogeneity can often be assumed (Ptak et al, 2004). In addition, due to the usually limited number of measurements available, there is always some remaining uncertainty in the investigation regarding the parameter estimations.

To illustrate the complexity of investigating groundwater flow and solute transport in a heterogeneous aquifer at intermediate scale, we look at tracer test results from Ptak and Teutsch at the Horkheimer Insel experimental field site (1994a).

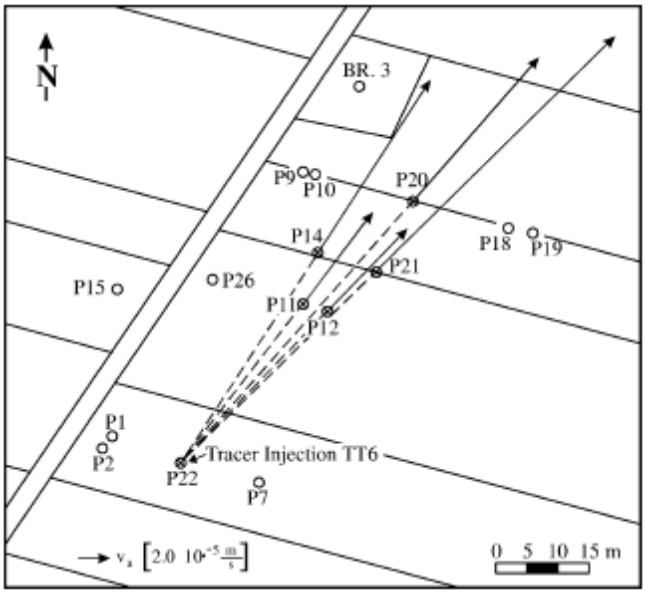

***Figure 6**: Distribution of transport velocities from a natural gradient tracer test (length of arrow indicates value of velocity; Ptak and Teutsch, 1994a).*

Figure 6 shows us the distribution of transport velocities derived from depth integrated sampling during a natural gradient tracer test with a transport distance of about 60 meters. Due to aquifer heterogeneity, Ptak and Teutsch did not manage to find a common transport velocity set for the entire ensemble of measured breakthrough curves. To illustrate the added complexity given by the aquifer heterogeneity, they decided to estimate the transport velocities for each individual breakthrough curve assuming an individual transport path within the aquifer with a transport direction parallel to the line connecting the injection point and the monitoring wells. The transport velocities range from 6,2 to 18,0 m/day. This example shows how transport predictions based on parameter values obtained at a limited number of borehole locations may be highly uncertain in heterogenous aquifers.

II.2.2. Type of tracers

The degree and extent to which a tracer test characterizes the subsurface depends on the type and number of tracers used. This is because each tracer has different properties and thus is used to investigate different properties. Therefore, a small overview of the different kinds of tracers available is necessary. Considering the multitude of existing tracers, I will mainly focus on the different tracer properties that could be useful for this study case.

Tracers are compounds that are inherent to or injected into the water cycle to study several properties of the subsurface (e.g. hydraulic conductivity, groundwater flow patterns, solute transport). A multitude of tracers can be used in hydrology, each of them with different properties, objectives, and sampling methods. For example, it is possible to use environmental tracers that are inherent compounds of the water cycle such as stable isotopes that naturally exist in water, or artificial tracers

that need to be added to the system by punctual injections such as fluorescent compounds, salts, radioactive compounds, and even viruses or spores.

Tracers are also categorized by how they interact with the subsurface, giving them different utilities in tracer test. *Conservative tracers*, also called non-reactive or ideal tracers, are biochemically stable tracers that show virtually no interaction with the porous media, and thus flow passively with the carrier fluid (e.g, salts, isotopes, dyes). They display only the purely hydrodynamic transport processes: advection, dispersion and diffusion. Therefore, they are generally used to investigate hydraulic properties (e.g., tracking aquifer connectivity, preferential flow pathways), to analyze travel times and flow velocities, and to estimate hydromechanical properties (e.g., dispersivity, porosity). In order to investigate these aquifer properties with great accuracy, the compounds are desired to behave ideally, meaning they should (1) behave conservatively (e.g., are transported with water velocity, not degradable), (2) have a low background concentration in the system, (3) be detectable in very low concentrations, and (4) have low or no toxicological environmental impact (Flury and Wai, 2003). Unfortunately, ideal tracers do not exist, all solute tracers are impacted to some degree by chemical, physical, and/or biological processes. This means some knowledge of the hydrological system is needed beforehand to verify the practicality of the tracer. A conservative tracer is only considered conservative under specific conditions, but it could be considered otherwise under other conditions.

Reactive tracers are compounds that undergo chemical reactions or physiochemical interactions in a predictable way under known conditions. By using specific features of reactive tracers, it is possible to investigate aquifer physicochemical properties (e.g., sorption capacity), water chemistry properties (e.g., redox condition, pH, ion concentrations), and other influencing parameters (e.g., temperatures, microbial activity) of the hydrological system beyond the capabilities of conservative tracers (Ptak et al., 2004; Luhmann et al., 2012). In order to identify and quantify the processes that take place in the subsurface with reactive tracers, it is necessary to combine them with at least one reference conservative tracer to identify purely hydrodynamic processes that affect both tracer types in a similar fashion. To go even further on reactive tracer types and applications, Cao et al. (2020) or Divine et al. (2005) have made further investigations and publications on the subject.

Regarding the Griftpark, given that this research merely focus on the hydrodynamic processes inside the Griftpark, conservative tracers should primarily be used. With several tracers arriving together, an easy comparison can be made and it would differentiate the signal from other injection locations in case one of them is re-used somewhere else. Salts, such as potassium iodide (KI), lithium chloride (LiCl), and sodium bromide (NaBr), are often used as conservative tracers due to their high stability, low toxicity, and low cost. Given that this project also focuses on the microbial remediation of pollutants, investigating the aquifer physicochemical properties with the already existing set-up could be very interesting for further research. For this purpose, a reactive tracer could be mixed with the conservative tracers.

II.2.3. Tracer test techniques

There exists a variety of ways to set up a tracer test depending on the objectives of the experiment, the subsurface concerned, and the investment considered. Two fundamentally different approaches can be distinguished among all the methods. The first approach accounts for tracer test applications at a local scale or point scale (very small REVs) to estimate subsurface parameters. These tracer tests are employed mainly in small-scale laboratory experiments (columns and tanks) or in small-scale field investigation, as for example Sutton did by combining a dipole flowmeter test with a tracer injection and detection (Sutton et al., 2000). The resulting small-scale measurements can be used for a variety of purposes, including understanding non-reactive and reactive transport processes, testing process-based transport models, and transport model predictions. In the case of heterogeneous aquifers, these

predictions should be performed within a stochastic modeling framework due to the remaining parameter uncertainty after investigation (Ptak et al., 2004).

The second approach deals with tracer tests that aim to directly measure effective subsurface parameters at field scale. This approach is often applied in situations where the cost to obtain the amount of data needed for stochastic simulations, the time needed to analyze the data, and the computation time become prohibitively high. It is also applied when some input parameters cannot be described with geostatistical methods (e.g., concentration within contaminant zones). Among this second approach, we distinguish tracer test performed under natural hydraulic conditions where the groundwater flow field is undisturbed, and tracer test performed under forced gradient conditions induced by groundwater pumping or tracer solute injections. The distinction is made because the experiment set-ups are quite different. Even though the Griftpark is designed to be under forced gradient conditions, I believe it is interesting to evaluate the implications of a tracer test under natural or close to natural conditions to understand the limitation of the planned tracer test in the Griftpark.

II.2.3.1. Natural gradient tracer tests

In natural gradient tracer tests (NGTT) at field scale, tracers are injected continuously over a period of time, or pulse-like into the undisturbed groundwater flow field. The tracer concentrations are then measured at different depth (multi-level) or along an entire section for which a weighted average value is computed (depth integrated). It is therefore essential for the experiment design to have an approximate mean transport direction. In addition, an approximation of the average transport velocity should be known in advance to coordinate the sampling activities.

One of the advantages of NGTT is that the investigation scale is in principle not limited. However, the duration and the experimental efforts may increase if the transport velocity is small, and/or the transport distance large. Another advantage is that NGTT can obtain proof of postulated position of contaminant sources, which not possible with forced gradient tracer tests (Ptak et al., 2004).

Another disadvantage of the NGTT may be that in heterogenous aquifers, a large number of monitoring wells may be needed to reliably identify the solute plume and its development. Furthermore, if the mean groundwater flow direction is shifting due to changes of boundary conditions of preferential flow pathways, the evaluation of solute concentration may become difficult.

II.2.3.2. Forced gradient tracer tests

Forced gradient tracer test (FGTTs) can be executed in convergent, divergent, and dipole flow fields, or in a subsequent application of divergent and convergent flow conditions (push and pull tests). Figure 7 shows a schematic example of a convergent a divergent flow field and Figure 7 in the following section of a dipole flow field. Because of the forced gradient, the flow direction is known, minimizing the effects of natural gradient variations and reducing the duration of the experiment in comparison with NGTTs. Possible field applications, considering advantages and disadvantages of NGTT and FGTT are summarized by Ptak et al. (2004).

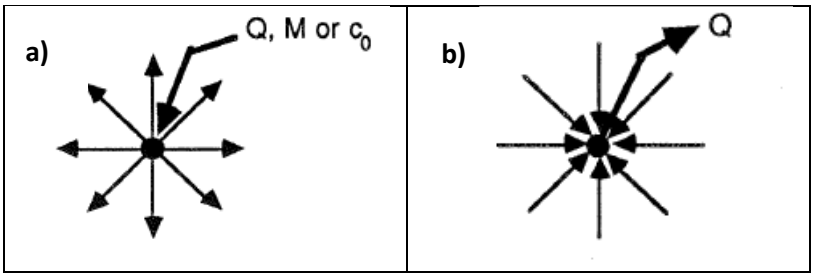

Figure 7: *Convergent flow field (a) and divergent flow field (b).*

In the divergent flow field approach, groundwater is injected into a well at a constant rate. Once a quasi-steady-state flow field is obtained, the tracer mass is added instantly or continuously over a period of time. Surrounding monitoring wells are then employed to measure depth integrated or multilevel tracer concentrations. Measurements can be procured in all directions using a single tracer.

The convergent flow field approach uses the same set-up, but groundwater is pumped out of the central well at a constant rate. Again, once quasi-steady-state is reached, the tracer is injected instantly or continuously over a period of time into the surrounding wells. Then, tracer concentrations are measured at the extraction location. If different flow directions have to be taken into account, different tracers must be used.

In the dipole flow field approach, groundwater is extracted from a well, and re-injected into another well. Sometimes it can be the same well but at a different depth, resulting in a vertical tracer test. This case will be further studied in the following section. The tracer is introduced into the injection well (pulse like, continuously, or pulse like with recirculation), and monitored at the extraction well. The nature of the of the dipole flow field might cause relatively long experimental times to obtain a satisfying tracer recovery. Therefore, this approach is often used at a small scale. Tracer recovery can be improved in an asymmetrical configuration by increasing the extraction rate compared to the infiltration rate.

A great example of FGTT and NGTT for the Griftpark with similar objectives and subsurface conditions is described by Ptak and Teutsh (1994a). They performed a NGTT and FGTTs with both divergent and convergent flow fields, in a highly heterogenous aquifer using non-reactive tracers. The objective of the many tests at Horkheimer Insel experimental field site was to investigate the aquifer structure by identifying preferential flow paths and estimating anisotropy, solute spreading, layers connectivity, and the spatially variable effective transport parameters. These are very similar objectives of this research. The results demonstrated that, for contaminant transport predictions in highly heterogenous aquifers, high resolution techniques are required in addition to a complex numerical and transport model to describe mass transport adequately. They were also confronted with the integration of horizontal and vertical flows when most of the tracer test only study horizontal flows. It is complex as well as expensive to have depth-accurate multilevel samplers for all types of wells. When comparing their experiment with the Griftpark, they still investigate mostly horizontal flows even if they take into account vertical flows given that their aquifer is only 3-5 meters deep. Still, it gives us a good idea on what to expect for the incoming tracer test in the Griftpark.

To resume which technique would be optimal for the Griftpark tracer test, a NGTT would be optimal to evaluate the connectivity of the first and second aquifers below the park. It would allow to investigate the risk of contaminant propagation under natural conditions even if it will probably take some time. However, the municipality will never take the risk of potentially contaminating the aquifer they use to produce drinking water. Regarding a dipole flow field tracer test, the scale at which they have been performed is too small for a case such as the Griftpark. Therefore, a FGTT will probably be

performed. Given the high experimental effort needed to perform a divergent FGTT, especially monitoring and sampling, a convergent FGTT would be more suited for the Griftpark tracer test.

II.2.4. Vertical tracer tests

Vertical tracer tests are highly unusual and unprecedent at the scale of the Griftpark. There has been some test at small scale executed in laboratories or as dipole flow test with a tracer (Sutton et al., 2000). At a larger scale, groundwater in the saturated porous media tends to flow mainly in a horizontal direction rather than vertical. The flow direction is dependent on the head gradient, which is generally more pronounced horizontally in saturated aquifers. In addition, all aquifers are, in some degree, anisotropic. This means that some of their physical properties, such as the hydraulic conductivity, vary with direction. Due to the layering of sediments, especially when combining sand and clay layers, vertical hydraulic conductivity is commonly orders of magnitude lower than horizontal hydraulic conductivity (Woessner and Poeter, 2020). This favorizes again groundwater flow in the horizontal direction. Therefore, there are not many situations at large scale where strictly vertical tracer tests have been performed. The tracer test planned in the Griftpark is then quite unique given its unusual groundwater flow field generated by the vertical bentonite barriers, pumps, and clay lenses.

Beside the fact that not many vertical tracer tests have been performed, doing so in a highly heterogenous, anisotropic, and partially connected aquifer may be challenging. Heterogeneity and anisotropy are both subsurface properties that can greatly affect groundwater flow and very difficult to estimate or evaluate its effects. As described by Ptak and Teutsh (1994a), high resolution techniques in time and space as well as a detailed numerical transport model are required to describe mass transport in heterogenous aquifers adequately. Small-scale studies and even some or large scale that, even though they do not focus specifically on vertical groundwater flow, have integrated depth into their investigation. Sutton et al. (2000) were the first to combine a dipole flow test, originally proposed by Kabala (1993), with a tracer to determine dispersivity as well as horizontal and vertical conductivity (K_r and K_z). Kabala's set-up is made out of three inflatable packers isolating two chambers in a cased well as shown in Figure 8. A submersible pump is located in the central packer and pumps water at a constant rate from the aquifer into the extraction chamber. At the same time, water from that chamber is transferred to an injection chamber where it is then released into the aquifer.

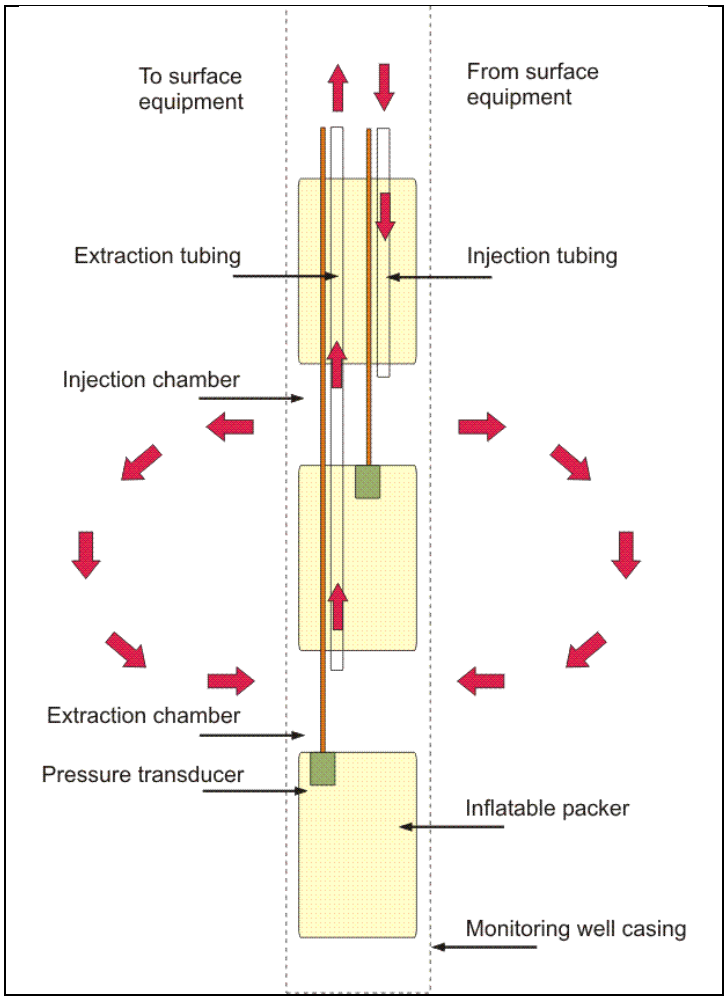

Figure 8: *Schematic of a dipole probe and tracer test set up (arrows indicate tracer flow direction; Roos et al., 2009)*

In the set up used by Sutton et al., once the dipole flow field has reached a steady state, a tracer is released into the injection chamber and the tracer concentration is monitored in the extraction chamber. However, this set-up is limited by the distance between the two chambers which, with less than a meter, limits its large-scale application. Further explanations and analysis have been described by Roos et al. (2008).

Even though large-scale vertical tracer tests are unprecedent, many tracer tests have managed to integrate depth in their investigation. Sampling groundwater at different depths is not uncommon. However, multilevel sampling is much more complex. Depth accurate multilevel groundwater sampling requires trustworthy seals to avoid water circulation within the well during and prior the sampling. Devices such as sampling pumps or bailers that are lowered to different depths are likely to disturb concentration gradients yielding mixed groundwater samples. Still, we distinguish two types of groundwater sampling devices designed to avoid vertical circulation within the well: samplers that are lowered into monitoring wells each time a sample need to be taken, and devices that are permanently installed in the well. With the first type, sampling complete profiles with multiple points is a very tedious and time-consuming task. Also, the free groundwater circulation within the well before the sampling might require extensive purging procedures to get representative samples. With the second type, specific well installations might be necessary and they are also not often retrievable. Furthermore, if samples at different locations are needed, this approach might become very expensive. Some companies and researchers have tried to develop new approaches to find a middle ground

between these two types of devices. For example, Solinst developed an inexpensive Multi-Level Sampling system (MLS) to monitor well systems. It is composed of 3 or 7 narrow tubes of different lengths that enable groundwater monitoring different discrete zones. The benefit of this system is that the tube design permits reliable seals between zones. The downside of this system is that certain application such as pumping are limited by the small diameter of the tubes (10mm). This is an aspect to take into consideration if a tracer needs to be injected into the subsurface. Figure 9 shows a picture of an MLS installed in the Griftpark.

Figure 9: *Multi-Level Sampler with 7 channels installed in the Griftpark subsurface.*

Another alternative for vertical tracer tests in saturated porous media could be to follow the principles of a convergent FGTT. One or many tracers could be injected deep into the subsurface and close to a pump generating a convergent field flow. Then, the water retrieved from that pump would need to be continuously or periodically analyzed to measure tracer concentrations. This is the approach considered for the Griftpark given the pre-existence of pumps, monitoring wells, and Multi-Level Sampling wells (MLSs).

III. Methodology

As previously stated, due to some pumps' failures a vertical tracer test has not been performed in the Griftpark. The pre-required pumping test needed for the later tracer test was performed instead. The original pumping test was also further expanded to suit this thesis objectives and timeline.

A pumping test consists of retrieving groundwater from a well, usually at a constant rate, and measuring the water level or hydraulic head changes in nearby wells. Hydraulic heads describe the mechanical energy per unit of weight of a fluid (Ge et al., 2015) and, as briefly explained in Darcy's law section, the retrieved hydraulic gradient between two points determines the groundwater flow direction. These mechanical energy measures are taken inside wells whose screen can either fully penetrate or partially penetrate an aquifer at specific depths. By spatially and temporally tracking hydraulic head changes in the subsurface and combining them with previously collected data (e.g. hydraulic conductivity field), several properties of the porous media can be retrieved (e.g. groundwater flow directions, confining layers locations), especially during a pumping test where these changes are forced and the hydrogeological conditions are controlled to some extent.

The objective of the pumping test in the Griftpark is to evaluate the connectivity of the 1st and 2nd aquifer, to obtain an increased understanding of the Griftpark soil's heterogeneity (layering) and its effects on groundwater flow, to parametrize aquifer properties. The parametrization will be done both analytically with the Stallman method for bounded aquifers and numerically using MODFLOW. Results obtained with a 3-layer and a 14-layer model will be compared to field measurements in order to evaluate the models.

III.1. Pumping tests

The pumping test was performed with pump B20 located in the central-east part of the Griftpark (Appendix A). This central eastern zone of the Griftpark was focused because it was believed to be the location with the biggest hydraulic connection between the 1st and 2nd aquifer (Figure 3; Grondmechanica Delft, 1988), also often called as the hydraulic hole between the two aquifers. This means the surrounding of pump B20 is the location where groundwater from the 2nd aquifer was believed to be seeping towards the 1st aquifer when the pumps of Griftpark are working (Figure 4, scenario A). Pump B20 is also the only pump of the park surrounded by a network of wells at different locations and depth allowing the investigation of vertical and horizontal groundwater flows. A pumping test with pump B20 should therefore unravel one of the biggest uncertainties of this investigation, whether the hydraulic connection between the 1st and 2nd aquifer is located in the central-east part of the Griftpark.

A constraint for the pumping test in the Griftpark is that the Municipality has required the park to respect a minimum total pumping rate to ensure groundwater seepage towards the park to avoid contamination propagation towards the 2nd aquifer. To fulfill this requirement, pumps B21 and B22 located in the northern part of the park were set to 3,5 m³/h and 4 m³/h respectively. Given their constant pumping rate, these two pumps should not be responsible for any changes of the hydrogeological conditions in the Griftpark.

During the course of the pumping tests, pump B20 was set to either 10 m³/h or 0 m³/h. The 10 m³/h pumping rate chosen is the maximum achievable rate with pump B20. We expect that at this rate, which overpass alone the minimum required by the municipality, hydraulic head changes in both the 1st and 2nd aquifer should be observable if they are closely connected. The collected hydraulic head

data should confirm or refute this hypothesis by analyzing possible patterns. It is also important to take into account that each one of the three pumps has a screen between 12-20 meters below ground level (bgl).

Regarding the monitoring network, we distinguish two types of wells. The first type are called observation wells, which have screens between 1-5m, and a diameter between 32-40mm in which a diver could fit. The second type of wells are called Multi-Level Sampling wells (MLS). They are composed of seven thin wells with a diameter of 10mm and screens of 0.25m located at different depths. To be able to compare hydraulic heads from both well types, the average depth of the screen has been taken in this case as the well depth. The properties of the three different locations around pump B20 are described on Table 1.

Table 1: *Specifications of each one of the three wells locations around pump B20*

Location	Number of Observation wells	Average depth [m - bgl]	Screen length [m]	Number of MLS wells	Average depth [m - bgl]	Screen Length [m]	Distance & Direction of B20 [m]
B	4 (BU1; BU2; BU3; BU4)	18; 44.5; 54.5; 63.5	2; 1; 1; 1	3 (BMLS1; BMLS2; BMLS3)	8.5-19; 20.75-31.25; 49.5-60	0.25	28m NW
B2	1 (B2)	65	1	2 (B2MLS1; B2MLS2)	6.75-17.5; 20-60	0.25	36m NE
Eastern border	2 (DV12; DV11)	31; 31.5	4; 5	0	-	-	43.5m & 50.5m E

Regarding the location at the eastern border of the Griftpark, pump DV12 is located inside the park bentonite barrier and DV11 is located outside the barrier. Figure 10 conceptually summarizes the location, depth, and screen length of wells of location B and B2 considering the cross section between these two points. A precise description of the depth of each well, their screen length, and their elevation can also be found in Appendix B.

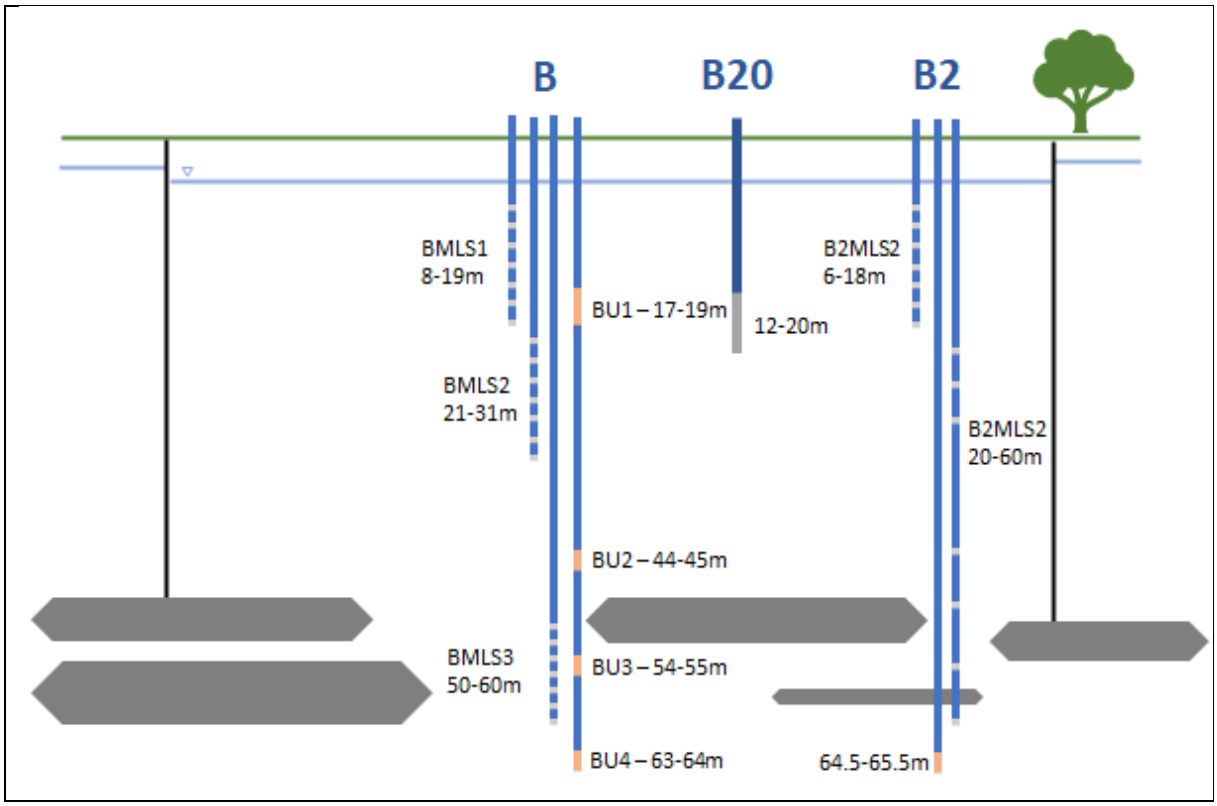

Figure 10: *Conceptual diagram of the subsurface between the cross-sectional area of location B and location B2.*

Hydraulic head measurements from each well were either taken manually with a Solinst 102M Mini Water Level Meter, or continuously with Van Essen Instruments' Divers. Divers are devices that are suspended inside observation wells and register the absolute pressure and water temperature. In this case, the divers were set to register hourly the absolute pressure and water temperature. To retrieve the hydraulic head of the water inside the well, the water column above the diver first needs to be computed based on the absolute pressure measured by the diver and the atmospheric pressure outside the well. Then, by knowing the length of the diver cable, the hydraulic head can be deduced. This can be summarized by the following equations:

$$WC = P_{diver} - \frac{P_{atm}}{\rho g} \quad 3.1$$

$$HH = L - WC \quad 3.2$$

where in equation 3.1 *WC* is the water column above the diver [m], P_{diver} is the absolute pressure measured by the diver [m], P_{atm} is the atmospheric pressure [Pa], ρ is the water density [kg/m³], and g is earth gravitational acceleration [m/s²]. The water density of equation 3.1 can also be calibrated for each measurement based on the temperature measured by the diver and the thermal expansion coefficient to account for the seasonal temperature change effects (The engineering ToolBox, 2003). In equation 3.2, HH is the hydraulic head of the water inside each well [m], *L* is the length of the diver cable [m], and *WC* is the water column above the diver measured with equation III.1.

Manual hydraulic head measurements have an accuracy of approximatively ± 1cm. Divers absolute pressure and temperature have a maximum accuracy of ± 2cm and ± 0.2°C but a typical accuracy of ± 0.5cm and ± 0.1°C respectively once calibrated (Source: manual). This has to be considered when comparing these two types of results. Another aspect to take into account is that each location and even well cap has a different elevation. To correct for the elevation difference between locations and

wells, all hydraulic head measurements have been referenced to the Normal Amsterdam Water Level (NAP in Dutch).

The atmospheric pressure used to compute the hourly hydraulic head measurements was downloaded from the Royal Netherlands Meteorological Institute open-source published dataset (KMNI, 2022). More specifically, these hourly atmospheric pressure measurements come from De Bilt station located 3.5 kilometers away from the Griftpark. It is to be noted that the diver absolute pressure and the atmospheric pressure were not always taken at the exact same time. To compute the groundwater hydraulic heads, the absolute pressure measured by the diver were matched with the closest atmospheric pressure time.

The water table and hydraulic heads in the subsurface can be affected by groundwater recharge variations. Therefore, hourly precipitation and daily evapotranspiration measurements were also retrieved from the dataset from the De Bilt station published by the KMNI and matched to the closest diver timelines. For the daily evapotranspiration, the values were converted into average hourly values by dividing them by 24. As such, the daily variations of evapotranspiration were not taken into account but, given that mostly the daily/weekly variations of hydraulic heads are studied, the hourly variations in evapotranspiration are considered negligeable. Based on these two measurements, hourly precipitation surplus or cumulative precipitation surplus were computed and compared to the diver results to understand the part recharge has over the hydraulic head changes. The distance between KMNI De Bilt meteorological station and the Griftpark was considered small enough to consider the variation of atmospheric pressure, precipitation, and evapotranspiration between these two locations insignificant.

Changes in atmospheric pressure also affect the water table. When the atmospheric pressure increases, water levels drop, and vice versa. This change can be estimated based on the barometric efficiency (BE) of the aquifer which is defined as the ratio of change in water level (Δh, m) in a well to the corresponding change in atmospheric pressure (Δp, Pa). The equation is formulated as:

$$BE = \frac{\gamma \Delta h}{\Delta p} \tag{3.3}$$

In which γ is the specific weight of water [kg m^{-2} s^{-2}]. This efficiency is dimensionless and range from 0 to 1. When the BE equal to 1 (100%) means the air pressure does not affect the total head within the aquifer. On the contrary, a BE efficiency of 0 (0%) means the air pressure travels fast through the soil. More details on how to compute the Barometric efficiency of an aquifer or how to graphically estimate it based on continuous data can be found in Gonthier publication in the US Geological Survey (2007).

From the changes in atmospheric pressure observed during a pumping test, and the known relationship between Δh and Δp, the water level changes due to changes in atmospheric pressure alone (Δh_p) can be calculated. Subsequently, the actual drawdown s' caused by the pumping test can be corrected for the water level changes du to atmospheric pressure:

$$s' = s + \Delta h_p \tag{3.4}$$

The Barometric Efficiency is generally computed during the pre-testing period where the water level is not influenced by the pumping test. In this case, the Barometric Efficiency has been computed based on the biggest period where the water table has not been influenced by any recharge and the aquifer is considered at equilibrium. Based on this efficiency, the effect that atmospheric pressure changes have on hydraulic heads has been estimated in order to purely investigate the hydraulic head variations caused by pumping.

III.1.1. Pumping tests timeline and set-ups

From mid-February to mid-March, the pumping test set-up was to weekly switch pump B20 on at 10 m^3/h or off. Hydraulic head measurements were taken through a diver placed in well BU1 (Location B, 17-19m bgl deep), and manual measurements in the other wells 5-6 days after switching the pump status.

Because of uncertainties remaining regarding the time for the aquifer to reach equilibrium, from mid-March to the end of June it was decided that pump B20 status will be switched every two weeks and manual measurements would be taken 12-13 days after the switch. In addition, five more divers were placed in wells BU3 (Location B, 54-55m bgl and where to aquitard is considered to be), BU4 (Location B, 63-64m bgl and where the 2nd aquifer is considered to be), B2 (Location B2, 64.5-65.5m bgl), DV11 (Outside the bentonite walls of the Griftpark, 29-33m bgl), and DV12 (Inside the bentonite walls of the Griftpark, 29-34m bgl).

Unfortunately for the Griftpark management but very interestingly for this research, all three pumps in the park had to be halted several times during the experiment timeline, disrupting the original experiment schedule. This enabled us to also study the effects of having all three pumps shut down on the Griftpark groundwater flows. The resulting timeline for the pumping tests can be seen in Table 2.

Table 2: *Timeline of the Griftpark pumping tests*

Date	Pump B20	Pump B21&B22	Comment
17-02-22 05:49	OFF	ON	Start
24-02-22 09:25	ON	ON	B20 switch on
03-03-22 06:55	OFF	ON	B20 switch off
10-03-22 07:30	ON	ON	B20 switch on
17-03-22 08:15	OFF	ON	B20 switch off
31-03-22 07:30	ON	ON	B20 switch on + 5 divers
14-04-22 13:43	OFF	ON	B20 switch off
24-04-22 21:30	OFF	OFF	All pumps off
09-05-22 11:30	OFF	ON	B21&B22 switch on
10-05-22 11:30	ON	ON	B20 switch on
13-05-22 17:40	OFF	OFF	All pumps off
24-05-22 10:40	ON	ON	All pumps on

III.2. Analysis of pumping test data

Hydrogeologists and engineers have developed several theoretical models over the past century to analyze and evaluate pumping test data. The solutions of these models were for a long time found analytically but, with the rise of computational power over the last decades, they have been more and more integrated into numerical models. Nowadays, 3D numerical models have even become the most established method to study groundwater flows.

III.2.1. Analytical solutions of aquifer properties

Multiple theoretical models exist to analyze pumping test data from different types of aquifers (confined, unconfined, leaky, bounded). The models can take a range of factors into consideration (e.g. steady or unsteady flows, fully or partially penetrating wells, anisotropy, heterogeneity) which complexify the pumping test analysis.

Given that groundwater flow in 1st aquifer of the Griftpark is characterized by the presence of a bentonite barrier and groundwater pumps, the Stallman method (as quoted by Ferris et al., 1962) for bounded confined or unconfined aquifers in unsteady-state flow was chosen to analyze our pumping test data analytically. The Griftpark boundary conditions do not allow to consider the general assumption that the aquifer's areal extent is infinite, which hinders the use of most methods.

This method for analyzing groundwater flow in bounded aquifers is based on the principle of superposition. According to this principle, the drawdown induced by two or more wells is equal to the sum of the drawdowns caused by each separate well. Therefore, by introducing imaginary wells, or image wells, it is possible to transform an aquifer of finite extent into one of seemingly infinite extent.

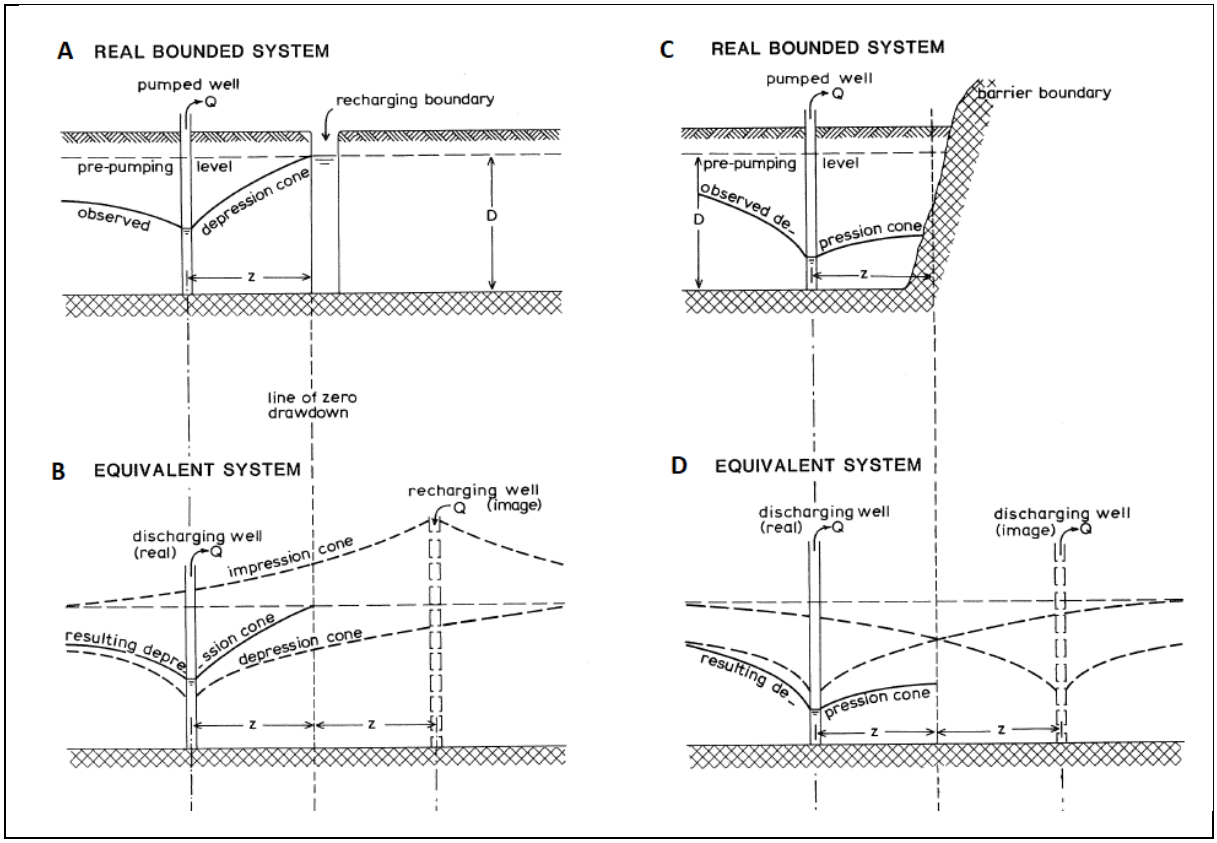

Figure 11: *Drawdowns in the water table of an aquifer bounded by:*

- *A) A recharging boundary*
- *C) A barrier boundary*
- *B) and D) Equivalent systems of infinite areal extent (Kruseman et al., 1994)*

As Figure 11 shows, recharging wells are placed to simulate recharging boundaries and discharging wells are placed to simulate barrier boundaries. The distance between the real well and a monitoring well is defined by r, the distance between the image well and the monitoring well is defined by r_i and their ratio is $r_i/r=r_r$. If all wells are discharge wells, the drawdown s in the nearby monitoring well can be estimated with the following equations (Kruseman et al., 1994):

$$s = \frac{Q}{4\pi KD}[W(u) + W(u_1) + W(u_2) + \cdots + W(u_n)] \quad 3.5$$

or

$$s = \frac{Q}{4\pi KD} W(u, r_{r1\to n}) \quad 3.6$$

Where Q is the well discharge [m³/h] which was 10 m³/h in this case, [-], K is the average hydraulic conductivity of the aquifer [m/h], D is the depth of the aquifer [m] which in our case was considered to be 50m, u and u_i are the dimensionless time of the real and imaginary wells respectively, and $W(u)$

and $W(u_i)$ are the dimensionless drawdown [-] of the real and imaginary wells respectively. The dimensionless time u and u_i are defined as:

$$u = \frac{r^2 S}{4KDt} \quad 3.7$$

and

$$u_i = \frac{{r_i}^2 S}{4KDt} = \frac{{r_r}^2 r^2 S}{4KDt} = {r_r}^2 u \quad 3.8$$

Where S is the Storativity of the aquifer [-], and t is the time since pumping started [h].

The number of terms inside equation 3.5 depends on the amount of imaginary wells. If there are two straight boundaries intersecting at right angles, a third image well is placed in the corner. With parallel boundaries, the number of image wells becomes infinite, but those where r_r>100 can be neglected. Image wells are placed at an image distance of real well from the barrier boundary.

Regarding the image well system for the Griftpark case, the shape of the boundary conditions has been simplified with a rectangular shape as shown on Figure 12, which illustrates the boundary and well configuration used to simulate the park. The Griftpark was considered to be 385m long and 215m wide. Pump B20 was placed 55m away from the eastern boundary, 160m from the western boundary, 185m from the northern boundary, and 200m from the southern boundary. As a result, the first four imaginary wells placed on the side of the Griftpark walls are 110m (Fig. 12 red arrows), 320m (Fig. 12 blue arrows), 370m (Fig. 12 green arrows), and 400m (Fig. 12 yellow arrows) away from pump B20. The monitoring well of location B was placed 28m north-west of pump B20.

Another real discharge well was placed to simulate the effects of pump B21 and B22. The discharge rate of this 2nd real discharge pump is also 10 m³/h because this method doesn't allow the placement of wells with a different rate than the real 1st one. As such, the distance from pump B20 of this second real pump has been increased in order to match the drawdown that by pump B21 and B22 would have generated according to Stallman's method. The pump was placed at 1260m away from pump B20 instead of the 121.5m and 139m from which pumps B21 and B22 are respectively separated from pump B20. This 2nd real discharge pump matched pump B21 and B22 estimated drawdown with a coefficient of determination R^2 of 0,9901.

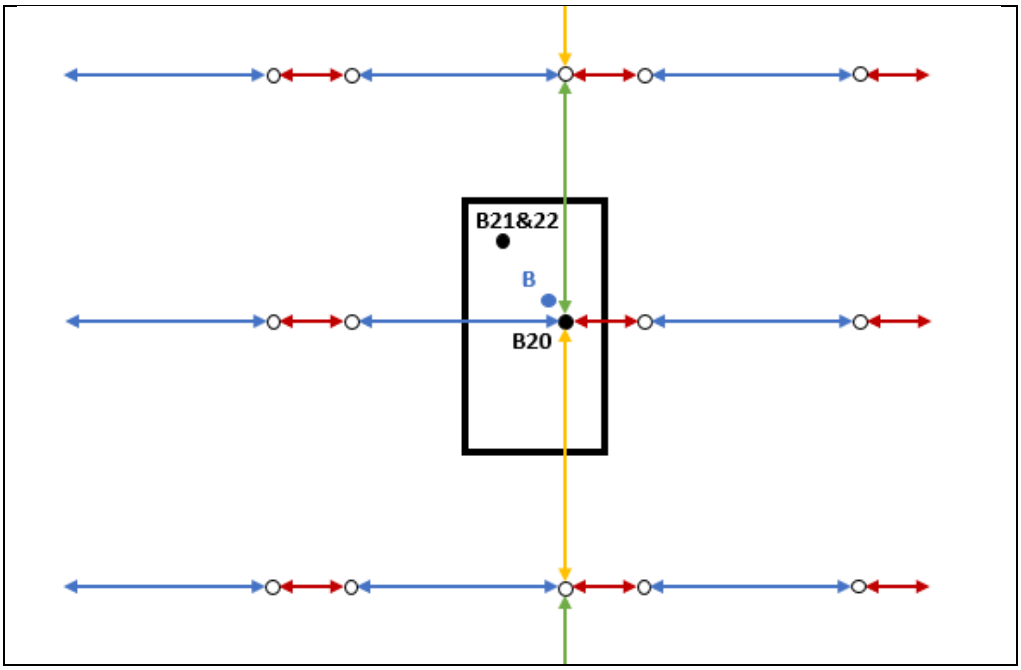

Figure 12: *Conceptual diagram of Stallman method adapted to the Griftpark case.*

- *Real discharging well*
- *Image discharging well*
- *(Blue) Measuring well*

In total, 65 imaginary wells were placed around pump B20 to simulate the groundwater flow boundaries of the Griftpark. For each well, $W(r_{rn}^2 u)$ were retrieved from Annex E based on their r_r ratio.

To estimate the aquifer average hydraulic conductivity and storativity, plots of $W(u, r_{r1\to n})$ versus u and the observed drawdown data versus 1/t, have to be matched on the same logarithmic scale. Based on the match points, *K* can be estimated from equation 3.6 and then *S* can be estimated from equation 3.7. As observed data from a pumping test, one of BU1 diver hydraulic heads measurements that has not been influenced by precipitation was used.

More details on Stallman method to analyze bounded aquifer pumping test data can be found in Ferris et al. (1962) or Kruseman et al. book on analysis of pumping test data (1994). Even though in this case all the presented equations were computed manually, many numerical programs such as AQTESOLV now combine analytical solutions with numerical estimations to have a more accurate result.

III.2.2. Numerical solutions of the aquifer behavior

One of the main objectives of this thesis is to update the already existing 3D MODFLOW groundwater model of the Griftpark with elements discovered during the pumping test, to run some parameter estimation based on pumping tests, and to deepen the investigation of some key parameters or features. Unfortunately, with the tracer test being cancelled, the pumping tests being delayed and running until the end of June, very little time was left to update the model and make some deep modelling analysis of the situation in the Griftpark.

Still, based on the data collected from the pumping tests and the sonic drills descriptions, the location of the clay lenses had to be corrected in the existing 14-layer model of the Griftpark. The defined clay lenses in the model have proven unsuccessfully model groundwater flows in the Griftpark. Therefore, for this new model, homogeneous clay layers along the entire area of the park were considered. The depth of each layer was defined based on the hydraulic head reactions shown during the pumping test

and the referenced depth where clay has been found according to the sonic drills. A 3-layer (1st aquifer, aquitard, and 2nd aquifer) model was also created to evaluate the effectiveness of using a simplified groundwater flow model. For this model, the hydraulic conductivities of the layers forming the 1st aquifer and the aquitard were averaged.

To compare the data collected with the model results, the model has been set up in a transient flow state. This allows to simulate consecutive pumping tests with several periods to simulate a few pumping and recovery phases. The simulations were based on a period when several pumping tests were realized and when weather conditions had only a small effect on the hydraulic heads. Also, several properties needed for a transient flow simulation had to be introduced such as the specific storage and specific yield.

Most initial properties of the models were based on data provided in the Woessner and Poeter book on Hydrogeologic properties of Earth Materials and Principles of Groundwater flow (2020). The models are also based on each layer composition described during sonic drilling. Appendix F contains the tables used to estimate the effective porosity (n_e), specific yield (*Sy*), and earth materials compressibility. Then, the specific storage [1/m] has been computed with the following equation:

$$S_s = \rho g\ (\alpha + n_e \beta) \qquad 3.9$$

Where ρ is the water density [kg/m³], g is the gravitational acceleration [m/s²], α is the aquifer material compressibility [m²/N], and β is the water compressibility [m²/N]. For each layer, the solution of equation 3.9 has been rounded to 0.0001 m^{-1}.

The initial horizontal hydraulic conductivity (*Kh*) values for each layer were based on Appendix F, Table 15, and past studies on the Griftpark subsurface. The selected values for each layer are shown on Table 3 for the 14-layer model and Table 4 for the 3-layer model. For the vertical hydraulic conductivity (*Kv*) values, an anisotropy ratio of 3 was used. A horizontal flow barrier has been placed in the model to simulate the bentonite wall around the Griftpark. Its effect on groundwater flow is defined as the barrier hydraulic conductivity over its thickness. For both models, it was considered equal to 0.006 day^{-1}.

In addition to comparing the 3 different model results (14-layer model, 3-layer model, and 3-layer set with the analytical solution) with the observed data, a small sensitivity analysis of several properties was done. For the sensitivity analysis, the 3-layer model was used to evaluate the effect of the 1st aquifer hydraulic conductivity, the aquitard hydraulic conductivity, and the barrier hydraulic conductivity/thickness on the hydraulic heads of well BU1. For each property, four different values were tested with values higher and lower than the initially used value in the previous 3-layer model. The objective is to determine which properties need further investigation.

A summary of the 14-layer model properties can be seen in Table 3, of the 3-layer model properties on Table 4, and of the 3-layer model properties incorporating the analytical solution in Table 5. The property values tested during the sensitivity analysis can also be seen in Table 6.

Table 3: *14-layer model properties*

Layer No.	Top (m - NAP)	Bottom (m - NAP)	Composition	Kh (m/day)	Kv (m/day)	n_e (-)	Ss (1/m)	Sy (-)
1	2	-5	Moderately fine sand	20	6	0,30	0,0001	0,30
2	-5	-12	Coarse sand	65	19,5	0,30	0,0001	0,30
3	-12	-30	Coarse sand	40	12	0,30	0,0001	0,30
4	-30	-37	Coarse sand	40	12	0,30	0,0001	0,30
5	-37	-41	Medium fine sand	15	4,5	0,25	0,0001	0,25
6	-41	-43	Medium fine sand	15	4,5	0,25	0,0001	0,25
7	-43	-45	Clay, moderately sandy	0,5	0,15	0,20	0,0001	0,20
8	-45	-46	Very fine sand	3	0,9	0,25	0,0001	0,25
9	-46	-49	Very fine and moderately fine sand	3	0,9	0,25	0,0001	0,25
10	-49	-51	Moderately fine sand + clay layers (no effect)	3	0,9	0,25	0,0001	0,25
11	-51	-53	Clay layers + fine sand	0,05	0,015	0,10	0,0001	0,10
12	-53	-55	Fine sand	5	1,5	0,25	0,0001	0,25
13	-55	-60	Moderately fine sand + clay	0,5	0,15	0,15	0,0001	0,15
14	-60	-90	Coarse sand	50	15	0,35	0,0001	0,35

Table 4: *Initial 3-layer model properties*

Layer No.	Top (m - NAP)	Bottom (m - NAP)	Kh (m/day)	Kv (m/day)	n_e (-)	Ss (1/m)	Sy (-)
1	2	-45	45	15	0,3	0,0001	0,30
2	-45	-65	10	3	0,15	0,0001	0,15
3	-65	-110	50	17	0,35	0,0001	0,35

Table 5: *3-layer model implementing analytical solution of horizontal hydraulic conductivity*

Layer No.	Top (m - NAP)	Bottom (m - NAP)	Kh (m/day)	Kv (m/day)	n_e (-)	Ss (1/m)	Sy (-)
1	2	-45	13	3,9	0,3	0,0001	0,30
2	-45	-65	0,05	0,015	0,15	0,0001	0,15
3	-65	-110	50	17	0,35	0,0001	0,35

Table 6: *Sensitivity analysis property values*

Models	**Kh (m/day)**	**Kv (m/day)**	**Barrier (1/day)**
3L_1Aquifer_1	**1**	0,3	0,006
3L_1Aquifer_2	**5**	1,5	0,006
3L_1Aquifer_3	**15**	4,5	0,006
3L_1Aquifer_4	**90**	27	0,006
3L_Aquitard_1	0,1	**0,03**	0,006
3L_Aquitard_2	1	**0,3**	0,006
3L_Aquitard_3	3,3	**1**	0,006
3L_Aquitard_4	20	**6**	0,006
3L_Barrier_1	-	-	**0,003**
3L_Barrier_2	-	-	**0,01**
3L_Barrier_3	-	-	**0,03**
3L_Barrier_4	-	-	**0,06**

IV. Results and discussions

In this chapter, firstly the pumping test results will be presented. Subsequently, the analytical solution of the aquifer hydraulic conductivity and storativity will be presented. At last, numerical solutions regarding groundwater flow in the Griftpark will be shown through a 14-layer model and a 3-layer model. These different solutions are then compared to evaluate which model has been so far the most effective in simulating groundwater flows in the Griftpark. However, due to the limited time available for modelling, these modelling results are just preliminary and need to be further developed.

IV.1. Pumping test

The results of the pumping test and their discussions will be presented in 3 steps. First, the recorded continuous data from divers in wells BU1 (1st aquifer), BU3 (aquitard), and BU4 (2nd aquifer) will be presented. Unfortunately, the diver in well B2 (2nd aquifer) did not register any data. Then, hydraulic head profiles through depth will be presented. Hydraulic head measurements were taken one or two weeks after switching pump B20 on or off. Finally, hydraulic head measurements from two sides of the Griftpark bentonite wall, at wells DV11 and DV12, will be presented.

IV.1.1. Continuous data

As explained in the methodology, the Griftpark 1st aquifer was monitored since mid-February through BU1, whereas the aquitard and 2nd aquifer were monitored from April through wells BU3 and BU4. Therefore, we will first look into the recorded hydraulic head variations of the 1st aquifer before looking at the aquitard and 2nd aquifer hydraulic heads. During this process, the impact of precipitation and atmospheric pressure variations on the hydraulic heads will also be evaluated.

IV.1.1.1. First aquifer

Figure 12.a shows the hydraulic head variations taken by the diver in well BU1 during the entire duration of the pumping test. The cumulative precipitation surplus is also displayed to verify the effect of groundwater recharge on the aquifer hydraulic heads. Precipitation will cause an increase of the cumulative precipitation surplus whereas evapotranspiration will cause a decrease.

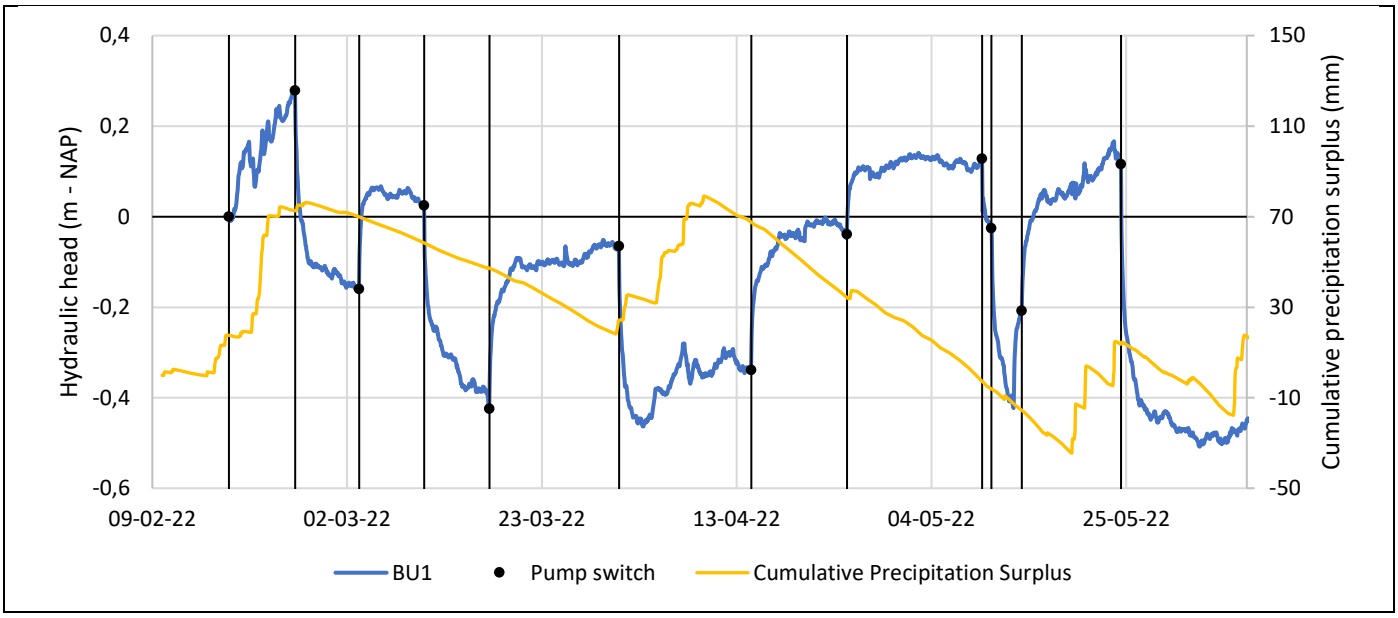

Figure 12.a: *Hydraulic head variations and cumulative precipitation surplus in the 1st aquifer of the Griftpark during the pumping test between February to June 2022.*

Periods when pump B20 pumping rate was set at 10 m³/h show a sharp decrease of the 1st aquifer hydraulic head until stabilizing. On the contrary, when the pump is switch off, we can see a sharp increase of the 1st aquifer hydraulic head until stabilizing. The same observation can be made when all three pumps are shut down or switched on at the same time in May and June. For a better understanding on when does the pumps are working or shut down, Figure 12.b is available in a larger format in Appendix G. The Figure has also been split into Figure 13.a and Figure 13.b showing the hydraulic head variations during the pumping test from February to March, and from March to June respectively.

IV.1.1.1.1. February – March pumping tests

From mid-February to mid-March a pumping test was performed during which pump B20 was weekly switched on and off. Figure 13.a shows the hydraulic head variations of the 1st aquifer of the Griftpark and the cumulative precipitation surplus from mid-February to March. From this figure, the reaction of the hydraulic head in the 1st aquifer to precipitation can be clearly seen. During the 1st week of the pumping test, where pump B20 has been turned off for a few days already, we can see several rises and drops of the hydraulic head of well BU1. They were caused by a storm during which more than 80mm of rain fell over 10 days. With the pump turned off for a few days, the hydraulic head of well BU1 is supposed to be quite stable as it can be seen in early March (04/03 – 10/03) and at the end of March (20/03 – 25/03).

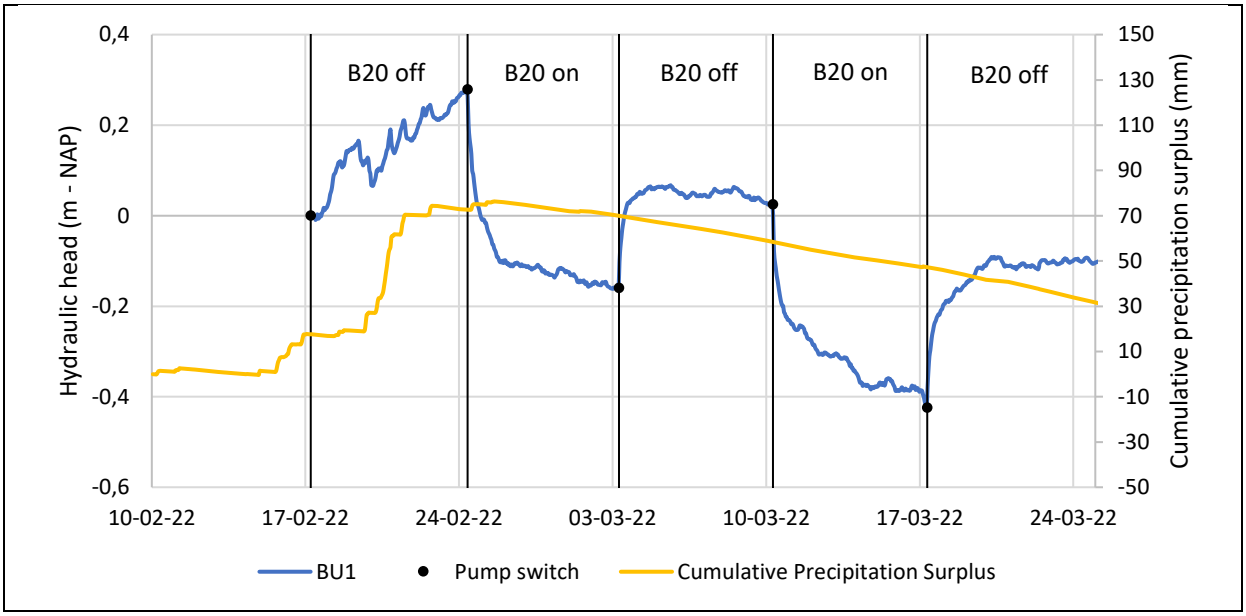

Figure 13.a: *Hydraulic head variations and cumulative precipitation surplus in the 1st aquifer of the Griftpark between February to March 2022.*

When pump B20 is switched on, hydraulic head in the 1st aquifer responds very fast and sharply decrease for a day until slowing down. However, it does not seem to be reaching an equilibrium after 7 days given that the hydraulic heads continue to decrease when the pump is switch off. This decrease in hydraulic head seems to follow an exponential decay even though it can be sometimes hard to see due to external factors. This can be seen when comparing the 2nd and 4th weeks of testing. The 2nd week of the pumping test show a trend almost exponential but is probably still influenced by the huge amount of rain fallen a few days earlier. The 4th week of the pumping test, which was impacted by precipitation, suggest an exponential decay trend.

When pump B20 is switch off, which can also be called a recovery test, the aquifer recovers very sharply from the provoked drawdown until settling. In this case, the hydraulic head of well BU1 seems to reach an equilibrium after 3-4 days. As opposed to when pump B20 is working, the rise of hydraulic head seems to follow an exponential decay upward trend.

These two trends are expected from early pumping and recovery tests of confined or unconfined aquifers. However, these two types of aquifer have a different behavior in the late stages of pumping tests. In a confined aquifer, the drawdown follows an exponential trend and reaches an equilibrium after some time. In unconfined aquifers, the drawdown also follows an exponential trend but, after appearing to reach an equilibrium thanks to surrounding recharge, increases again with an exponential trend. This behavior can be seen in Figure 14 which shows log-log plots of the theoretical time-drawdown relationship for confined aquifer (Fig. 14.A) and unconfined aquifer (Fig. 14.B). Unfortunately, because these pumping tests were not long enough to clearly define when the Griftpark 1st aquifer has reached an equilibrium, it is hard to evaluate if the aquifer is behaving more as a confined or unconfined aquifer. This could help understanding further reactions.

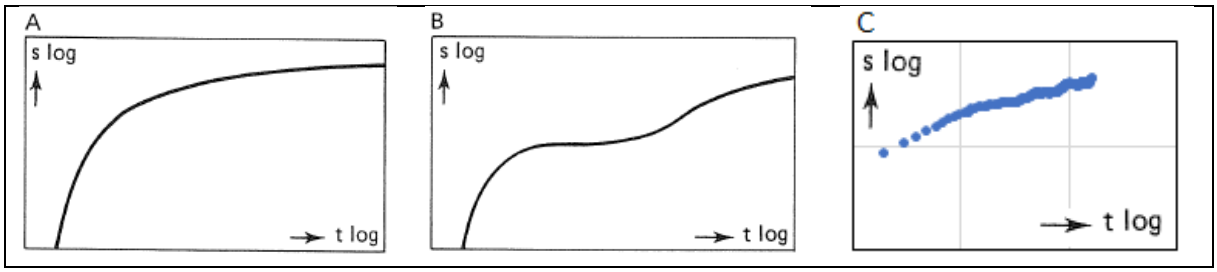

Figure 14: *Theoretical time-drawdown relationships during pumping tests for confined (A) and unconfined aquifers (B) compared with the real time-drawdown relationship from early March pumping test (10/03-17/03; C) (Kruseman et al., 1994).*

The effect of daily evapotranspiration can also be seen in Figure 13.a with very short rises and drops in hydraulic heads. One could think that the cumulative effect of evapotranspiration is responsible for continuous decrease of hydraulic head when pump B20 is on. The effect of evapotranspiration is also combined with the effect of pumping during this period. This would mean that the 1st aquifer has indeed reached an equilibrium. However, since the aquifer does not seem to have difficulties to reach and stay at equilibrium when affected by evapotranspiration and when pump B20 is off, the previous hypothesis is probably false. The ability of the aquifer to recover from hydraulic head changes seems bigger than the effect of evapotranspiration. This should be also true when the is on and thus the continuous decrease of the hydraulic head when the pump is caused by the pumping, meaning the aquifer has not reached an equilibrium yet. The aquifer seems to also recover faster from hydraulic head changes caused by evapotranspiration than precipitation. This means evapotranspiration has probably a low mid-term impact on the aquifer hydraulic heads, especially compared to precipitation.

One can also notice that between the two periods where pump B20 is off and the aquifer has reached equilibrium, the hydraulic head at which equilibrium is reached has decreased. If the negative precipitation surplus would be responsible for this lower hydraulic head equilibrium, it should also progressively decrease the hydraulic heads while the aquifer stays at equilibrium (i.e. when pump B20 stays off). However, we do not see a continuous decrease of the hydraulic head when pump B20 is off. This proves that with these pumping rates (3.5, 4.5, and 10 m^3/h = 17.5 m^3/h), the 1st aquifer of the Griftpark loses more water through the pumps than it gains through leakages from the surrounding aquifers.

IV.1.1.1.2. Mid-March to June pumping tests

From mid-March to June, the aim was to switch pump B20 on and off every 2 weeks. However, during this period all three pumps shut down two times due to pump failures. Although this disrupted the original plans, it gave the opportunity to study the effects of pumps B21 and B22 on the hydraulic heads at B, B2, DV11 and DV12. Furthermore, rainfall in early April also interfered with the pumping test, which was key to understand the aquifer behavior. Figure 13.b shows the hydraulic head variations measured in well BU1 during this period.

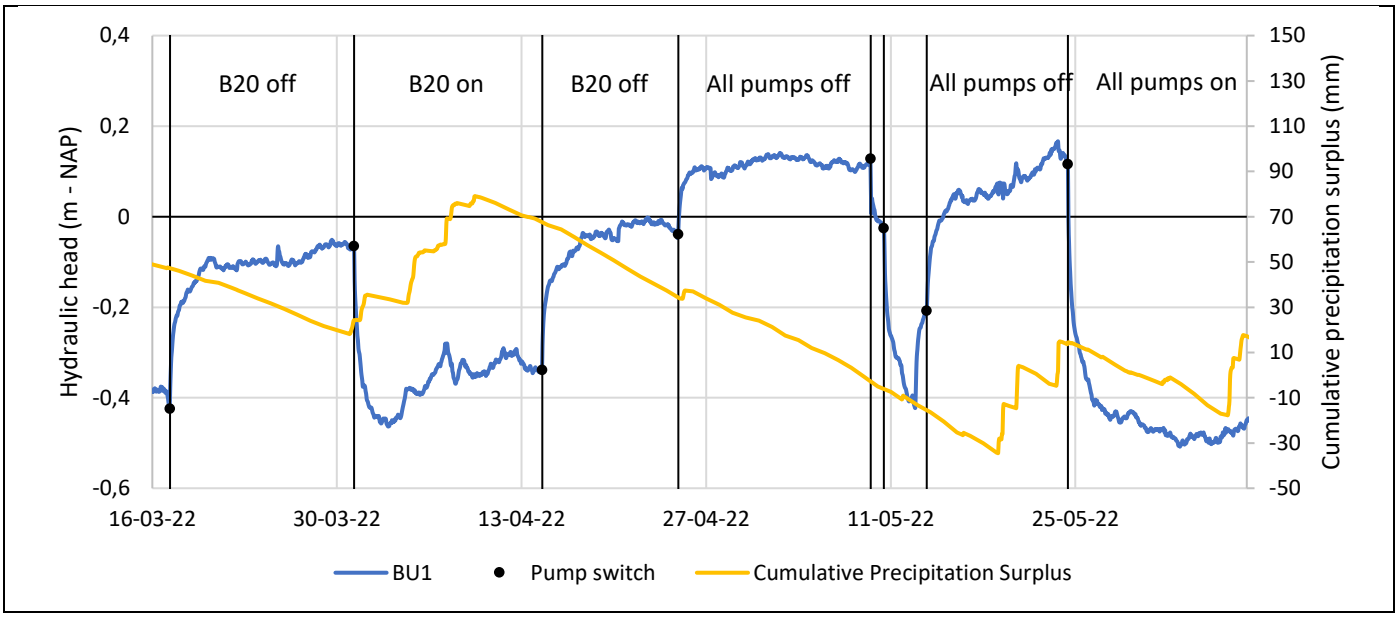

Figure 13.b: *Hydraulic head variations and cumulative precipitation surplus in the 1st aquifer of the Griftpark between mid-March to June 2022.*

Regarding the hydraulic head behavior during the recovery phases with a longer timeline, Figure 13.b does not show any new developing processes compared to Figure 13.a. The early April pumping test did not either show the intended objective of reaching an aquifer equilibrium due to precipitation. However, these precipitation do confirm that precipitation increase the aquifer hydraulic head equilibrium as it can be seen from Figure 13.b first two periods with pump B20 off (17/03 - 31/03 and 14/04 - 24/04). Without any precipitation, the aquifer would have lost more water than it gained through leakages.

The last period of Figure 13.b does show a clear exponential decay trend of hydraulic head during the test and the aquifer seems to be reaching equilibrium within 10 days. This trend seems to indicate that this bounded aquifer behaves as a confined aquifer. A longer than two weeks timeline without precipitation would be needed to confirm the absence of the second slump of drawdown expected for unconfined aquifers during a pumping test (Figure 14.B).

During late April's recovery test (14/04 – 24/04) during which the 1st aquifer had reached an equilibrium, pumps B21 and B22 had to be switched off. As a result, the hydraulic head of well BU1 sharply increased before slowing down, as when pump B20 is switched off. This rise of BU1 hydraulic head demonstrates that the surrounding of pump B20 are indeed affected by pumps B21 and B22 even though they are more than 100m away.

IV.1.1.2. First aquifer, aquitard, and second aquifer

Figure 15.a shows the hydraulic head measurements from the divers placed in wells BU1, BU3 and BU4, which correspond to the 1st aquifer, the aquitard, and the 2nd aquifer respectively. The figure can be seen in a larger format in Appendix G, Figure 15.b. It is important to remember that the aquitard in this case is not formed by a continuous layer but by several clay lenses whose cumulative effect on groundwater flow is still unknown.

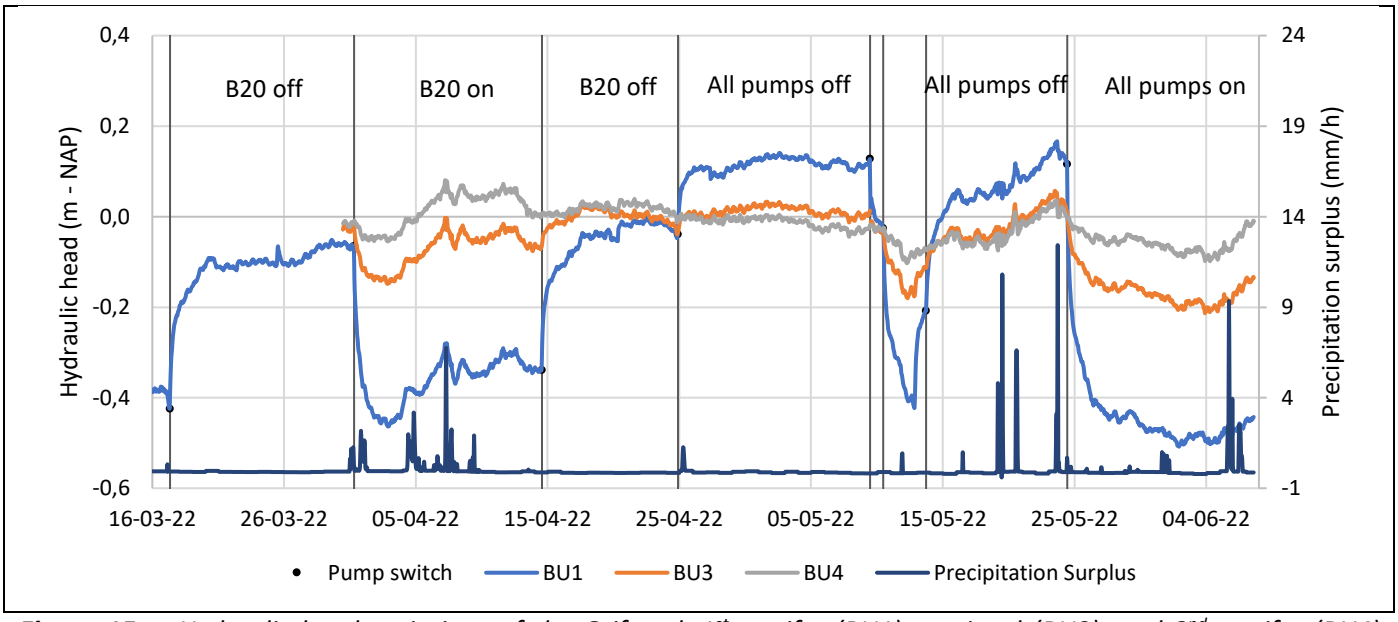

Figure 15.a: *Hydraulic head variations of the Griftpark 1st aquifer (BU1), aquitard (BU3), and 2nd aquifer (BU4) between April and June 2022.*

Early April's pumping test shows that the hydraulic head of the 1st aquifer of the Griftpark measured by well BU1 is greatly affected by pump B20, the hydraulic head in the aquitard measured by well BU3 is mildly affected, and the hydraulic head in the 2nd aquifer measured by well BU4 is barely affected. The following two recovery phases, pump B20 off and all three pumps off, the hydraulic head of the first aquifer is again greatly affected, of BU3 is mildly affected, and of the 2nd aquifer it does not seem affected at all.

This pattern behavior can also be seen in June's pumping test when the hydraulic head of the 1st aquifer is greatly affected, of the aquitard is mildly affected, and of the 2nd aquifer is lightly but clearly affected. This proves that the 1st and 2nd aquifers are connected, but not as much as it was anticipated in previous studies (Grondmechanica Delft, 1988). The presence of clay lenses prevents groundwater to flow easily between the two aquifers, making the hydraulic connection weak.

From Figure 15.a, we can also see that the hydraulic head of the aquitard almost matched the 2nd aquifer hydraulic head when recovering from pumping. This is clear in the two periods when all three pumps were off in late April (24/04 – 09/05) and mid-May (14/05 – 24/05), indicating that at 53-54m bgl (equivalent to 50-51m NAP) the aquitard is more connected to the 2nd than to the 1st aquifer. This means that most of the confining clay lenses, or the most effective confining clay lens, lies above the screen of well BU3.

Given that the 2nd aquifer hydraulic heads at location B were only weakly affected by the pumping test, the 1st aquifer nearby pump B20 is probably barely connected locally. However, as can be seen in Figure 15.a, the three sections of the subsurface are similarly affected by the pressure variation caused by precipitation and atmospheric pressure variations, which is a clear indication that all three sections are hydraulically connected regionally. We will analyze these effects in the section below.

IV.1.1.3. Precipitations and atmospheric pressure variations impact on hydraulic heads

Figure 16 shows the hydraulic head in wells BU1, BU3 and BU4, together with the precipitation surplus during early April's pumping test (03/04 – 11/04). As the pump was working during the depicted period, it would be expected that the hydraulic heads would decrease until reaching an equilibrium. However, as the aquifer is replenished due to precipitation, the water table rises.

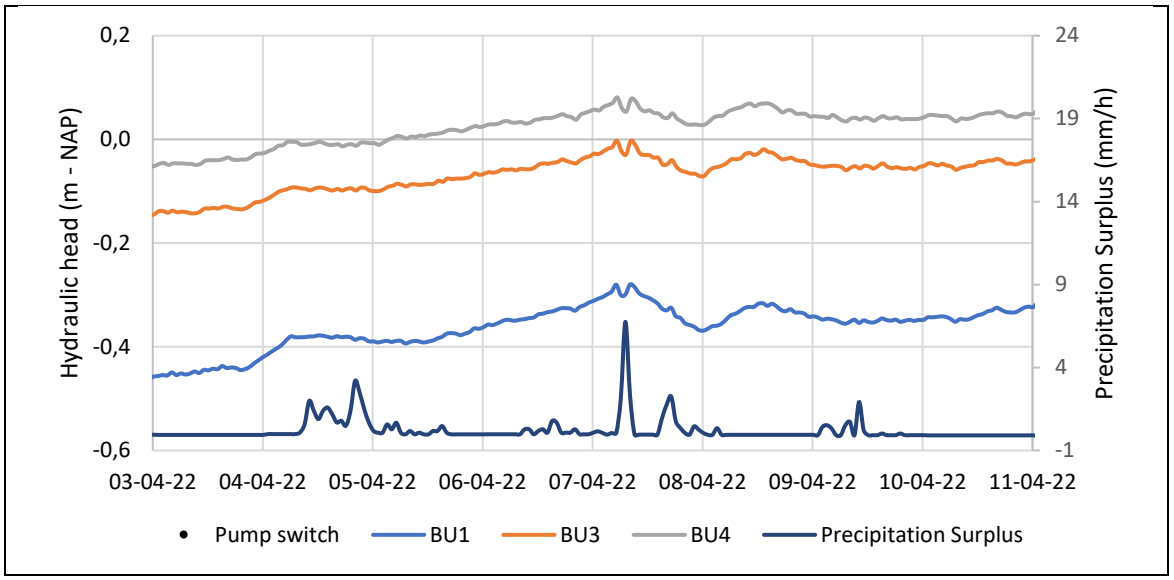

Figure 16: *Effect of precipitation on the hydraulic heads of wells BU1, BU3, and BU4 during early April's pumping test (31/03 – 14/04) where pump B20 was working.*

There is a delay between the time of precipitation and the rise of the water table. The added water still needs to infiltrate the porous media and reach the water table, a process which can take some time. This is clearly seen in Figure 16 where the hydraulic heads in the three wells increase during evening of the 3rd of April while it has not rained for at least a day. It can only mean the hydraulic heads rises are caused by previous precipitations or atmospheric pressure variations. It is to be noted that the precipitation data has been taken from De Bilt station of the KNMI located 3.5 km away from the Griftpark. The exact time at which precipitation have fallen on the Griftpark is thus unknown but this one should be quite close to the times from De Bilt station, probably with times within the same hour.

In this case, it seems like the precipitation of the 4th of June caused the hydraulic head peaks of the 7th of June. This means precipitation seems to take two to three days to reach the water table. This time can fluctuate depending on the height of the water table, the saturation state of the porous media, and the hydraulic conductivity of this last one. The higher the water table, the more saturated the porous media, and the bigger the hydraulic conductivity, the faster precipitation will reach the water table.

Precipitation is not the only cause of hydraulic head fluctuations. Changes in atmospheric pressure also generate fluctuations in hydraulic heads. To evaluate the effect of this fluctuation, the barometric efficiency of the 1st aquifer has been computed based on several periods of BU1 hydraulic head measurements. The barometric efficiency was based on periods when no precipitation was recorded and the aquifer was at equilibrium. Figure 17 shows the barometric efficiency computed with 26th of June to 9th of May hydraulic heads registered in BU1.

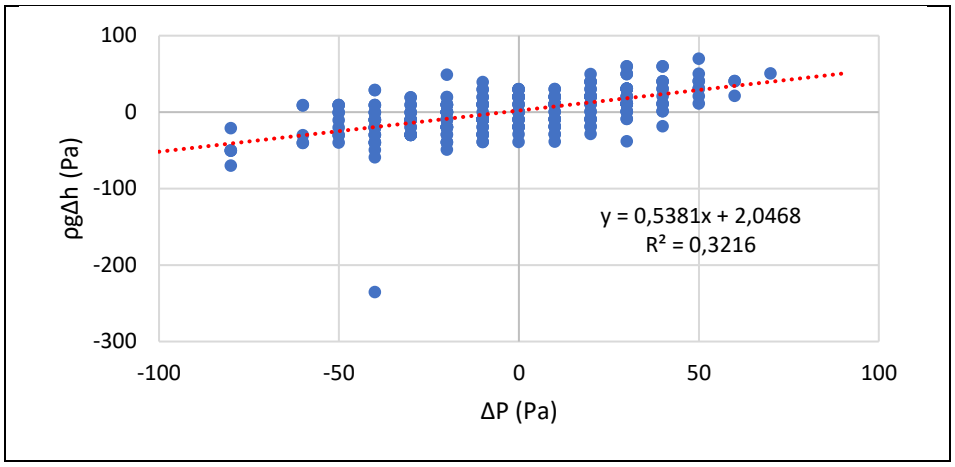

Figure 17: *Barometric efficiency of the Griftpark 1st aquifer*

According to equation 3.3 and Figure 17 data, the barometric efficiency (BE) of the 1st aquifer in the Griftpark is around 0.5381. Other periods had a barometric efficiency between 0.45 and 0.55. This indicates that the load generated by atmospheric pressure changes is taken almost half by the pore water, and the other half by the aquifer material (Chowdhury, 2020).

Typically, the Barometric Efficiency of aquifers range from 0.2 to 0.7 (Todd 1980), meaning the found values of BE seem reasonable. However, in our case, the coefficient of determination R^2 is quite low for all the periods where it was computed, around 0.3. This might be due to the lack of precision of the atmospheric pressure measurement collected from KMNI database which have a precision of 10 Pascals. This low value of R^2 raises some accuracy concern on the determination of the barometric efficiency.

To evaluate the impact of the atmospheric pressure fluctuations, the hydraulic head changes due to the atmospheric pressure variations alone (Δh_p) has been computed considering a barometric efficiency of 0.5. To account to possible inaccuracy of the barometric efficiency compute, Δh_p has also been computed with a barometric efficiency of 0, meaning the groundwater in the porous media takes the entirety of impact of the atmospheric pressure changes. The impact of these fluctuations are shown on Table 7.

Table 7: *Atmospheric pressure fluctuations impact on Griftpark 1st aquifer hourly hydraulic heads*

Barometric Efficiency	Mean (cm)	St dev (cm)	Increase (cm)	Decrease (cm)	5% percentile	95% percentile
0	-0,0026	0,5340	2,551	-3,571	-0,8163	0,8162
0,5	-0,0013	0,2670	1,275	-1,786	-0,4081	0,4081

The mean hourly impact of the atmospheric fluctuations on the 1st aquifer hydraulic head is less than a millimeter. If the utmost barometric efficiency is considered (BE = 0), 90% of the 2643 hydraulic head measurements in BU1 have been impacted by less than 8.2mm. The biggest impact possibly caused on the hydraulic heads is a drop of 3.5cm. As such, compared to the impact of pumping on the 1st aquifer hydraulic heads which range between 30cm and 50cm (Figure 12.a or 12.b), the impact of atmospheric pressure fluctuations are negligeable.

According to Table 7, the maximum increase of hydraulic head caused by hourly atmospheric pressure fluctuations is lower than the maximum decrease. The effects are probably similar but a drop in atmospheric pressure, which would lead to an increase of the hydraulic head in BU1, often comes along with precipitation. As we have previously seen, precipitation takes some time to reach the water table but, if it rains for a while, it will increase the hydraulic head in the well and buffer the effect of

an atmospheric pressure drop. Atmospheric pressure rise does not come with the same effect because it often comes along with good weather.

A point to take in consideration when looking at these results is that it might take a bit more than 1h for the aquifer to account the atmospheric pressure changes. Therefore, the impact might be slightly different than presented in Table 7 even though in a similar order of magnitude. However, when comparing to the impact of precipitation on the hydraulic heads, the impact of the atmospheric pressure fluctuation is much lower than the ones caused by precipitation. When looking at Figure 16 or 15, we can see that precipitation can easily produce a rise of hydraulic heads of the order of 5 to 15 centimeters. This impact of precipitations cannot be neglected when studying the impact of pumping on the 1st aquifer hydraulic head.

IV.1.2. Hydraulic head profiles

With the three MLS wells at location B and two MLS wells at B2, both in the vicinity of pumping well B20, hydraulic head profiles were recorded throughout depths between 7 and 65 meters below ground level during the pump and recovery tests. These profiles offer more detailed information in groundwater flow and the heterogeneity of the subsurface than the three diver datasets from location B. In addition, hydraulic head profiles from location B and B2, separated by 60 meters, could be compared. This would determine if location B is representative of the surroundings of pump B20.

Hydraulic head profiles with only pump B20 off as well as with all three pumps off will be first presented. Then, the hydraulic head profiles with all pumps on will be presented .Finally, a comparison of location B and B2 profiles will be shown.

IV.1.2.1. Pump B20 off

With pump B20 off, if the 1st and 2nd aquifer would be hydraulically disconnected, we should expect straight hydraulic head sections with different values for each aquifer given that there is no vertical groundwater flow. It is possible that both aquifers have the same hydraulic head value without being connected, but this would be a rare case. If the two aquifers are connected, we should expect a hydraulic gradient between these two or a straight hydraulic head profile if the two aquifers have reached an equilibrium.

Figure 18 presents the hydraulic head profiles from location B and location B2 measured after each pumping test. The x-axis shows the measured hydraulic head, and the y-axis shows the well screen average depth below the Amsterdam Ordnance Datum (m – NAP). The profiles, which were recorded at different times, do not show the same hydraulic heads values due to natural fluctuations in precipitation, evapotranspiration, or atmospheric pressures. Precipitation events, which we have seen greatly influence the aquifers' hydraulic heads, have been registered in mid-February (15th to 20th of February), at the beginning of April (31 of March to 10th of April), and in mid-May (19th to 24th of May), as shown on Figure 12.a. As such, the idea is not only to directly compare the hydraulic heads values of each profile, but to identify the shared trends between these profiles.

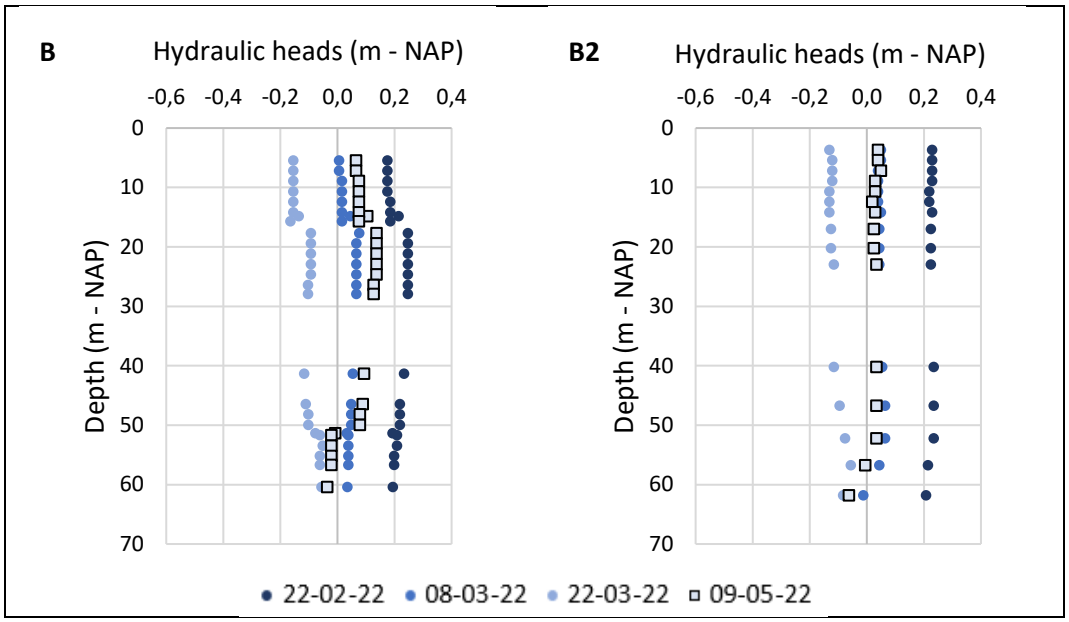

Figure 18: *Hydraulic head profiles at location B (left) and B2 (right) with pump B20 off.*

- Measurements taken 5-6 days after pump B20 was switched off or on
- Measurements taken 13 days after all three pumps were switched off

When looking at profiles from location B in Figure 18, we can notice that the first eight points, taken from wells BMLS1 and BU1, show the same value. The following seven points, taken from BMLS2 wells, show also the same hydraulic head value as each other, but higher than the value of the eight points above. This change in water level at 16-17m-NAP suggests that an obstacle is impeding groundwater flow vertically, forcing it to go around and increasing the fluid pressure. However, the obstacle only affects groundwater flow locally, as the hydraulic difference is always the same. If the obstacle would act as a confining layer, the hydraulic head in the wells above and below would not respond to precipitation in the same manner. In contrast, another obstacle impeding groundwater flow at 51m deep is seen in Figure 18. This obstacle affects groundwater flow at a bigger scale than the one at 16-17m NAP as it seems to confine the porous media below. As a result, the hydraulic difference before and after this confining layer is always different. The upper and lower sections of this confining layer in the porous media respond differently to groundwater recharge (i.e. precipitation). The reaction caused by the layer at 51m NAP will be further developed later. Another possibility that needs to be taken into account for small hydraulic jump at 16-17m-NAP but that considered less probable is that there might be a mistake in the alignment of wells BMLS1 and BMLS2, causing a small hydraulic difference between the wells.

The obstacle at 16-17m NAP is believed to be some remaining of DNAPL that has been retained by the porous media, forming a small impermeable lens obstructing vertical groundwater flow. According to the drilling description of well B (Appendix C), a weak smell of carbolineum was detected, which could indicate the presence of residuals of coal tar, as DNAPLs penetrate the groundwater zone because of their higher density compared to water. Some local physical conditions such as compaction or specific grain sizes might have increased the capillary forces of the porous media at this depth which could facilitate the retention of residual DNAPL.

From Figure 18 it can be seen that although the section between 17-51m-NAP has the same hydraulic head trend at the different dates, the hydraulic heads between 51-60m-NAP respond differently. This deeper section has at times lower (09/05), higher (22/03), or almost identical (22/02 and 08/03) hydraulic head values compared the 17-51m sections. Small hydraulic jumps mark the presence of another obstacle impeding vertical groundwater flow. In this case, the hydraulic jumps, especially the

one at 51m NAP, mark the presence of clay layers or lenses. The impact of the clay layers or lenses at 51m on vertical groundwater flows is much more significant than the NAPL lens at 16-17m-NAP given that the sections above and below these layers are not identically affected by precipitation. This explains why this deeper section (51-60m-NAP), which includes the 2nd aquifer, has sometimes a different hydraulic head value than the 1st aquifer. The biggest hydraulic jump at 51m depth can be observed when all three pumps were switched off and the measurements taken 13 days after the pump switch. According to the drilling descriptions, other clay layers have been identified at 44m, 48m, and 57m NAP in location B, but their effect on the groundwater hydraulic heads cannot be seen in Figure 18. A forced hydraulic head gradient caused by pumping might help to determine their effect.

It is to be noted that values collected from observation wells have slightly different hydraulic heads than the ones collected from MLS wells. This is mainly due to the longer screens of the observations wells compared to the MLS wells and because the average screen depth was taken for the hydraulic head profiles. As a result, the depth of well BU1 in Figure 18 was set at 14.8m-NAP, in between the depth considered for wells BMLS1U6 (14.2m-NAP) and BMLS1U7 (15.7m-NAP). In reality, the screen of well BU1 is so long (2m, 13.8-15.8m-NAP) that it also takes into account the depths of wells BMLS1U6 (14.1-14.3m-NAP) and BMLS1U7 (15.6-15.8m-NAP).

When looking at B2 hydraulic head profiles in Figure 18, the trend is similar as at location B, but with some slight differences. First, we do not see any hydraulic jump at 16-17m in all four profiles. There is a lower resolution to find potential vertical groundwater flow obstacles due to the lower number of wells in the deeper sections of the aquifer. This prevents us from evaluating whether there is also a hydraulic jump between 52-62m at B2. The fact that the deepest two wells, located in the 2nd aquifer, show a different trend as in the wells above, indicates that clay layers also impede vertical groundwater flow here. From the drilling descriptions of location B2, clay layers have been identified at 41m, 48m, 53m, and 62m NAP. Their effects on the groundwater hydraulic head are hard to see in Figure 18 but will be evaluate later on with a forced hydraulic head gradient.

IV.1.2.2. Pump B20 on

With pump B20 at a pumping rate of 10m³/h, the hydraulically connected upper part of the profiles is expected to show a substantial decrease in hydraulic heads until reaching the clay lenses in the deeper part. These clay lenses have such a low hydraulic conductivity that for most of the groundwater, it will be easier to flow around the lenses through the porous media with a higher hydraulic conductivity, in this case mostly sand, than to flow through them. As such, the clay lenses increase the distance groundwater has to travel to reach pump B20 and thus lower the impact of the pump on their hydraulic heads. The impact of the pump decreases depending on size, thickness, and hydraulic conductivity of the clay lenses. This will be seen through the size of the hydraulic jump they generate.

It is to be noted that, the deeper we look, the bigger the distance is to reach the pump and thus a hydraulic gradient should be seen when looking at a continuous aquifer. However, sudden hydraulic jumps are not the consequence of only increased distance with depth but also increased groundwater travel distance. The groundwater path to reach discharge pumps is not necessarily a straight line due to the presence of obstacles such as clay lenses of confining layers.

Figure 19 presents the hydraulic head profiles at location B and B2 with pump B20 on. From location B profiles, the same hydraulic jump, with the same hydraulic head difference between wells BMLS1U7 and BMLS2U1 can be seen at 16-17m as when pump B20 was off, confirming again the NAPL residuals are only locally impeding vertical groundwater flow. If the NAPL lens would impede regionally vertical groundwater flow, the size of the hydraulic jump would have been affected by the changed pumping conditions. A second small hydraulic jump can be noticed between 41-46m, marking the presence of

the clay lenses at 44m NAP. Finally, a third and significant hydraulic jump can be seen between 51-52m, exactly where the BU3 1m screen is located, explaining why the manual measurement at BU3 is always between BMLS3U3 and BMLS3U4. This means that at location B, clay lenses occur at:

- 44m deep has a small impact on vertical groundwater flows, similar to the NAPL pool at 16-17m.
- 48m deep does not have any impact on vertical groundwater flows.
- 51m deep has a significant impact on vertical groundwater flow, possibly disconnecting the 1st and 2nd aquifer at a medium scale. We have already proved in section IV.1.1 that the aquifer must be connected at a larger scale.
- 57m deep do not have any impact on vertical groundwater flows, or the clay layers just before are so extensive that groundwater past it is not affected anymore by pump B20. As a result, the impact of the clay layer could not be seen.

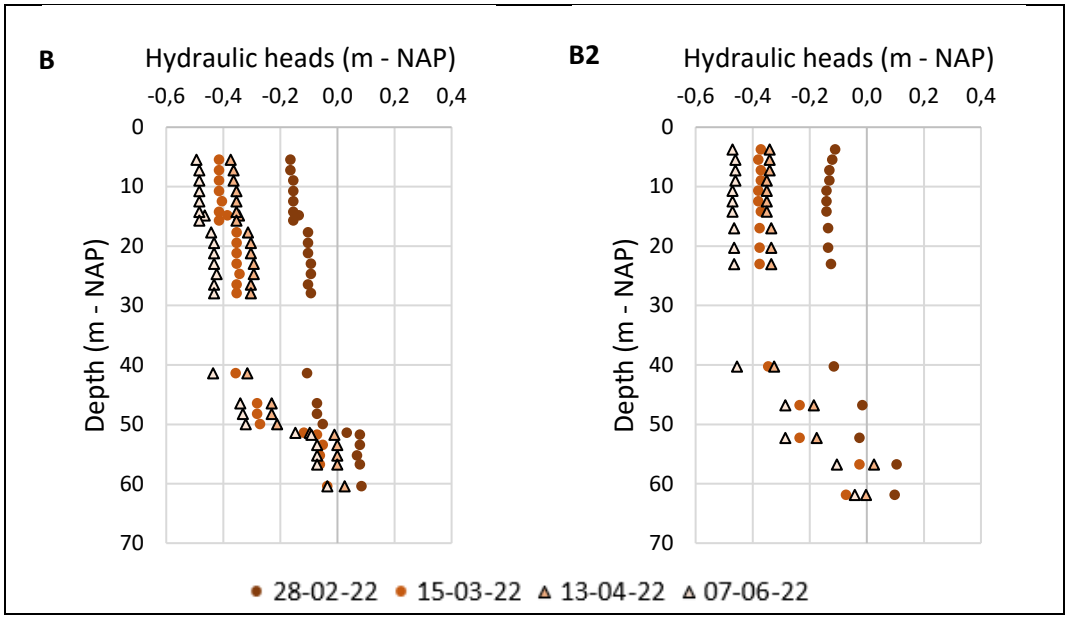

Figure 19: *Hydraulic head profiles of location B (left) and B2 (right) with pump B20 on.*

- Measurements taken 5-6 days after pump B20 was switched off or on

Δ Measurements taken 13 days after pump B20 was switched on

When looking at hydraulic head profiles at location B2 in Figure 19, no hydraulic jump can be seen at 16-17m, and the first 40m have the same hydraulic head value. Then, between 40-46m and 52-57m hydraulic jumps can be seen, the second one more significant than the first one. These hydraulic jumps are the result of the clay layers present at 41m and 53m according to the drillings descriptions. These profiles also indicate that the clay lenses registered at 48m do not affect vertical groundwater flow. Nothing can be said of the clay lenses at 62m given that we do not have a deeper well. . It looks like location B and location B2 respond very similarly to the forced hydraulic gradient generated by pump B20 with slight differences regarding the depth of the clay lenses or the presence of a NAPL lens. Regarding the hydraulic head profiles which measurements were taken 13 days after pump B20 was switched (Figure 19, location B and location B2), no particular difference is noted with the profiles which measurements were taken 5-6 days after the pump switch

IV.1.2.3. Comparing profiles of location B and location B2

To directly compare the hydraulic head reaction to pumping of location B and location B2, hydraulic head profiles of each location have been put together in Figure 20. These profiles come from

measurements taken the 15th of March when pump B20 was off, and the 22nd of March when the pump was on.

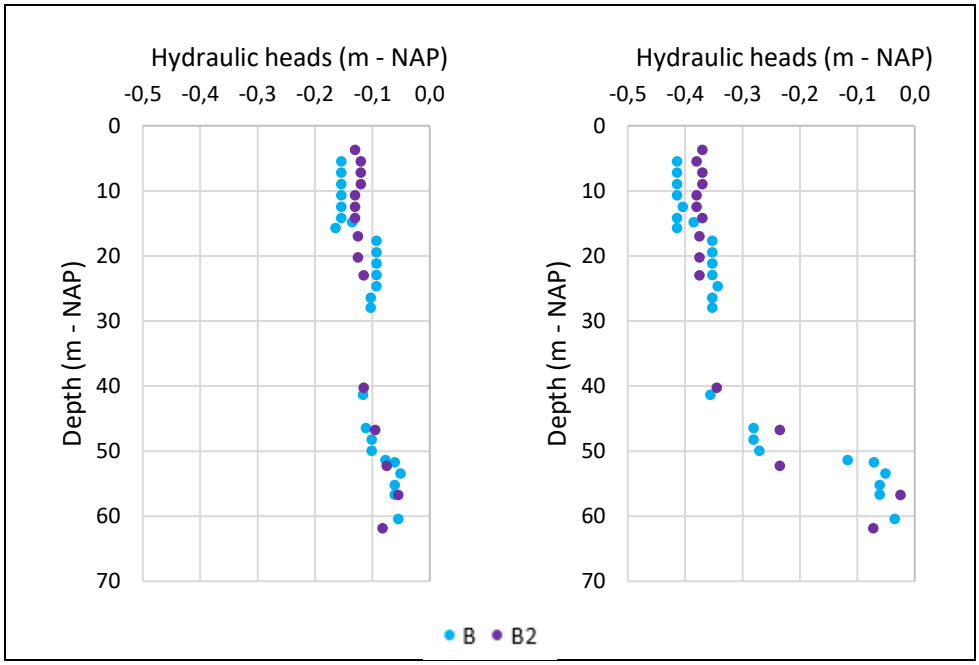

Figure 20: *Hydraulic head profiles of location B and location B2 from the 15th (left, pump B20 off) and 22nd (right, pump B20 on) of March.*

We can easily see in Figure 20, that location B and B2 generate very similar hydraulic head reactions. If location B did not have a NAPL pool at 16-17m NAP, both first 40m sections might behave exactly alike. When reaching the clay lenses below these first 40m, it can be seen that each clay lens positions are not exactly at the same depth and thus cause a slightly different hydraulic head reaction. The difference in depth might be the reflection of large clay lenses connecting both locations and with a slight slope. This does not mean all clay layers are connected, but some might be.

IV.1.3. Barrier data

Hydraulic head measurements have been taken from two wells installed on two sides of the Griftpark bentonite barrier to obtain more information on leakage of groundwater through the barrier. Each well is less than 4 meters away from the barrier. Measurements were taken manually since mid-February and with divers since April. The analysis of manual measurements has the disadvantage to be highly susceptible to the fluctuations of the hydraulic heads (e.g. precipitation, atmospheric pressure changes, pumping). Measurements from divers do not encounter the same problem since the evolution of these fluctuations can be easily followed. Hence, only the diver measurements of wells DV11 and DV12 will be presented in this section.

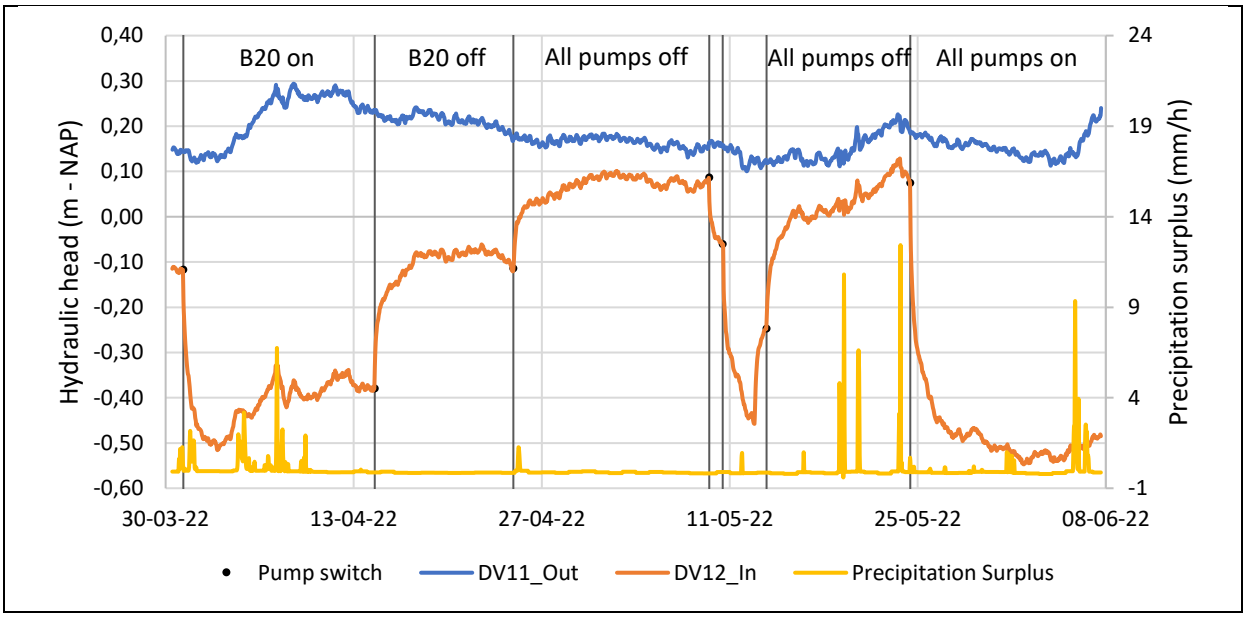

Figure 21: *Hourly hydraulic head measurements from well DV11 (outside of the park barrier) and DV12 (inside of the park barrier) April and June 2022.*

Figure 21 show the hourly hydraulic head variations of wells DV11 and DV12, located respectively outside and inside the park bentonite barrier. Firstly, when comparing Figure 21 and Figure 13.b, it can be seen that the hydraulic head reaction of DV12 during is almost alike BU1 reaction from location B. Both wells are located in the 1st aquifer and inside the Griftpark bentonite barriers. The subsurface at DV12 is presumed to be similar to that at location B given that location B2 has also a very similar layering and is only 20m away from well DV12.

From Figure 21, it can be seen that at well DV11, which is outside of the Griftpark bentonite barriers, the water table is higher than inside the park. Through pumping, a lower hydraulic head inside than out is also established, so that, in case of leakage, contaminants will not spread out of the containment. It can also be seen that the water table at DV11 reacts very differently to the pumping test than at DV12. It appears that the hydraulic head of well DV11 is hardly affected by the pumping and aquifer recovery phases. If there is any effect from the pumping, it is overshadowed by the fluctuations caused by precipitation, to which there does appear to be a reaction.

During the intervals where no precipitation was recorded, it can be seen that the hydraulic heads of DV11 constantly decrease. This constant decrease might be a natural reaction of the 1st aquifer water level following a precipitation event as the aquifer needs to reach a new equilibrium with this groundwater recharge. The constant decrease after precipitation can also be a potential sign of groundwater leakage through the bentonite walls.

IV.2. Analytical solution of the aquifer Transmissivity and Storativity

The data collected from well BU1 from the 10th to 17th of March was selected to estimate analytically with Stallman's method the aquifer transmissivity and storativity. Even though the aquifer has not reached equilibrium yet, this pumping test has the advantage of not being affected by precipitation during the entirety of the test. To simulate the boundary conditions of the Griftpark, 65 imaginary wells have been placed following the configuration shown in Figure 11. The drawdown trend of well BU1 could then be computed using equation 3.5 with values of $W(u_n)$ from Appendix E. Then, three match sections between curves $W(u, r_{r1\rightarrow n})$ versus u and the observed drawdown versus 1/t were found. For each section, the observed drawdown value could be related to a dimensionless drawdown value

($W(u, r_{r1\rightarrow n})$), enabling the estimation of the aquifer storativity (KD) with equation 3.6. The aquifer storativity was then found with equation 3.7. The resulting estimations for each match section can be seen in Table 8. A drawdown versus time plot with each section estimation can also be seen on Figure 22.

Table 8: *Matching sections with observed pumping test data*

Match sections	u	W(u, r²)	s	1/t	t	KD	K_diag	S
	-	-	m	1/h	h	m²/h	m/day	-
1	6,50E-03	6,5	0,196	1,00E-01	10	26,4	12,7	8,74E-03
2	2,00E-03	1,5	0,148	1,67E-01	6	8,1	3,9	4,95E-04
3	2,00E-02	6,0	0,203	8,33E-02	12	23,5	11,3	2,88E-02

Aquifer transmissivities between 8.1 m²/h and 26.4 m²/h were found from the match sections. If an aquifer depth of 50m is presumed, hydraulic conductivities lie between 3.9 m/day and 12.7 m/day. However, considering that BU1 is located 28m away from pump B20 and at a different depth, these computed hydraulic conductivities are probably a mix between vertical and horizontal hydraulic conductivities. This would mean the horizontal hydraulic conductivity is higher than the estimated value and the vertical one is lower than the estimated value. These estimated values of hydraulic conductivities are close to the values expressed by Dinoloket, maybe even slightly higher. Dinoloket BRO REGIS II v2.2 model estimates a horizontal hydraulic conductivity between 2.5-5m/day for the porous media at 5-10m-bgl, between 10-25m/day at 10-20m-bgl, and between 5-10m/day at 20-35m-bgl. If averaged, the model estimates a horizontal hydraulic conductivity between 6.25-12.5m/day for the porous media between 5-35m-bgl. The estimated storativities from these match sections lie between 2.88 $x10^{-2}$ and 4.95 $x10^{-4}$.

When looking at Figure 22 illustrating each match section drawdown solution, we easily see that match sections 1 and 2 overlap part of the observed drawdown. The drawdown computed from match section 1 results overlaps the early points of the observed data (t = 1→10) whereas the drawdown computed from match section 2 overlaps the late points (t = 50→200). Stallman indicates in his publication that the determination of the aquifer transmissibility and storage should be based on the early drawdown data (Ferris et al., 1962). In the later stage of the pumping test, the measured drawdowns reflect the net effect of the pumped well but also the effects caused by the boundary conditions. This complicates the analysis of the aquifer transmissibility and storativity. As such, match section 1 seems to be the best estimation for the 1st aquifer transmissivity and storativity, meaning the average horizontal hydraulic conduct of the 1st aquifer is closer to 12.7m/day than 11.3m/day.

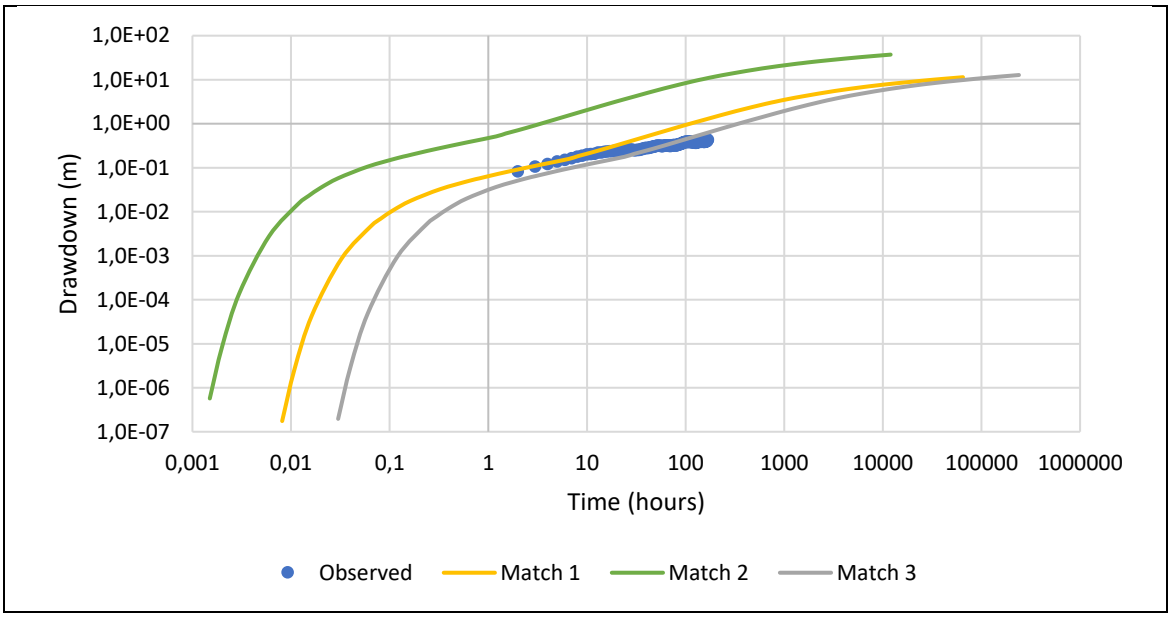

Figure 22: *Analytical solutions of the Griftpark 1st aquifer drawdown during a pumping test.*

We can also notice from Figure 22 that the observed drawdown data from BU1 does not follow the expected trend of unconfined aquifers. We do not observe a second increase in drawdown, which are generally seen from unconfined aquifer pumping tests. As previously mentioned, a longer dataset might be needed to fully confirm this trend.

It is to be noted from Figure 22 that no drawdown can be compute at t = 0 as a hydraulic head reference is needed to compute the drawdown. Also, in this case, at t = 1h, the drawdown observed was equal to 0. In case more pumping test would be performed in the future, measuring very early drawdowns (i.e. seconds and minutes) would be greatly beneficial to the analysis of the pumping test results.

IV.3. Numerical solutions for groundwater flows

Three 3D groundwater models were created to simulate the complex groundwater flows below the Griftpark. A 14-layer model offering a detailed projection of the subsurface layering (Table 3), a 3-layer model only includes the 1st and 2nd aquifer and aquitard with averaged conductivities, and a 3-layer model with the analytically found hydraulic conductivity. In order to accurately model groundwater flows, models need to be calibrated with real data. Unfortunately, with the limited time available, a full calibration of two models based on the collected data during the pumping tests could not be done. Still, basic testing and comparisons were performed to understand the challenges and limitations of creating a groundwater flow model for the Griftpark.

IV.3.1. Models simulations

Figure 23 illustrates the projected hydraulic heads of well BU1 obtained with the 14-layer model, the 3-layer model, and the 3-layer model incorporating the previously obtained analytical solution of the aquifer hydraulic conductivity. As mentioned before, this last solution of hydraulic conductivity is probably a little underestimated because it represents a diagonal hydraulic conductivity. The three projections are compared with the observed hydraulic heads in well BU1 during pumping tests. The hydraulic head measured between February 24th to March 17th have been used as a point of comparison for the models. This period was selected because of the low impact from external fluctuations and because it included two consecutive pumping and recovery phases.

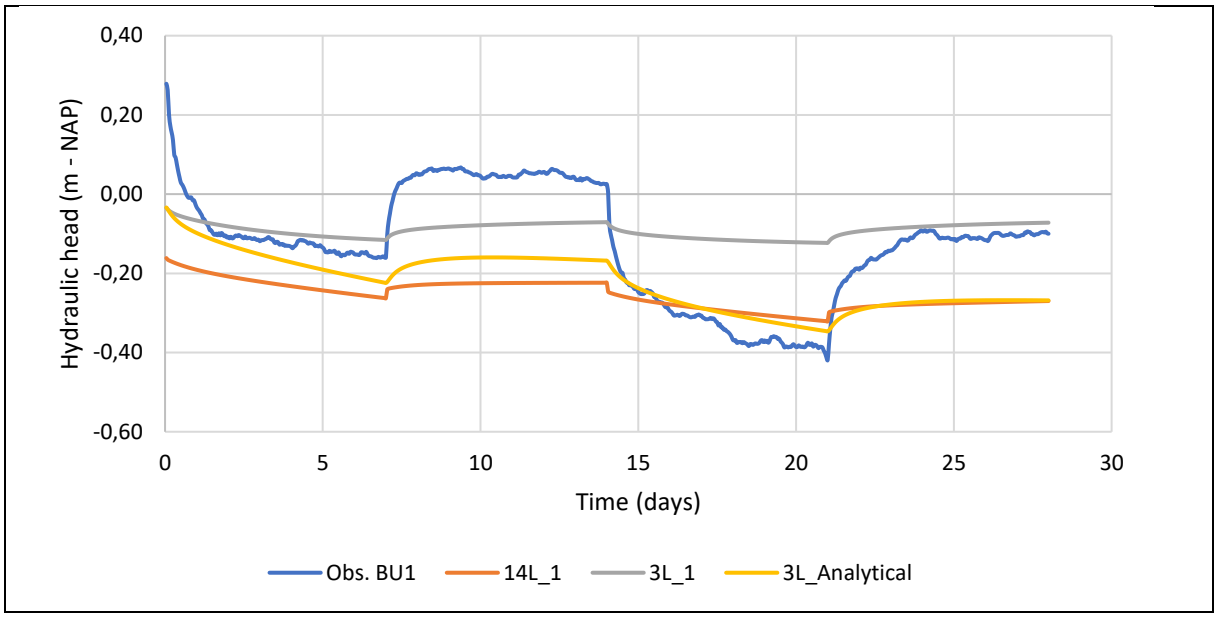

Figure 23: *Numerical solution of the Griftpark 1st aquifer drawdown from a 14-layer model, 3-layer model, and 3-layer model incorporating IV.2 analytical solution during several pumping tests.*

We can notice that none of the models simulation match the observed data. They do not come close in matching the drawdown generated by the pumping phases, or the water table rise from the recovery phases. Yet, insightful information can be deduced from each model. The original 3-layer model projects only little reaction of the hydraulic heads. The aquifer recovers groundwater almost as fast as it is extracted through pump B20. This is due to the elevated hydraulic conductivities values used for the 1st aquifer (Kh = 45m/day, Kv = 15m/day) and aquitard (Kh = 10m/day, Kv = 3m/day). As a point of comparison, the horizontal hydraulic conductivity is more than 3 times higher than what Dinoloket model estimates (6.25-12.5m/day for 5-35m-bgl). As a result of this overestimation, groundwater from the 2nd aquifer can easily flow through the aquitard and balance the water pumped from the 1st aquifer. The recovery phases and pumping phases of the 3-layer model have almost identical hydraulic heads (Figure 23, 3L_1).

The 14-layer model projects some drawdown during pumping but significantly less than the observed drawdown. The aquifer also recovers groundwater a bit too fast compared to the water pumping by pump B20. However, compared to the 3-layer model, we have a decrease of the water table during the consecutive pumping tests. This means that with this 14-layer model, the 1st aquifer below the Griftpark is losing after a pumping and recovery phase. From this 14-layer model estimation, we can also see a sharp reaction of the 1st aquifer hydraulic head to the pump switch as with the observed data. This impact is sought but still too small compared the observed data. Given the many layer properties, it is hard to determine what exactly causes these impacts.

The 3-layer model incorporating the previously obtained analytical solution of the aquifer hydraulic conductivity projects a slightly stronger variation in hydraulic head. Still, it is lower than what has been observed. The increased drop and rise of the water table during the pumping phases and recovery phases respectively is better than the previous two models. It is probably due to the lower hydraulic conductivity of the 1st aquifer of this model. However, during early pumping phases and recovery phases, this model lack of sharpness to react to pump B20 changing status. This could be due to a too high hydraulic conductivity of the aquitard as the 14-layer model, which has confining clay layers with a much lower hydraulic conductivity, showed a much sharper reaction to the pump switch.

By combining several of the layer properties responsible for some of these hydraulic head reactions, the models could be improved. To do so, a good understanding of the impacts of each property on groundwater flow is needed. Thus, a sensitivity analysis of a few properties is needed.

IV.3.2. Sensitivity analysis

The impact of the hydraulic conductivity of the 1st aquifer, the aquitard, and the barrier on the hydraulic heads of the Griftpark's 1st aquifer were tested with the 3-layer model. The objective was to test a range of hydraulic conductivity values including some much higher and much lower than what we would have expected from the previous model simulations. The results of the sensitivity analyses can be seen in Figures 24, 25, and 26 respectively.

IV.3.2.1. Hydraulic conductivity of the 1st aquifer

The values tested for the 1st aquifer horizontal hydraulic conductivities are 1 m/day, 5 m/day, 15 m/day, and 90 m/day. An anisotropy ratio of 3 has been kept for the vertical hydraulic conductivities.

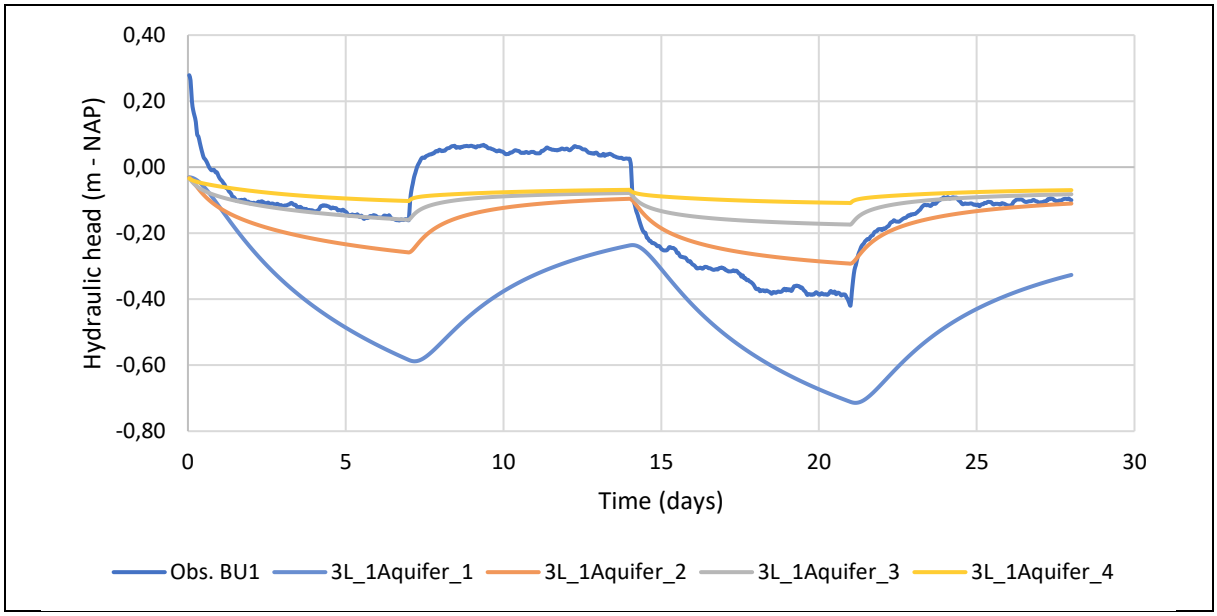

Figure 24: *Sensitivity analysis of Griftpark 1st aquifer hydraulic conductivity (3L_1Aquifer_1 → Kh=1m/day; 3L_1Aquifer_2 → Kh=5m/day; 3L_1Aquifer_3 → Kh=15m/day; 3L_1Aquifer_4 → Kh=90m/day)*

Figure 24 shows that the bigger the hydraulic conductivity, the smaller the drawdown and the faster the recovery. Also, smaller is the hydraulic conductivity, longer it takes for the aquifer to reach an equilibrium and slower is the aquifer to react to the changed pumping conditions. When the horizontal hydraulic conductivity was equal to 90m/day (3L_1Aquifer_4, yellow curve), the 1st aquifer hydraulic conductivity is almost not affected by the pumping test. On the contrary, when the hydraulic conductivity was equal to 1m/day (3L_1Aquifer_1, blue curve), The hydraulic conductivity of the 1st aquifer is greatly affected by the pumping test. The hydraulic head decreases and increases even more than the observed data during the pumping and recovery phases respectively. However, it seems that the aquifer is still far from reaching an equilibrium as the hydraulic head of the aquifer does not settle after the pumps have been switched.

When comparing the observed drawdown with Figure 24 4 projections, it seems that the 1st aquifer has a horizontal hydraulic conductivity close to than the one used during 3L_1Aquifer_2 model run (5m/day). This estimation is lower than the estimation established with Stallman's method or by Dinoloket although it should also be taken with precaution as a combination of factors can influence

the hydraulic heads of the 1st aquifer. Still, the estimation gives an idea of the hydraulic conductivity range that should be tested in a subsequent model simulation.

Figure 24 also shows that changing the 1st aquifer hydraulic conductivity does not affect the sharpness at which the aquifer reacts when the pumping conditions are changed. For all 4 projections, the rise or drop of the hydraulic head when pump B20 is switched is progressive and not as sharp as the results from the real pumping test. Changing the 1st aquifer hydraulic conductivity does not cause a big drop of the aquifer water table after a pumping and recovery phase. In contrary with what is observed in reality, the hydraulic head of the 1st aquifer at 7 and 21 days in Figure 24, just before pump B20 is to be switched off, are very close. This is also true for the hydraulic heads at 14 and 28 days, 7 days after pump B20 was switched.

IV.3.2.2. Hydraulic conductivity of the aquitard

The values tested for the aquitard vertical hydraulic conductivities are 0,03 m/day, 0,3 m/day, 1 m/day, and 6 m/day. Again, an anisotropy ratio of 3 has been kept for the horizontal hydraulic conductivities.

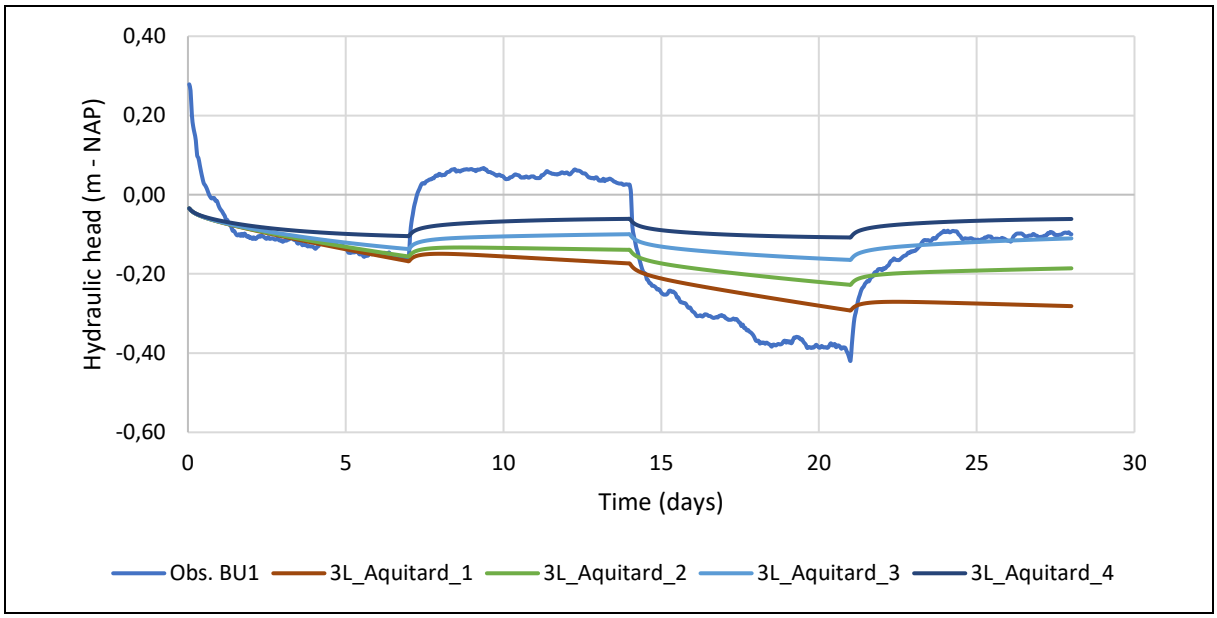

Figure 25: *Sensitivity analysis of the Griftpark aquitard hydraulic conductivity (3L_Aquitard_1 → Kv=0.03m/day; 3L_Aquitard_2 → Kv=0.3m/day; 3L_Aquitard_3 → Kv=1m/day; 3L_Aquitard_4 → Kv=6m/day)*

Figure 25 shows that the projection with the biggest vertical hydraulic conductivity for the aquitard (3L_Aquitard_4, Kv=6m/day) show a very small decrease in hydraulic during the pumping phases which is almost completely recovered during the recovery phases. By contrast, the projection with the lowest hydraulic conductivity (3L_Aquitard_1, Kv=0.03m/day), shows a bigger decrease of hydraulic head and which its recovery phase is not able to recover from. This means that the lower the hydraulic conductivity of the aquitard, bigger the drawdown during the pumping phase and the bigger the loss of groundwater in the 1st aquifer. Considering the significant drawdown observed during the performed pumping tests, this indicates that the aquitard has on average a low vertical hydraulic conductivity, at least in the surroundings of pump B20. It's value is probably nearby the vertical hydraulic conductivity tested with 3L_Aquitard projections (Kv=0.03m/day), in the same range as clay layers.

Figure 25 also shows that the hydraulic conductivity of the aquifer is not responsible for the intensity of the rise or drop of hydraulic head when pumps. The four projections on Figure 25 show the same sharpness regarding the rises and drops after pump switches. This means that in the previously seen

14-layer model, the hydraulic conductivity of the clay layers are not responsible for these sharp rises or drops in hydraulic head when pump B20 status is switched. The reason for this intense impact is still unknown.

IV.3.2.3. Hydraulic conductivity and thickness of the barrier

The values tested for the barrier thickness/conductivity are 0,003 m/day, 0,01 m/day, 0,03 m/day, and 0,06 m/day.

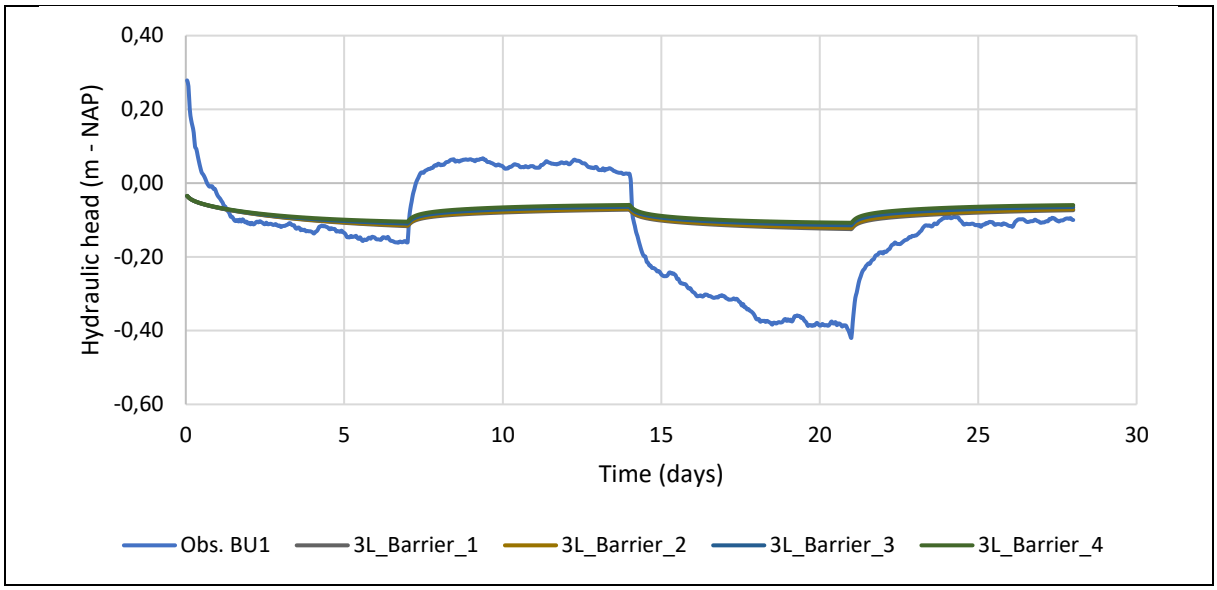

Figure 26: *Sensitivity analysis of the Griftpark bentonite barrier thickness/conductivity.*

Figure 26 shows that increasing the hydraulic conductivity by 10 does not have much impact on the hydraulic head of the 1st aquifer. If groundwater is leaking through the walls, it is probably because the bentonite walls have been severely damaged, generating holes where groundwater flows substantially faster than with the walls.

Testing the effect of including hydraulic holes in the aquitard or the bentonite walls could be quite interesting for further research given that we know water has been leaking into the Griftpark 1st aquifer.

V. Conclusion

This research aimed to evaluate the connectivity of the 1st and 2nd aquifer of the Griftpark, notably nearby pump B20, to obtain an increased understanding of the Griftpark soil's heterogeneity and its effect on groundwater flow, and to assess the best way to model the Griftpark subsurface. Additionally, it sought to evaluate the necessity of doing a tracer test in the Griftpark as the pumping test was performed in preparation for a tracer test.

The pumping test confirmed that the 1st and 2nd aquifer below the Griftpark are indeed hydraulically connected as pressure is able to travel through both aquifers. However, in contrary with what we believed, the hydraulic connection is very weak nearby pump B20. This means groundwater and potentially DNAPL are not leaking to the 2nd aquifer in this part of the park. We have also seen that groundwater is not leaking through the bentonite wall in this central-east sector. As such, the hydraulic connection between the two aquifers is elsewhere in the Griftpark, as potentially groundwater is leaking through the bentonite walls elsewhere, or a combination or both. A potential leakage location through the walls that needs to be investigated is the north-west part of the Griftpark where pumps B21 and pumps B22 are located.

The hydraulic head profiles confirmed the location of some clay lenses described by the sonic drills results. They also evaluated which one of these lenses has an effect on the groundwater hydraulic heads, and thus on groundwater flow. Not all of the described lenses in the sonic drills were sufficiently big or thick to affect the groundwater hydraulic heads. The hydraulic separation of the 1st and 2nd aquifer nearby pump B20 is mainly due to a clay lenses located between 54-56m below ground level. These clay lenses have also a small slope as the two monitored locations around pump B20 have very similar hydraulic head reactions but at a slightly different depth. The hydraulic head profiles also revealed a potential location where remnants of coal tar are locally obstructing vertical groundwater flows in the porous media. These remnants of coal tar have probably formed a small lens in the porous media below location B at 19-20m below ground level.

Regarding how to model the Griftpark subsurface, the 14-layer and 3-layer models used showed promising results even though many improvements can be made. Several hydraulic head reactions shown with the pumping test data have yet to be understood in order to accurately simulate groundwater flows below the Griftpark. For example, the hydraulic conductivity of the 1st aquifer has not been clearly estimated. With Stallman method, a diagonal hydraulic conductivity of 12,7m/day was estimated, meaning the horizontal hydraulic conductivity is probably around 15-20m/day. The model results and sensitivity analysis of the 1st aquifer hydraulic conductivity suggests the same. While homogeneous clay layers are considered to model the aquitard, the 3-layer model seems to be the better choice to continue future model improvements. The 14-layer model complexifies the groundwater flow simulations without returning much information on the driving processes managing these flows.

For a future tracer test, injecting a multitude of conservative tracers in the MLS wells around pump B20 would evaluate with more precision the hydraulic connection between the 1st and 2nd aquifer. The multitude of tracers from different locations and different depths would also enable the investigation of the extent of clay lenses However, given that the hydraulic connection between the two aquifers is weak nearby pump B20, I would suggest focusing on finding the location of hydraulic connection than on doing a tracer test. A water budget analysis defining how much water is leaking into the 1st aquifer would also help to understand the size of the hydraulic connection between the two aquifers.

Appendix A: Griftpark pumps, wells, and clay layer locations

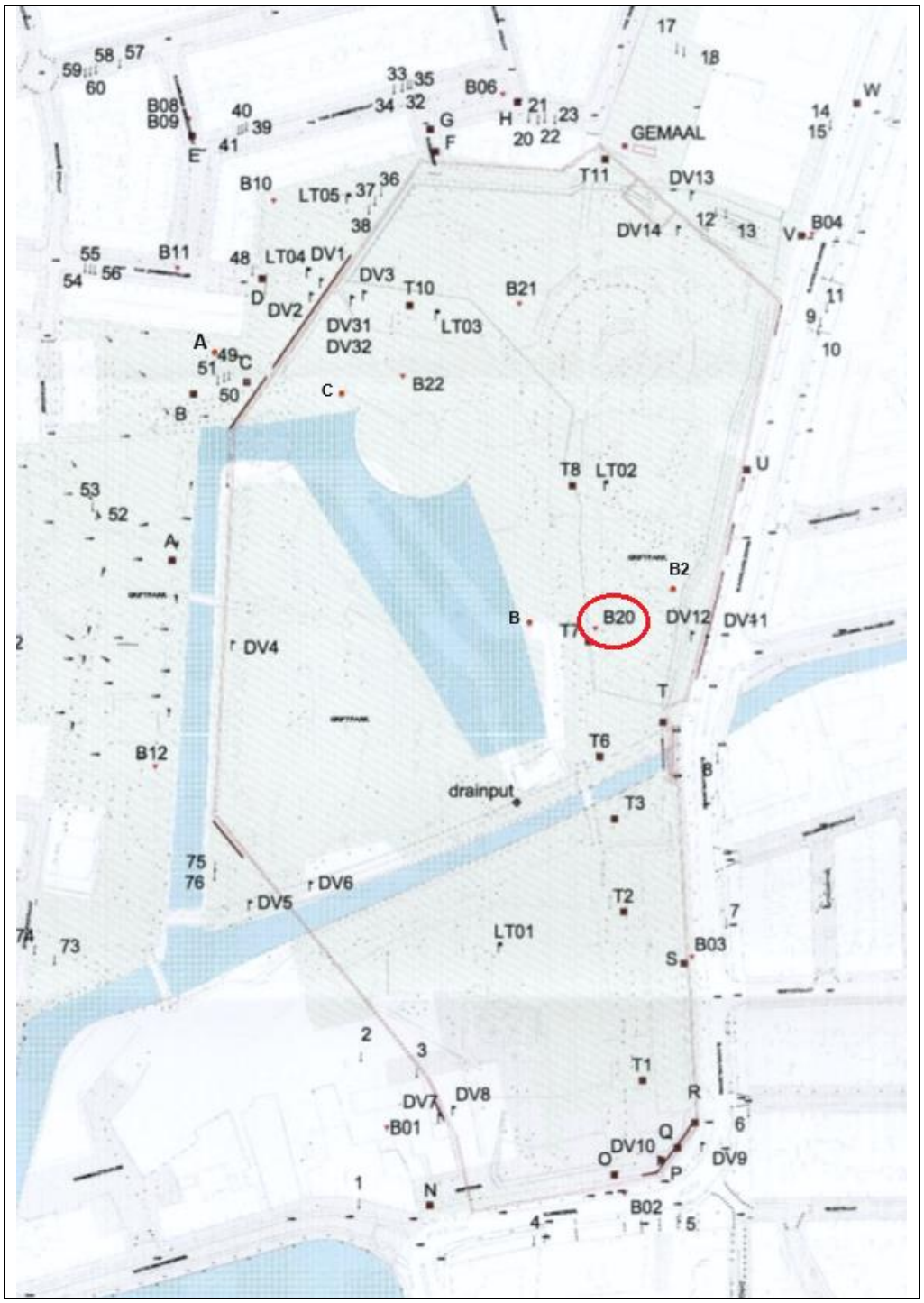

Figure 27: *Griftpark pumps and wells locations*

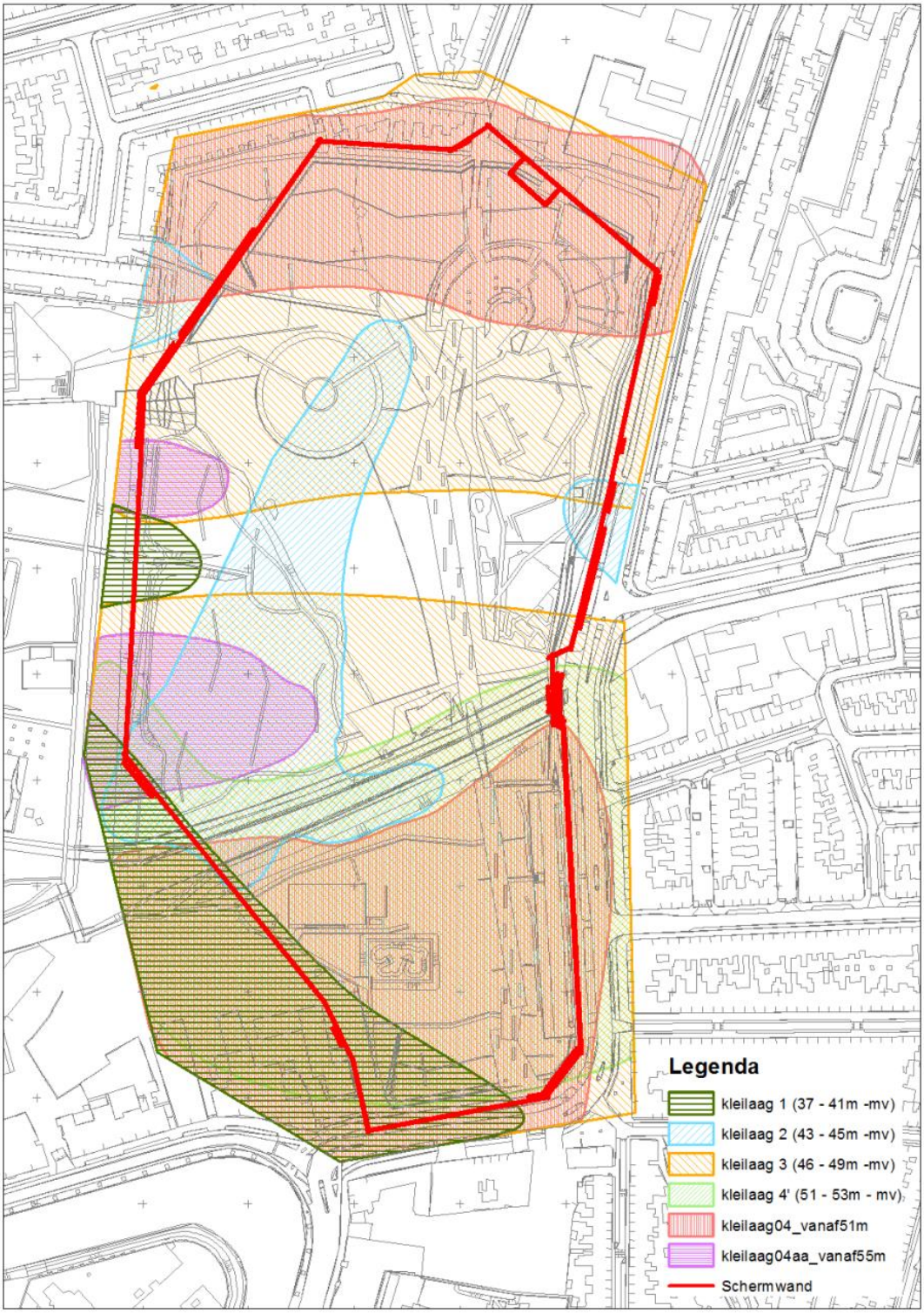

Figure 3: *Griftpark clay layer formations (Grondmechanica Delft, 1988)*

Appendix B: Well descriptions

Table 9: *Depth of wells in location B, B2, and at the eastern border of the Griftpark*

ASSET	TOP OF FILTER [cm-bgl]	BOTTOM OF FILTER [cm-bgl]	AVG. FILTER DEPTH [cm-bgl]	CAP HEIGHT (m-NAP)	AVG. FILTER DEPTH [m-NAP]
BU1	1700	1900	1800	3,145	14,855
BU2	4400	4500	4450	3,114	41,386
BU3	5400	5500	5450	3,093	51,407
BU4	6300	6400	6350	3,065	60,435
BMLS1U1	850	875	862,5	3,146	5,479
BMLS1U2	1025	1050	1037,5	3,146	7,229
BMLS1U3	1200	1225	1212,5	3,146	8,979
BMLS1U4	1375	1400	1387,5	3,146	10,729
BMLS1U5	1550	1575	1562,5	3,146	12,479
BMLS1U6	1725	1750	1737,5	3,146	14,229
BMLS1U7	1875	1900	1887,5	3,146	15,729
BMLS2U1	2075	2100	2087,5	3,167	17,708
BMLS2U2	2250	2275	2262,5	3,167	19,458
BMLS2U3	2425	2450	2437,5	3,167	21,208
BMLS2U4	2600	2625	2612,5	3,167	22,958
BMLS2U5	2775	2800	2787,5	3,167	24,708
BMLS2U6	2950	2975	2962,5	3,167	26,458
BMLS2U7	3100	3125	3112,5	3,167	27,958
BMLS3U1	4950	4975	4962,5	3,139	46,486
BMLS3U2	5125	5150	5137,5	3,139	48,236
BMLS3U3	5300	5325	5312,5	3,139	49,986
BMLS3U4	5475	5500	5487,5	3,139	51,736
BMLS3U5	5650	5675	5662,5	3,139	53,486
BMLS3U6	5825	5850	5837,5	3,139	55,236
BMLS3U7	5975	6000	5987,5	3,139	56,736
B2	6450	6550	6500	3,128	61,872
B2MLS1U1	675	700	687,5	3,15	3,725
B2MLS1U2	850	875	862,5	3,15	5,475
B2MLS1U3	1025	1050	1037,5	3,15	7,225
B2MLS1U4	1200	1225	1212,5	3,15	8,975
B2MLS1U5	1375	1400	1387,5	3,15	10,725
B2MLS1U6	1550	1575	1562,5	3,15	12,475
B2MLS1U7	1725	1750	1737,5	3,15	14,225
B2MLS2U1	2000	2025	2012,5	3,105	17,020
B2MLS2U2	2325	2350	2337,5	3,105	20,270
B2MLS2U3	2600	2625	2612,5	3,105	23,020
B2MLS2U4	4325	4350	4337,5	3,105	40,270
B2MLS2U5	4975	5000	4987,5	3,105	46,770
B2MLS2U6	5525	5550	5537,5	3,105	52,270
B2MLS2U7	5975	6000	5987,5	3,105	56,770
DV11	2900	3300	3100	1,898	29,102
DV12	2900	3400	3150	1,873	29,627

Appendix C: Wells drilling descriptions

B

Boormeester: M. Murray
13-11-2018

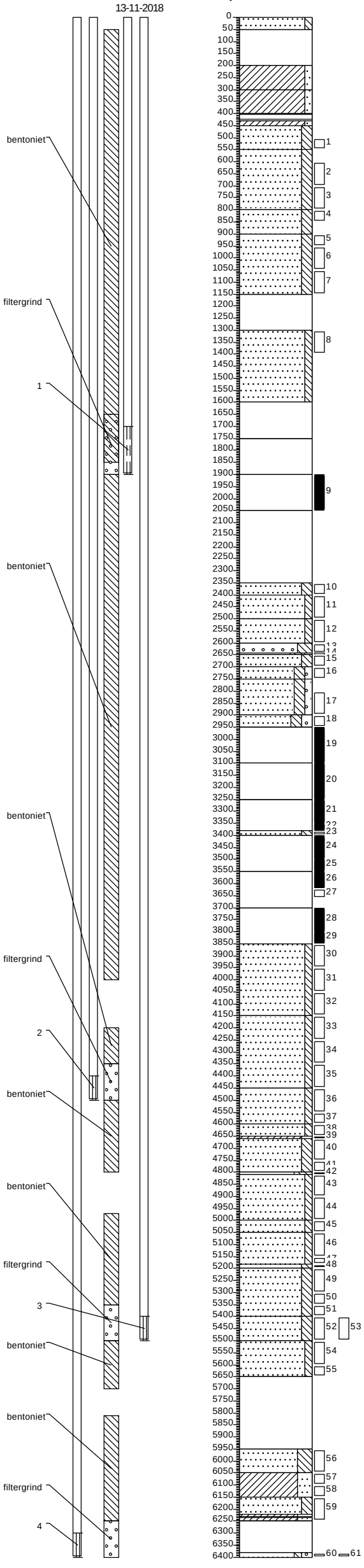

0 gras

-50 Zand, uiterst fijn, zwak siltig, Graven

Matig puinhoudend, antropogeen, matig kolengruishoudend, antropogeen, grijsbruin, Edelmanboor, Voorboren / voorgraven

-200

Klei, zwak zandig, sterk puinhoudend, antropogeen, pid (0 ppm), neutraalgrijs, Sonic Drill

-300 Klei, zwak zandig, Sonic Drill

-400

-430 Veen, mineraalarm, donker zwartbruin, Sonic Drill

-450 Klei, zwak zandig, lichtgrijs, Sonic Drill

-550 Zand, zeer fijn, matig siltig, pid (0 ppm), licht beigegrijs, Sonic Drill, CO 52 ppm, H2S 2,1 ppm

Zand, zeer fijn, matig siltig, pid (0 ppm), lichtgrijs, Sonic Drill, CO 0 ppm, H2S 0 ppm

-800 Zand, zeer fijn, matig siltig, laagjes veen, gebiedseigen, pid (0 ppm), lichtgrijs, Sonic Drill, CO 0 ppm, H2S 0 ppm

-900 Zand, matig fijn, matig siltig, pid (0 ppm), lichtgrijs, Sonic Drill, CO 0 ppm, H2S 0 ppm

-1150 Aqualock-sampler, Geen beschrijving. Geen monster zuiger bleef hangen

-1300 Zand, matig fijn, zwak siltig, pid (0 ppm), lichtgrijs, Sonic Drill, vermoedelijk grove zandlaag uit barrel gevallen, monster +/- 13-14 l corecacher boven in barrel | CO 30 ppm, H2S 0,7 ppm

-1600 Sonic Drill, Geen beschrijving | linergestoken geen zand

-1750 Sonic Drill, Geen beschrijving | linergestoken geen zand

-1900 Zwakke carbolineumgeur, Sonic Drill, Geen beschrijving | linergestoken zand achergebleven tussen 19-20,5 -mv

-2050 Sonic Drill, Geen beschrijving | geen zand achter gebleven in core barrel

-2350

-2400 Zand, zeer fijn, matig siltig, pid (0 ppm), lichtgrijs, Sonic Drill, CO 0 ppm, H2S 0 ppm

-2500 Zand, matig fijn, zwak siltig, pid (0 ppm), lichtgrijs, Sonic Drill, CO 0 ppm, H2S 0 ppm

Zand, matig fijn, zwak siltig, laagjes veen, gebiedseigen, laagjes grind, gebiedseigen, pid (0 ppm), lichtgrijs, Sonic Drill, CO 0 ppm, H2S 0 ppm

-2600

-2650 Grind, fijn, siltig, pid (0 ppm), lichtgrijs, Sonic Drill, CO 0 ppm, H2S 0 ppm

-2700 Zand, uiterst fijn, sterk siltig, zwak humeus, matig veenhoudend, gebiedseigen, pid (0 ppm), neutraalgrijs, Sonic Drill, CO 0 ppm, H2S 0 ppm

-2750 Zand, zeer fijn, matig siltig, pid (0 ppm), lichtgrijs, Sonic Drill, CO 0 ppm, H2S 0 ppm

Zand, zeer grof, matig siltig, zwak grindig, pid (0 ppm), lichtgrijs, Sonic Drill, CO 0 ppm, H2S 0 ppm

-2900

-2950 Zand, matig grof, matig siltig, zwak grindig, pid (0 ppm), lichtgrijs, Sonic Drill, CO 0 ppm, H2S 0 ppm

Zand, uiterst grof, matig siltig, matig grindig, laagjes klei, gebiedseigen, pid (0 ppm), lichtgrijs, Sonic Drill, CO 0 ppm, H2S 0 ppm

-3100 Sonic Drill, Geen beschrijving | zand achter gebleven tussen 27,5-31 m -mv

Sonic Drill, Geen beschrijving liner gestoken | zand traject tussen 31-32,5 m - mv

-3250 Sonic Drill, geen beschrijving Liner gestoken

-3380

-3400 Zand, zeer fijn, matig siltig, geen olie-water reactie, pid (0 ppm), lichtgrijs, Sonic Drill, Zand uit boorkop

Geen olie-water reactie, Sonic Drill, Geen beschrijving liner gestoken | zand matig fijn

-3550 Geen olie-water reactie, Sonic Drill, Geen beschrijving liner gestoken | zand matig fijn

-3700 Sonic Drill, Geen beschrijving liner gestoken | zand matig fijn | vermoedelijk "fingers" (puur product)

-3850 Zand, matig fijn, zwak siltig, geen olie-water reactie, pid (0 ppm), lichtgrijs, Sonic Drill, Vermoedelijk een gedeelte van een zandlaag verloren gegaan (1 linerzak) | CO 0-5 ppm, H2S 0 ppm

-4150 Zand, matig fijn, zwak siltig, geen olie-water reactie, pid (0 ppm), lichtgrijs, Sonic Drill, Vermoedelijk een gedeelte van een zandlaag verloren gegaan (1 linerzak) | CO 0-18 ppm, H2S 0 ppm

-4450 Zand, matig fijn, zwak siltig, geen olie-water reactie, pid (0 ppm), lichtgrijs, Sonic Drill, CO 0 ppm, H2S 0 ppm

-4600

-4660 Zand, zeer fijn, zwak siltig, geen olie-water reactie, pid (0 ppm), lichtgrijs, Sonic Drill, CO 0 ppm, H2S 0 ppm

Klei, matig zandig, geen olie-water reactie, pid (0 ppm), lichtgrijs, Sonic Drill, CO 0 ppm, H2S 0 ppm

-4810 Zand, zeer fijn, matig siltig, geen olie-water reactie, pid (0 ppm), lichtgrijs, Sonic Drill, enkel veenlaagje (4700) CO 0 ppm, H2S 0 ppm

Zand, uiterst fijn, uiterst siltig, zwak kleihoudend, gebiedseigen, geen olie-water reactie, pid (0 ppm), lichtgrijs, Sonic Drill, CO 0 ppm, H2S 0 ppm

Zand, zeer fijn, zwak siltig, geen olie-water reactie, pid (0 ppm), lichtgrijs, Sonic Drill, CO 0 ppm, H2S 0 ppm

-5000

-5050 Zand, zeer fijn, zwak siltig, geen olie-water reactie, pid (0 ppm), lichtgrijs, Sonic Drill, CO 0-17 ppm, H2S 0 ppm

Zand, matig fijn, zwak siltig, geen olie-water reactie, pid (0 ppm), lichtgrijs, Sonic Drill, CO 0 ppm, H2S 0 ppm

-5200 Zand, uiterst fijn, matig siltig, laagjes klei, gebiedseigen, geen olie-water reactie, pid (0 ppm), lichtgrijs, Sonic Drill, CO 120 ppm, H2S 2,8 ppm

Zand, matig fijn, matig siltig, geen olie-water reactie, pid (0 ppm), lichtgrijs, Sonic Drill, CO 0 ppm, H2S 0 ppm

-5400

Zand, zeer fijn, matig siltig, laagjes klei, gebiedseigen, geen olie-water reactie, pid (0 ppm), lichtgrijs, Sonic Drill, CO 17 ppm, H2S 0 ppm

-5500 Zand, matig fijn, zwak siltig, geen olie-water reactie, pid (0 ppm), lichtgrijs, Sonic Drill, CO 0 ppm, H2S 0 ppm

-5650 Sonic Drill, Geen beschrijving | geen zand in core barrel

-5950

Zand, zeer fijn, sterk siltig, laagjes klei, gebiedseigen, geen olie-water reactie, pid (0 ppm), neutraalgrijs, Sonic Drill, kleilagen max 10 cm | CO 0 ppm, H2S 0 ppm

-6050 Klei, sterk zandig, geen olie-water reactie, pid (0 ppm), neutraalgrijs, Sonic Drill, CO 0 ppm, H2S 0 ppm

-6150

Zand, matig grof, matig siltig, laagjes klei, gebiedseigen, geen olie-water reactie, pid (0 ppm), neutraalgrijs, Sonic Drill, CO 0 ppm, H2S 0 ppm

-6250 Klei, sterk zandig, geen olie-water reactie, pid (0 ppm), neutraalgrijs, Sonic Drill, CO 0 ppm, H2S 0 ppm

-6380 Zand, zeer grof, zwak siltig, zwak grindig, geen olie-water reactie, pid (0 ppm), neutraalgrijs, Sonic Drill, CO 0 ppm, H2S 0 ppm

-6400 Klei, sterk zandig, geen olie-water reactie, pid (0 ppm), neutraalgrijs, Sonic Drill, CO 0 ppm, H2S 0 ppm

Lichtgrijs, Sonic Drill, Geen beschrijving | Geen zand in liner

Zand, uiterst grof, zwak siltig, matig grindig, geen olie-water reactie, lichtgrijs, Sonic Drill, Restand zand uit boorkop

BMLS1

Boormeester: M. Murray
7-5-2019

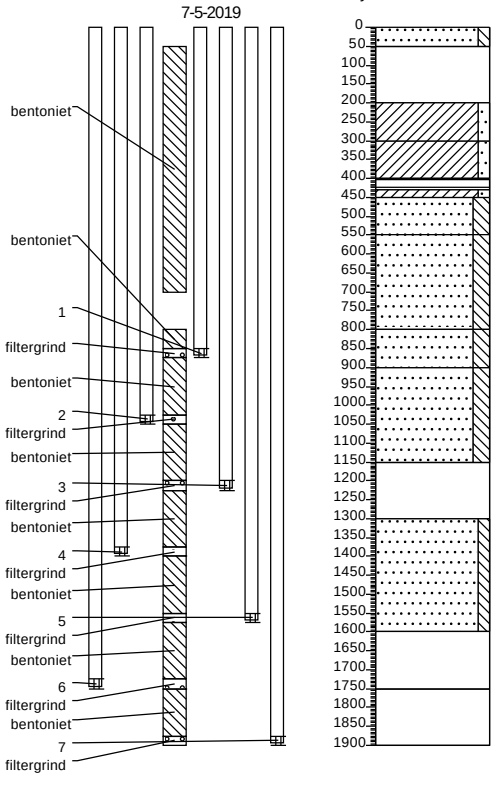

0 gras

-50 Zand, uiterst fijn, zwak siltig, Graven

Matig puinhoudend, antropogeen, matig kolengruishoudend, antropogeen, grijsbruin, Edelmanboor, Voorboren / voorgraven

-200

Klei, zwak zandig, sterk puinhoudend, antropogeen, pid (0 ppm), neutraalgrijs, Sonic Drill

-300

Klei, zwak zandig, Sonic Drill

-400

-430 Veen, mineraalarm, donker zwartbruin, Sonic Drill

-450 Klei, zwak zandig, lichtgrijs, Sonic Drill

-550 Zand, zeer fijn, matig siltig, pid (0 ppm), licht beigegrijs, Sonic Drill, CO 52 ppm, H2S 2,1 ppm

Zand, zeer fijn, matig siltig, pid (0 ppm), lichtgrijs, Sonic Drill, CO 0 ppm, H2S 0 ppm

-800

Zand, zeer fijn, matig siltig, laagjes veen, gebiedseigen, pid (0 ppm), lichtgrijs, Sonic Drill, CO 0 ppm, H2S 0 ppm

-900

Zand, matig fijn, matig siltig, pid (0 ppm), lichtgrijs, Sonic Drill, CO 0 ppm, H2S 0 ppm

-1150

Sonic Drill, Geen beschrijving. Geen monster zuiger bleef hangen

-1300

Zand, matig fijn, zwak siltig, pid (0 ppm), lichtgrijs, Sonic Drill, vermoedelijk grove zandlaag uit barrel gevallen, monster +/- 13-14 l corecacher boven in barrel | CO 30 ppm, H2S 0,7 ppm

-1600

Sonic Drill, Geen beschrijving | linergestoken geen zand

-1750

Sonic Drill, Geen beschrijving | linergestoken geen zand

-1900

BMLS2

Boormeester: M. Murray
7-5-2019

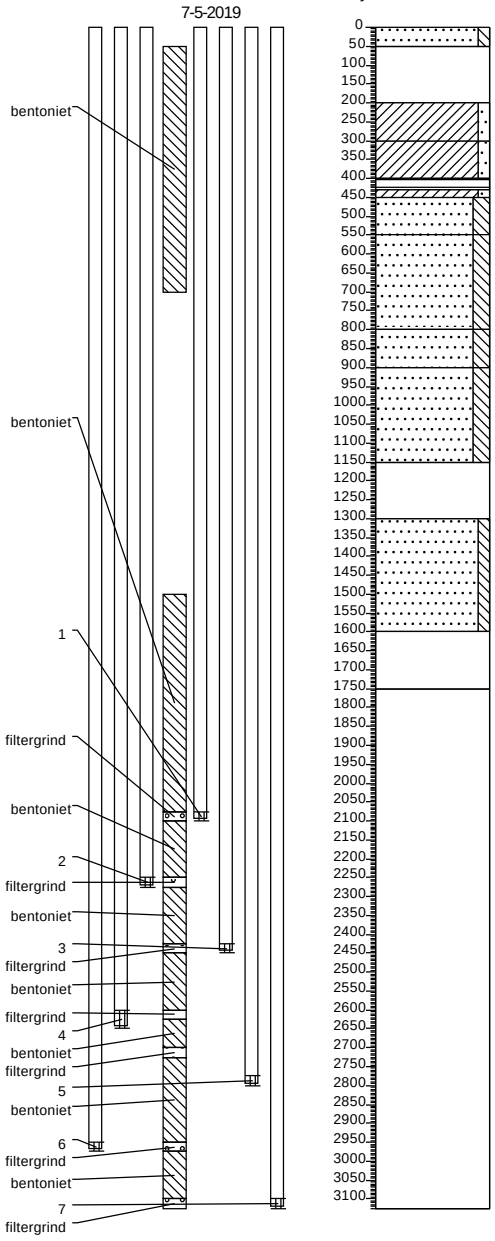

0 gras

-50 Zand, uiterst fijn, zwak siltig, Graven

Matig puinhoudend, antropogeen, matig kolengruishoudend, antropogeen, grijsbruin, Edelmanboor, Voorboren / voorgraven

-200

Klei, zwak zandig, sterk puinhoudend, antropogeen, pid (0 ppm), neutraalgrijs, Sonic Drill

-300

Klei, zwak zandig, Sonic Drill

-400

-430 Veen, mineraalarm, donker zwartbruin, Sonic Drill

-450 Klei, zwak zandig, lichtgrijs, Sonic Drill

-550 Zand, zeer fijn, matig siltig, pid (0 ppm), licht beigegrijs, Sonic Drill, CO 52 ppm, H2S 2,1 ppm

Zand, zeer fijn, matig siltig, pid (0 ppm), lichtgrijs, Sonic Drill, CO 0 ppm, H2S 0 ppm

-800

Zand, zeer fijn, matig siltig, laagjes veen, gebiedseigen, pid (0 ppm), lichtgrijs, Sonic Drill, CO 0 ppm, H2S 0 ppm

-900

Zand, matig fijn, matig siltig, pid (0 ppm), lichtgrijs, Sonic Drill, CO 0 ppm, H2S 0 ppm

-1150

Sonic Drill, Geen beschrijving. Geen monster zuiger bleef hangen

-1300

Zand, matig fijn, zwak siltig, pid (0 ppm), lichtgrijs, Sonic Drill, vermoedelijk grove zandlaag uit barrel gevallen, monster +/- 13-14 l corecacher boven in barrel | CO 30 ppm, H2S 0,7 ppm

-1600

Sonic Drill, Geen beschrijving | linergestoken geen zand

-1750

Sonic Drill, Geen beschrijving | linergestoken geen zand

-3125

BMLS3

Boormeester: M. Murray
30-4-2019

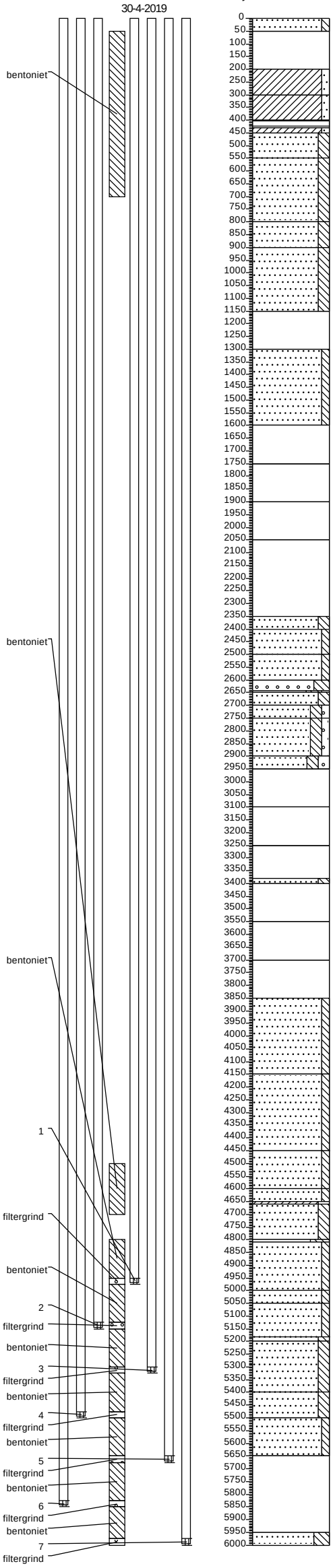

0		gras
-50		Zand, uiterst fijn, zwak siltig, Graven
	▲	Matig puinhoudend, antropogeen, matig kolengruishoudend, antropogeen, grijsbruin, Edelmanboor, Voorboren / voorgraven
-200		
	▲	Klei, zwak zandig, sterk puinhoudend, antropogeen, pid (0 ppm), neutraalgrijs, Sonic Drill
-300		Klei, zwak zandig, Sonic Drill
-400		
-430		Veen, mineraalarm, donker zwartbruin, Sonic Drill
-450		Klei, zwak zandig, lichtgrijs, Sonic Drill
-550		Zand, zeer fijn, matig siltig, pid (0 ppm), licht beigegrijs, Sonic Drill, CO 52 ppm, H2S 2,1 ppm
		Zand, zeer fijn, matig siltig, pid (0 ppm), lichtgrijs, Sonic Drill, CO 0 ppm, H2S 0 ppm
-800		
		Zand, zeer fijn, matig siltig, laagjes veen, gebiedseigen, pid (0 ppm), lichtgrijs, Sonic Drill, CO 0 ppm, H2S 0 ppm
-900		Zand, matig fijn, matig siltig, pid (0 ppm), lichtgrijs, Sonic Drill, CO 0 ppm, H2S 0 ppm
-1150		Sonic Drill, Geen beschrijving. Geen monster zuiger bleef hangen
-1300		Zand, matig fijn, zwak siltig, pid (0 ppm), lichtgrijs, Sonic Drill, vermoedelijk grove zandlaag uit barrel gevallen, monster +/- 13-14 l corecacher boven in barrel | CO 30 ppm, H2S 0,7 ppm
-1600		Sonic Drill, Geen beschrijving | linergestoken geen zand
-1750		Sonic Drill, Geen beschrijving | linergestoken geen zand
-1900		Zwakke carbolineumgeur, Sonic Drill, Geen beschrijving | linergestoken zand achergebleven tussen 19-20,5 -mv
-2050		Sonic Drill, Geen beschrijving | geen zand achter gebleven in core barrel
-2350		
-2400		Zand, zeer fijn, matig siltig, pid (0 ppm), lichtgrijs, Sonic Drill, CO 0 ppm, H2S 0 ppm
		Zand, matig fijn, zwak siltig, pid (0 ppm), lichtgrijs, Sonic Drill, CO 0 ppm, H2S 0 ppm
-2500		Zand, matig fijn, zwak siltig, laagjes veen, gebiedseigen, laagjes grind, gebiedseigen, pid (0 ppm), lichtgrijs, Sonic Drill, CO 0 ppm, H2S 0 ppm
-2600		
-2650		Grind, fijn, siltig, pid (0 ppm), lichtgrijs, Sonic Drill, CO 0 ppm, H2S 0 ppm
-2700		Zand, uiterst fijn, sterk siltig, zwak humeus, matig veenhoudend, gebiedseigen, pid (0 ppm), neutraalgrijs, Sonic Drill, CO 0 ppm, H2S 0 ppm
-2750		Zand, zeer fijn, matig siltig, pid (0 ppm), lichtgrijs, Sonic Drill, CO 0 ppm, H2S 0 ppm
-2900		Zand, zeer grof, matig siltig, zwak grindig, pid (0 ppm), lichtgrijs, Sonic Drill, CO 0 ppm, H2S 0 ppm
-2950		Zand, matig grof, matig siltig, zwak grindig, pid (0 ppm), lichtgrijs, Sonic Drill, CO 0 ppm, H2S 0 ppm
		Zand, uiterst grof, matig siltig, matig grindig, laagjes klei, gebiedseigen, pid (0 ppm), lichtgrijs, Sonic Drill, CO 0 ppm, H2S 0 ppm
-3100		Sonic Drill, Geen beschrijving | zand achter gebleven tussen 27,5-31 m -mv
		Sonic Drill, Geen beschrijving liner gestoken | zand traject tussen 31-32,5 m - mv
-3250		Sonic Drill, geen beschrijving Liner gestoken
-3380		
-3400		Zand, zeer fijn, matig siltig, geen olie-water reactie, pid (0 ppm), lichtgrijs, Sonic Drill, Zand uit boorkop
		Geen olie-water reactie, Sonic Drill, Geen beschrijving liner gestoken | zand matig fijn
-3550		Geen olie-water reactie, Sonic Drill, Geen beschrijving liner gestoken | zand matig fijn
-3700		Sonic Drill, Geen beschrijving liner gestoken | zand matig fijn | vermoedelijk "fingers" (puur product)
-3850		Zand, matig fijn, zwak siltig, geen olie-water reactie, pid (0 ppm), lichtgrijs, Sonic Drill, Vermoedelijk een gedeelte van een zandlaag verloren gegaan (1 linerzak) | CO 0-5 ppm, H2S 0 ppm
-4150		Zand, matig fijn, zwak siltig, geen olie-water reactie, pid (0 ppm), lichtgrijs, Sonic Drill, Vermoedelijk een gedeelte van een zandlaag verloren gegaan (1 linerzak) | CO 0-18 ppm, H2S 0 ppm
-4450		Zand, matig fijn, zwak siltig, geen olie-water reactie, pid (0 ppm), lichtgrijs, Sonic Drill, CO 0 ppm, H2S 0 ppm
-4600		
-4660		Zand, zeer fijn, zwak siltig, geen olie-water reactie, pid (0 ppm), lichtgrijs, Sonic Drill, CO 0 ppm, H2S 0 ppm
		Klei, matig zandig, geen olie-water reactie, pid (0 ppm), lichtgrijs, Sonic Drill, CO 0 ppm, H2S 0 ppm
-4810		Zand, zeer fijn, matig siltig, geen olie-water reactie, pid (0 ppm), lichtgrijs, Sonic Drill, enkel veenlaagje (4700) CO 0 ppm, H2S 0 ppm
		Zand, uiterst fijn, uiterst siltig, zwak kleihoudend, gebiedseigen, geen olie-water reactie, pid (0 ppm), lichtgrijs, Sonic Drill, CO 0 ppm, H2S 0 ppm
-5000		Zand, zeer fijn, zwak siltig, geen olie-water reactie, pid (0 ppm), lichtgrijs, Sonic Drill, CO 0 ppm, H2S 0 ppm
-5050		Zand, zeer fijn, zwak siltig, geen olie-water reactie, pid (0 ppm), lichtgrijs, Sonic Drill, CO 0-17 ppm, H2S 0 ppm
		Zand, matig fijn, zwak siltig, geen olie-water reactie, pid (0 ppm), lichtgrijs, Sonic Drill, CO 0 ppm, H2S 0 ppm
-5200		Zand, uiterst fijn, matig siltig, laagjes klei, gebiedseigen, geen olie-water reactie, pid (0 ppm), lichtgrijs, Sonic Drill, CO 120 ppm, H2S 2,8 ppm
		Zand, matig fijn, matig siltig, geen olie-water reactie, pid (0 ppm), lichtgrijs, Sonic Drill, CO 0 ppm, H2S 0 ppm
-5400		Zand, zeer fijn, matig siltig, laagjes klei, gebiedseigen, geen olie-water reactie, pid (0 ppm), lichtgrijs, Sonic Drill, CO 17 ppm, H2S 0 ppm
-5500		Zand, matig fijn, zwak siltig, geen olie-water reactie, pid (0 ppm), lichtgrijs, Sonic Drill, CO 0 ppm, H2S 0 ppm
-5650		Sonic Drill, Geen beschrijving | geen zand in core barrel
-5950		
-6000		Zand, zeer fijn, sterk siltig, laagjes klei, gebiedseigen, geen olie-water reactie, pid (0 ppm), neutraalgrijs, Sonic Drill, kleilagen max 10 cm | CO 0 ppm, H2S 0 ppm

B2

Boormeester: M. Murray
8-4-2019

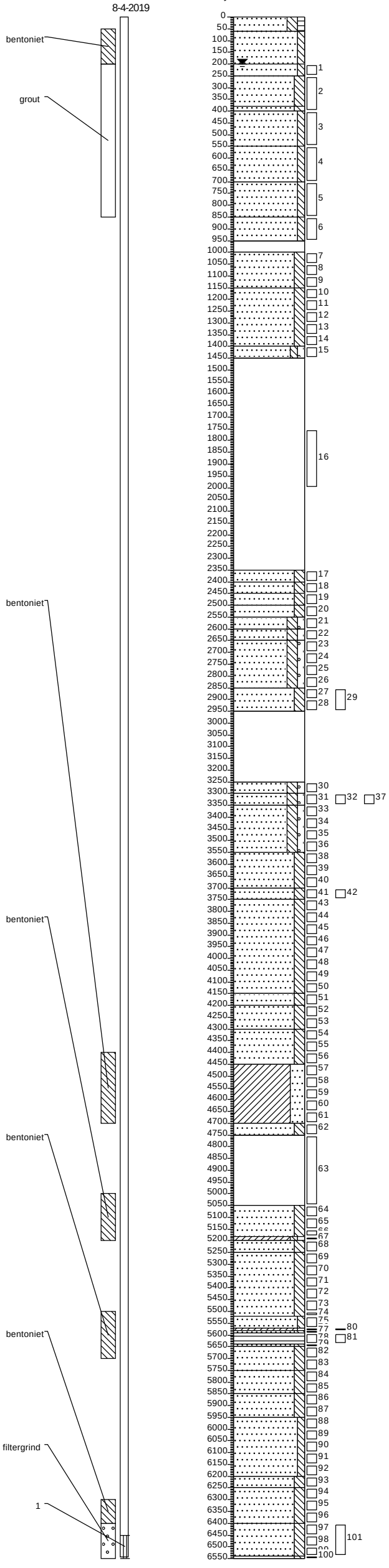

0		gras
0		
-60		Zand, zeer fijn, matig siltig, zwak humeus, donkerbruin, Graven
		Zand, uiterst fijn, zwak siltig, Edelmanboor
-200		
-250		Zand, matig fijn, zwak siltig, lichtgrijs, Sonic Drill, Liner gestoken
		Zand, matig fijn, matig siltig, lichtgrijs, Sonic Drill, Liner gestoken
-380		
-400		Zand, matig fijn, matig siltig, donker bruingrijs, Sonic Drill, Liner gestoken | zaklaag
		Zand, uiterst fijn, zwak siltig, sterke carbolineumgeur, donker roodbruin, Sonic Drill, liner gestoken | zaklaag waarneembaar
-550		Zand, uiterst fijn, zwak siltig, Sonic Drill, Liner gestoken | laagjes DNALP
-700		Zand, uiterst fijn, zwak siltig, lichtgrijs, Sonic Drill, Liner gestoken | "druppels" DNALP
-850		Zand, uiterst fijn, zwak siltig, lichtgrijs, Sonic Drill, Liner gestoken
-950		
-1000		Sonic Drill, Geen materiaal
		Zand, zeer fijn, matig siltig, geen olie-water reactie, pid (1 ppm), lichtgrijs, Sonic Drill, 24 ppm CO , 2,3 ppm H2S
-1150		Zand, zeer fijn, matig siltig, geen olie-water reactie, pid (0 ppm), lichtgrijs, Sonic Drill, 0 ppm CO , 0 ppm H2S |
-1400		
-1450		Zand, zeer grof, zwak siltig, zwak grindig, geen olie-water reactie, pid (0 ppm), licht beigegrijs, Sonic Drill, 0 ppm CO , 0 ppm H2S |
		Licht beigegrijs, Sonic Drill, Geen materiaal | zeer grof zand zwak ziltig zwak grindig
-2350		
-2400		Zand, matig grof, matig siltig, geen olie-water reactie, pid (0 ppm), lichtgrijs, Sonic Drill, CO 5-10 ppm, H2S 0 ppm
-2450		Zand, matig fijn, matig siltig, laagjes grind, gebiedseigen, geen olie-water reactie, pid (0 ppm), lichtgrijs, Sonic Drill, CO 5-10 ppm, H2S 0 ppm
-2500		Zand, matig fijn, matig siltig, geen olie-water reactie, pid (0 ppm), lichtgrijs, Sonic Drill, CO 5-10 ppm, H2S 0 ppm
-2550		
-2600		Zand, matig fijn, matig siltig, laagjes klei, gebiedseigen, geen olie-water reactie, pid (17 ppm), lichtgrijs, Sonic Drill, CO 0 ppm, H2S 0 ppm
-2650		Zand, matig grof, matig siltig, zwak grindig, geen olie-water reactie, pid (17 ppm), lichtgrijs, Sonic Drill, CO 0 ppm, H2S 0 ppm
		Zand, matig grof, matig siltig, zwak grindig, geen olie-water reactie, pid (63 ppm), lichtgrijs, Sonic Drill, CO 62 ppm, H2S 4,7 ppm
-2850		Zand, zeer grof, matig siltig, zwak grindig, geen olie-water reactie, pid (0 ppm), lichtgrijs, Sonic Drill, CO 0 ppm, H2S 0 ppm
-2950		Zand, zeer fijn, matig siltig, geen olie-water reactie, pid (0 ppm), lichtgrijs, Sonic Drill, CO 0 ppm, H2S 0 ppm
		Sonic Drill, Geen materiaal | zeer grof zand
-3250		
-3300		Zand, matig fijn, matig siltig, zwak grindig, geen olie-water reactie, pid (0 ppm), lichtgrijs, Sonic Drill, CO 0 ppm, H2S 0 ppm
-3350		Zand, matig fijn, matig siltig, zwak grindig, laagjes klei, gebiedseigen, geen olie-water reactie, pid (0 ppm), lichtgrijs, Sonic Drill, CO 0 ppm, H2S 0 ppm
		Zand, matig fijn, matig siltig, zwak grindig, laagjes klei, gebiedseigen, geen olie-water reactie, pid (0 ppm), lichtgrijs, Sonic Drill, CO 0 ppm, H2S 0 ppm
-3550		Zand, matig fijn, matig siltig, geen olie-water reactie, pid (0 ppm), lichtgrijs, Sonic Drill, CO 0 ppm, H2S 0 ppm
-3700		
-3750		Zand, matig fijn, matig siltig, resten hout, gebiedseigen, zwak leemhoudend, gebiedseigen, laagjes klei, gebiedseigen, geen olie-water reactie, pid (0 ppm), lichtgrijs, Sonic Drill, CO 0 ppm, H2S 0 ppm
		Zand, zeer fijn, matig siltig, geen olie-water reactie, pid (0 ppm), lichtgrijs, Sonic Drill, CO 0 ppm, H2S 0 ppm
-4150		
-4200		Zand, zeer fijn, matig siltig, geen olie-water reactie, pid (0 ppm), lichtgrijs, Sonic Drill, CO 10-15 ppm, H2S 0-1 ppm
-4300		Zand, zeer fijn, matig siltig, geen olie-water reactie, pid (0 ppm), lichtgrijs, Sonic Drill, CO 0 ppm, H2S 0 ppm
		Zand, zeer fijn, matig siltig, geen olie-water reactie, pid (0 ppm), lichtgrijs, Sonic Drill, CO 0 ppm, H2S 0 ppm
-4450		Klei, sterk zandig, geen olie-water reactie, pid (0 ppm), lichtgrijs, Sonic Drill, CO 0 ppm, H2S 0 ppm
-4700		
-4750		Zand, matig fijn, matig siltig, geen olie-water reactie, pid (0 ppm), lichtgrijs, Sonic Drill, CO 0 ppm, H2S 0 ppm
		Geen olie-water reactie, pid (0 ppm), lichtgrijs, Sonic Drill, CO 0 ppm, H2S 0 ppm | zeer weinig monstermateriaal | Z2S3K1 ligr
-5050		
		Zand, matig fijn, matig siltig, geen olie-water reactie, pid (0 ppm), lichtgrijs, Sonic Drill, CO 0 ppm, H2S 0 ppm
-5200		Klei, zwak siltig, zwak humeus, resten veen, gebiedseigen, geen olie-water reactie, pid (0 ppm), lichtgrijs, Sonic Drill, CO 0 ppm, H2S 0 ppm
-5250		Zand, matig fijn, matig siltig, laagjes klei, gebiedseigen, geen olie-water reactie, pid (0 ppm), lichtgrijs, Sonic Drill, CO 0 ppm, H2S 0 ppm
		Zand, matig fijn, matig siltig, geen olie-water reactie, pid (0 ppm), lichtgrijs, Sonic Drill, CO 0 ppm, H2S 0 ppm
-5520		
-5590		Zand, matig grof, zwak siltig, geen olie-water reactie, pid (0 ppm), lichtgrijs, Sonic Drill, CO 0-15 ppm, H2S 0 ppm
-5650		Klei, zwak zandig, geen olie-water reactie, pid (0 ppm), lichtgrijs, Sonic Drill, CO 0-15 ppm, H2S 0 ppm
-5750		Zand, matig grof, matig siltig, geen olie-water reactie, pid (0 ppm), lichtgrijs, Sonic Drill, CO 0-15 ppm, H2S 0 ppm
-5850		Veen, mineraalarm, laagjes zand, gebiedseigen, geen olie-water reactie, pid (0 ppm), donkerbruin, Sonic Drill, CO 0-15 ppm, H2S 0 ppm
-5950		Zand, uiterst fijn, matig siltig, geen olie-water reactie, pid (0 ppm), lichtgrijs, Sonic Drill, CO 0-15 ppm, H2S 0 ppm
		Zand, matig fijn, matig siltig, geen olie-water reactie, pid (0 ppm), lichtgrijs, Sonic Drill, CO 0 ppm, H2S 0 ppm
		Zand, matig fijn, matig siltig, resten veen, gebiedseigen, geen olie-water reactie, pid (0 ppm), lichtgrijs, Sonic Drill, CO 0 ppm, H2S 0 ppm
		Zand, matig fijn, matig siltig, sporen veen, gebiedseigen, geen olie-water reactie, pid (0 ppm), lichtgrijs, Sonic Drill, CO 0 ppm, H2S 0 ppm
-6200		Zand, matig grof, zwak siltig, geen olie-water reactie, pid (0 ppm), licht beigegrijs, Sonic Drill, CO 0 ppm, H2S 0 ppm
-6250		Zand, matig fijn, matig siltig, geen olie-water reactie, pid (0 ppm), licht beigegrijs, Sonic Drill, CO 0 ppm, H2S 0 ppm
		Zand, matig fijn, matig siltig, geen olie-water reactie, pid (0 ppm), licht beigegrijs, Sonic Drill, CO 0 ppm, H2S 0 ppm
-6400		Zand, matig fijn, matig siltig, geen olie-water reactie, pid (0 ppm), lichtgrijs, Sonic Drill, CO 0 ppm, H2S 0 ppm
-6550		Zand, matig fijn, matig siltig, resten klei, gebiedseigen, geen olie-water reactie, pid (0 ppm), lichtgrijs, Sonic Drill, CO 0 ppm, H2S 0 ppm

B2MLS1

Boormeester: M. Murray
30-4-2019

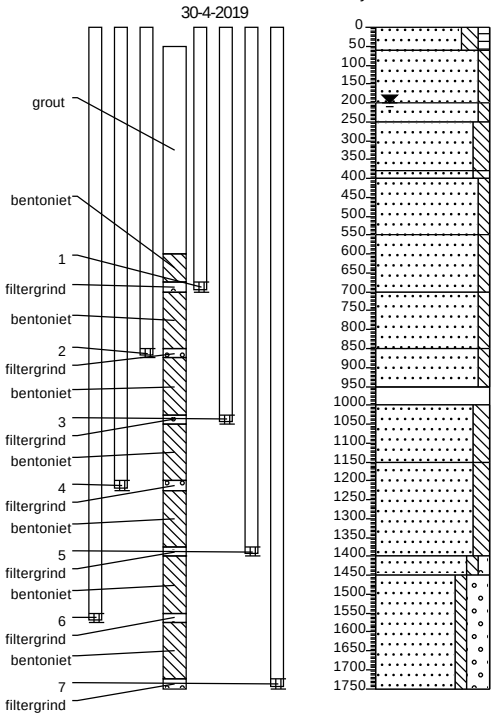

0 gras

-60 Zand, zeer fijn, matig siltig, zwak humeus, donkerbruin, Graven

Zand, uiterst fijn, zwak siltig, Edelmanboor

-200

-250 Zand, matig fijn, zwak siltig, lichtgrijs, Sonic Drill, Liner gestoken

Zand, matig fijn, matig siltig, lichtgrijs, Sonic Drill, Liner gestoken

-380
-400 Zand, matig fijn, matig siltig, donker bruingrijs, Sonic Drill, Liner gestoken | zaklaag

Zand, uiterst fijn, zwak siltig, sterke carbolineumgeur, donker roodbruin, Sonic Drill, liner gestoken | zaklaag waarneembaar

-550 Zand, uiterst fijn, zwak siltig, Sonic Drill, Liner gestoken | laagjes DNALP

-700 Zand, uiterst fijn, zwak siltig, lichtgrijs, Sonic Drill, Liner gestoken | "druppels" DNALP

-850 Zand, uiterst fijn, zwak siltig, lichtgrijs, Sonic Drill, Liner gestoken

-950
-1000 Sonic Drill, Geen materiaal

Zand, zeer fijn, matig siltig, geen olie-water reactie, pid (1 ppm), lichtgrijs, Sonic Drill, 24 ppm CO , 2,3 ppm H2S

-1150 Zand, zeer fijn, matig siltig, geen olie-water reactie, pid (0 ppm), lichtgrijs, Sonic Drill, 0 ppm CO , 0 ppm H2S |

-1400
-1450 Zand, zeer grof, zwak siltig, zwak grindig, geen olie-water reactie, pid (0 ppm), licht beigegrijs, Sonic Drill, 0 ppm CO , 0 ppm H2S |

Zand, matig grof, zwak siltig, sterk grindig, neutraalbeige, Sonic Drill

-1750

B2MLS2

Boormeester: M. Murray
17-4-2019

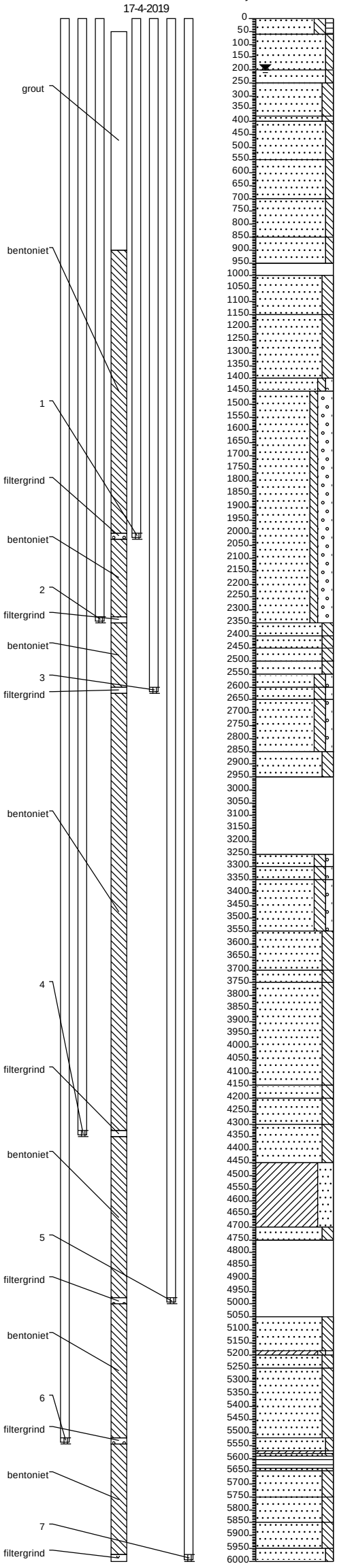

0		gras
-60		Zand, zeer fijn, matig siltig, zwak humeus, donkerbruin, Graven
		Zand, uiterst fijn, zwak siltig, Edelmanboor
-200		
-250		Zand, matig fijn, zwak siltig, lichtgrijs, Sonic Drill, Liner gestoken
		Zand, matig fijn, matig siltig, lichtgrijs, Sonic Drill, Liner gestoken
-380		
-400		Zand, matig fijn, matig siltig, donker bruingrijs, Sonic Drill, Liner gestoken | zaklaag
		Zand, uiterst fijn, zwak siltig, sterke carbolineumgeur, donker roodbruin, Sonic Drill, liner gestoken | zaklaag waarneembaar
-550		Zand, uiterst fijn, zwak siltig, Sonic Drill, Liner gestoken | laagjes DNALP
-700		Zand, uiterst fijn, zwak siltig, lichtgrijs, Sonic Drill, Liner gestoken | "druppels" DNALP
-850		Zand, uiterst fijn, zwak siltig, lichtgrijs, Sonic Drill, Liner gestoken
-950		
-1000		Sonic Drill, Geen materiaal
		Zand, zeer fijn, matig siltig, geen olie-water reactie, pid (1 ppm), lichtgrijs, Sonic Drill, 24 ppm CO , 2,3 ppm H2S
-1150		Zand, zeer fijn, matig siltig, geen olie-water reactie, pid (0 ppm), lichtgrijs, Sonic Drill, 0 ppm CO , 0 ppm H2S |
-1400		
-1450		Zand, zeer grof, zwak siltig, zwak grindig, geen olie-water reactie, pid (0 ppm), licht beigegrijs, Sonic Drill, 0 ppm CO , 0 ppm H2S |
		Zand, matig grof, zwak siltig, sterk grindig, licht beigegrijs, Sonic Drill, zeer grof zand
-2350		
-2400		Zand, matig grof, matig siltig, geen olie-water reactie, pid (0 ppm), lichtgrijs, Sonic Drill, CO 5-10 ppm, H2S 0 ppm
-2450		Zand, matig fijn, matig siltig, laagjes grind, gebiedseigen, geen olie-water reactie, pid (0 ppm), lichtgrijs, Sonic Drill, CO 5-10 ppm, H2S 0 ppm
-2500		Zand, matig fijn, matig siltig, geen olie-water reactie, pid (0 ppm), lichtgrijs, Sonic Drill, CO 5-10 ppm, H2S 0 ppm
-2550		Zand, matig fijn, matig siltig, laagjes klei, gebiedseigen, geen olie-water reactie, pid (17 ppm), lichtgrijs, Sonic Drill, CO 0 ppm, H2S 0 ppm
-2600		Zand, matig grof, matig siltig, zwak grindig, geen olie-water reactie, pid (17 ppm), lichtgrijs, Sonic Drill, CO 0 ppm, H2S 0 ppm
-2650		Zand, matig grof, matig siltig, zwak grindig, geen olie-water reactie, pid (63 ppm), lichtgrijs, Sonic Drill, CO 62 ppm, H2S 4,7 ppm
-2850		Zand, zeer grof, matig siltig, zwak grindig, geen olie-water reactie, pid (0 ppm), lichtgrijs, Sonic Drill, CO 0 ppm, H2S 0 ppm
-2950		Zand, zeer fijn, matig siltig, geen olie-water reactie, pid (0 ppm), lichtgrijs, Sonic Drill, CO 0 ppm, H2S 0 ppm
		Sonic Drill, Geen materiaal | zeer grof zand
-3250		
-3300		Zand, matig fijn, matig siltig, zwak grindig, geen olie-water reactie, pid (0 ppm), lichtgrijs, Sonic Drill, CO 0 ppm, H2S 0 ppm
-3350		Zand, matig fijn, matig siltig, zwak grindig, laagjes klei, gebiedseigen, geen olie-water reactie, pid (0 ppm), lichtgrijs, Sonic Drill, CO 0 ppm, H2S 0 ppm
		Zand, matig fijn, matig siltig, zwak grindig, laagjes klei, gebiedseigen, geen olie-water reactie, pid (0 ppm), lichtgrijs, Sonic Drill, CO 0 ppm, H2S 0 ppm
-3550		Zand, matig fijn, matig siltig, geen olie-water reactie, pid (0 ppm), lichtgrijs, Sonic Drill, CO 0 ppm, H2S 0 ppm
-3700		
-3750		Zand, matig fijn, matig siltig, resten hout, gebiedseigen, zwak leemhoudend, gebiedseigen, laagjes klei, gebiedseigen, geen olie-water reactie, pid (0 ppm), lichtgrijs, Sonic Drill, CO 0 ppm, H2S 0 ppm
		Zand, zeer fijn, matig siltig, geen olie-water reactie, pid (0 ppm), lichtgrijs, Sonic Drill, CO 0 ppm, H2S 0 ppm
-4150		
-4200		Zand, zeer fijn, matig siltig, geen olie-water reactie, pid (0 ppm), lichtgrijs, Sonic Drill, CO 10-15 ppm, H2S 0-1 ppm
-4300		Zand, zeer fijn, matig siltig, geen olie-water reactie, pid (0 ppm), lichtgrijs, Sonic Drill, CO 0 ppm, H2S 0 ppm
		Zand, zeer fijn, matig siltig, geen olie-water reactie, pid (0 ppm), lichtgrijs, Sonic Drill, CO 0 ppm, H2S 0 ppm
-4450		Klei, sterk zandig, geen olie-water reactie, pid (0 ppm), lichtgrijs, Sonic Drill, CO 0 ppm, H2S 0 ppm
-4700		
-4750		Zand, matig fijn, matig siltig, geen olie-water reactie, pid (0 ppm), lichtgrijs, Sonic Drill, CO 0 ppm, H2S 0 ppm
		Geen olie-water reactie, pid (0 ppm), lichtgrijs, Sonic Drill, CO 0 ppm, H2S 0 ppm | zeer weinig monstermateriaal | Z2S3K1 ligr
-5050		Zand, matig fijn, matig siltig, geen olie-water reactie, pid (0 ppm), lichtgrijs, Sonic Drill, CO 0 ppm, H2S 0 ppm
-5200		Klei, zwak siltig, zwak humeus, resten veen, gebiedseigen, geen olie-water reactie, pid (0 ppm), lichtgrijs, Sonic Drill, CO 0 ppm, H2S 0 ppm
-5250		Zand, matig fijn, matig siltig, laagjes klei, gebiedseigen, geen olie-water reactie, pid (0 ppm), lichtgrijs, Sonic Drill, CO 0 ppm, H2S 0 ppm
		Zand, matig fijn, matig siltig, geen olie-water reactie, pid (0 ppm), lichtgrijs, Sonic Drill, CO 0 ppm, H2S 0 ppm
-5520		
-5590		Zand, matig grof, zwak siltig, geen olie-water reactie, pid (0 ppm), lichtgrijs, Sonic Drill, CO 0-15 ppm, H2S 0 ppm
-5650		Klei, zwak zandig, geen olie-water reactie, pid (0 ppm), lichtgrijs, Sonic Drill, CO 0-15 ppm, H2S 0 ppm
-5750		Zand, matig grof, matig siltig, geen olie-water reactie, pid (0 ppm), lichtgrijs, Sonic Drill, CO 0-15 ppm, H2S 0 ppm
-5850		Veen, mineraalarm, laagjes zand, gebiedseigen, geen olie-water reactie, pid (0 ppm), donkerbruin, Sonic Drill, CO 0-15 ppm, H2S 0 ppm
-5950		Zand, uiterst fijn, matig siltig, geen olie-water reactie, pid (0 ppm), lichtgrijs, Sonic Drill, CO 0-15 ppm, H2S 0 ppm
-6000		Zand, matig fijn, matig siltig, geen olie-water reactie, pid (0 ppm), lichtgrijs, Sonic Drill, CO 0 ppm, H2S 0 ppm
		Zand, matig fijn, matig siltig, resten veen, gebiedseigen, geen olie-water reactie, pid (0 ppm), lichtgrijs, Sonic Drill, CO 0 ppm, H2S 0 ppm
		Zand, matig fijn, matig siltig, sporen veen, gebiedseigen, geen olie-water reactie, pid (0 ppm), lichtgrijs, Sonic Drill, CO 0 ppm, H2S 0 ppm
		Zand, matig grof, zwak siltig, geen olie-water reactie, pid (0 ppm), licht beigegrijs, Sonic Drill, CO 0 ppm, H2S 0 ppm

Appendix D: Hydraulic heads profile data

Table 10: *Hydraulic heads of location B, B2, and the eastern border of the Griftpark manually measured*

ASSET	AVG. FILTER DEPTH [m-NAP]	22-02-22	28-02-22	08-03-22	15-03-22	22-03-22	13-04-22	27-04-22	09-05-22	07-06-22
BU1	14,855	0,215	-0,135	0,045	-0,385	-0,135	-0,345	0,075	0,105	-0,465
BU2	41,386	0,234	-0,106	0,054	-0,356	-0,116	-0,316	0,074	0,094	-0,436
BU3	51,407	0,193	0,033	0,033	-0,117	-0,077	-0,097	-0,017	-0,007	-0,147
BU4	60,435	0,195	0,085	0,035	-0,035	-0,055	0,025	-0,025	-0,035	-0,035
BMLS1U1	5,479	0,176	-0,164	0,006	-0,414	-0,154	-0,374	0,036	0,066	-0,494
BMLS1U2	7,229	0,176	-0,164	0,006	-0,414	-0,154	-0,364	0,036	0,066	-0,484
BMLS1U3	8,979	0,176	-0,154	0,016	-0,414	-0,154	-0,364	0,036	0,076	-0,484
BMLS1U4	10,729	0,176	-0,154	0,016	-0,414	-0,154	-0,354	0,036	0,076	-0,484
BMLS1U5	12,479	0,186	-0,154	0,016	-0,404	-0,154	-0,354	0,036	0,076	-0,484
BMLS1U6	14,229	0,186	-0,154	0,016	-0,414	-0,154	-0,354	0,036	0,076	-0,484
BMLS1U7	15,729	0,186	-0,154	0,016	-0,414	-0,164	-0,354	0,036	0,076	-0,484
BMLS2U1	17,708	0,247	-0,103	0,077	-0,353	-0,093	-0,313	0,097	0,137	-0,443
BMLS2U2	19,458	0,247	-0,103	0,067	-0,353	-0,093	-0,303	0,097	0,137	-0,433
BMLS2U3	21,208	0,247	-0,103	0,067	-0,353	-0,093	-0,303	0,097	0,137	-0,433
BMLS2U4	22,958	0,247	-0,093	0,067	-0,353	-0,093	-0,293	0,097	0,137	-0,433
BMLS2U5	24,708	0,247	-0,093	0,067	-0,343	-0,093	-0,293	0,097	0,137	-0,423
BMLS2U6	26,458	0,247	-0,103	0,067	-0,353	-0,103	-0,303	0,097	0,127	-0,433
BMLS2U7	27,958	0,247	-0,093	0,067	-0,353	-0,103	-0,303	0,097	0,127	-0,433
BMLS3U1	46,486	0,219	-0,071	0,049	-0,281	-0,111	-0,231	0,049	0,089	-0,341
BMLS3U2	48,236	0,219	-0,071	0,049	-0,281	-0,101	-0,231	0,059	0,079	-0,331
BMLS3U3	49,986	0,219	-0,051	0,049	-0,271	-0,101	-0,211	0,059	0,079	-0,321
BMLS3U4	51,736	0,209	0,079	0,039	-0,071	-0,061	-0,011	-0,011	-0,021	-0,091
BMLS3U5	53,486	0,209	0,079	0,039	-0,051	-0,051	-0,001	-0,001	-0,021	-0,071
BMLS3U6	55,236	0,199	0,069	0,039	-0,061	-0,061	-0,001	-0,031	-0,021	-0,071
BMLS3U7	56,736	0,199	0,079	0,039	-0,061	-0,061	-0,001	-0,011	-0,021	-0,071
B2	61,872	0,208	0,098	-0,012	-0,072	-0,082	-0,002	-0,062	-0,062	-0,042
B2MLS1U1	3,725	0,230	-0,110	0,050	-0,370	-0,130	-0,340	0,070	0,040	-0,470
B2MLS1U2	5,475	0,230	-0,120	0,050	-0,380	-0,120	-0,340	0,070	0,040	-0,460
B2MLS1U3	7,225	0,230	-0,130	0,040	-0,370	-0,120	-0,340	0,070	0,050	-0,460
B2MLS1U4	8,975	0,230	-0,130	0,040	-0,370	-0,120	-0,350	0,070	0,030	-0,460
B2MLS1U5	10,725	0,220	-0,140	0,040	-0,380	-0,130	-0,350	0,070	0,030	-0,470
B2MLS1U6	12,475	0,220	-0,140	0,040	-0,380	-0,130	-0,350	0,070	0,020	-0,470
B2MLS1U7	14,225	0,230	-0,140	0,050	-0,370	-0,130	-0,350	0,070	0,030	-0,470
B2MLS2U1	17,020	0,225	-0,135	0,045	-0,375	-0,125	-0,335	0,075	0,025	-0,465
B2MLS2U2	20,270	0,225	-0,135	0,045	-0,375	-0,125	-0,335	0,075	0,025	-0,465
B2MLS2U3	23,020	0,225	-0,125	0,045	-0,375	-0,115	-0,335	0,075	0,035	-0,465
B2MLS2U4	40,270	0,235	-0,115	0,055	-0,345	-0,115	-0,325	0,075	0,035	-0,455
B2MLS2U5	46,770	0,235	-0,015	0,065	-0,235	-0,095	-0,185	0,065	0,035	-0,285
B2MLS2U6	52,270	0,235	-0,025	0,065	-0,235	-0,075	-0,175	0,055	0,035	-0,285
B2MLS2U7	56,770	0,215	0,105	0,045	-0,025	-0,055	0,025	-0,005	-0,005	-0,105
DV11	29,102	0,528	0,388	0,298	0,248	0,218	0,318	0,238	0,218	0,308
DV12	29,627	0,213	-0,137	0,043	-0,347	-0,127	-0,357	0,073	-0,007	-0,467

Appendix E: Values of Stallman's function $W_R(u,r_r)$

Table 11.a: *Values of Stallman's function $W(r^2_r,u)$ for bounded confined and unconfined aquifer (Kruseman et al., 1994)*

u	1/u	$r_r = 1.0$	1.1	1.2	1.3	1.4	1.5	1.6	1.7	1.8	1.9	2.0	2.2	2.4	2.6	2.8	3.0	3.3	3.6	4.0	4.5
1(−6)	1.00(6)	13.23	13.05	12.87	12.70	12.54	12.42	12.30	12.17	12.07	11.96	11.05	11.67	11.48	11.33	11.18	11.04	10.95	10.67	10.47	10.24
2(−6)	5.00(5)	12.54	12.36	12.17	12.01	11.88	11.73	11.61	11.48	11.37	11.26	11.16	10.97	10.80	10.63	10.50	10.35	10.24	9.98	9.77	9.53
4(−6)	2.50(5)	11.85	11.67	11.48	11.32	11.84	11.04	10.94	10.80	10.67	10.56	10.47	10.27	10.10	9.94	9.80	9.65	9.33	9.29	9.08	8.72
6(−6)	1.66(5)	11.45	11.26	11.08	10.93	10.75	10.64	10.53	10.40	10.27	10.15	10.06	9.87	9.68	9.53	9.39	9.25	9.15	8.88	8.67	8.45
8(−6)	1.25(5)	11.16	10.97	10.80	10.64	10.47	10.35	10.22	10.10	9.98	9.87	9.77	9.57	9.41	9.25	9.09	8.96	8.87	8.58	8.37	8.16
1(−5)	1.00(5)	10.93	10.75	10.56	10.41	10.24	10.12	9.98	9.87	9.77	9.65	9.55	9.36	9.18	9.02	8.88	8.74	8.64	8.37	8.16	7.94
2(−5)	5.00(4)	10.24	10.06	9.87	9.71	9.57	9.43	9.30	9.17	9.06	8.96	8.86	8.66	8.59	8.23	8.19	8.04	7.94	7.68	7.47	7.23
4(−5)	2.50(4)	9.549	9.367	9.178	9.019	8.882	8.739	8.633	8.494	8.371	8.262	8.163	7.965	7.800	7.640	7.502	7.353	7.024	6.985	6.777	6.426
6(−5)	1.66(4)	9.144	8.954	8.784	8.633	8.451	8.333	8.228	8.103	7.965	7.845	7.758	7.569	7.381	7.225	6.086	6.947	6.858	6.580	6.372	6.149
8(−5)	1.25(4)	8.856	8.664	8.594	8.333	8.163	8.045	7.915	7.800	7.678	7.569	7.470	7.272	7.107	6.947	6.793	6.660	6.567	6.283	6.069	5.862
1(−4)	1.00(4)	8.633	8.451	8.263	8.103	7.940	7.822	7.678	7.569	7.470	7.353	7.247	7.065	6.876	6.723	6.580	6.437	6.342	6.069	5.862	5.639
2(−4)	5.00(3)	7.940	7.758	7.569	7.410	7.272	7.129	7.004	6.876	6.762	6.660	6.554	6.362	6.193	6.032	5.944	5.745	5.639	5.378	5.171	4.935
4(−4)	2.50(3)	7.247	7.065	6.876	6.717	6.580	6.437	6.331	6.193	6.069	5.960	5.862	5.664	5.500	5.340	5.202	5.053	4.726	4.687	4.481	4.131
6(−4)	1.66(3)	6.842	6.652	6.482	6.331	6.149	6.032	5.927	5.802	5.664	5.544	5.457	5.269	5.081	4.935	4.788	4.649	4.561	4.284	4.078	3.858
8(−4)	1.25(3)	6.554	6.362	6.193	6.032	5.862	5.745	5.614	5.500	5.378	5.269	5.171	4.973	4.809	4.649	4.496	4.364	4.272	3.990	3.778	3.574
1(−3)	1.00(3)	6.331	6.149	5.961	5.802	5.639	5.522	5.378	5.269	5.171	5.053	4.948	4.666	4.578	4.427	4.284	4.142	4.048	3.778	3.574	3.355
2(−3)	5.00(2)	5.639	5.457	5.269	5.110	4.973	4.831	4.706	4.578	4.465	4.364	4.259	4.068	3.900	3.736	3.605	3.458	3.355	3.098	2.896	2.669
4(−3)	2.50(2)	4.948	4.767	4.579	4.420	4.284	4.142	4.038	3.900	3.778	3.664	3.574	3.379	3.218	3.061	2.927	2.783	2.468	2.431	2.235	1.909
6(−3)	1.66(2)	4.545	4.356	4.187	4.038	3.858	3.742	3.637	3.514	3.379	3.261	3.176	2.992	2.810	2.269	2.527	2.395	2.311	2.050	1.860	1.659
8(−3)	1.25(2)	4.259	4.068	3.900	3.742	3.574	3.458	3.330	3.218	3.098	2.992	2.896	2.706	2.547	2.395	2.249	2.125	2.039	1.784	1.589	1.409
1(−2)	1.00(2)	4.038	3.858	3.671	3.514	3.355	3.239	3.098	2.992	2.896	2.783	2.681	2.506	2.327	2.184	2.050	1.919	1.832	1.589	1.409	1.223
2(−2)	5.00(1)	3.355	3.176	2.992	2.838	2.706	2.568	2.449	2.327	2.220	2.125	2.027	1.850	1.698	1.556	1.436	1.309	1.223	1.014	0.858	0.694
4(−2)	2.50(1)	2.681	2.507	2.327	2.178	2.050	1.919	1.823	1.698	1.589	1.524	1.409	1.242	1.110	0.985	0.881	0.774	0.560	0.536	0.420	0.256
6(−2)	1.66(1)	2.295	2.117	1.960	1.823	1.659	1.556	1.464	1.358	1.243	1.145	1.076	0.931	0.794	0.694	0.598	0.514	0.464	0.322	0.235	0.158
8(−2)	1.25(1)	2.027	1.850	1.698	1.556	1.409	1.309	1.202	1.109	1.014	0.931	0.858	0.719	0.611	0.514	0.428	0.360	0.316	0.202	0.135	0.086
1(−1)	1.00(1)	1.822	1.659	1.494	1.358	1.223	1.122	1.014	0.931	0.858	0.774	0.702	0.584	0.473	0.392	0.322	0.260	0.223	0.135	0.086	0.049
2(−1)	5.00	1.222	1.076	0.930	0.815	0.719	0.625	0.548	0.473	0.411	0.360	0.311	0.231	0.172	0.126	0.091	0.065	0.049	0.022	0.010	0.003
4(−1)	2.50	0.702	0.585	0.473	0.388	0.322	0.260	0.219	0.172	0.135	0.108	0.086	0.052	0.032	0.019	0.011	0.006	0.001	0.001	0.000	
6(−1)	1.66	0.454	0.356	0.279	0.219	0.158	0.126	0.100	0.075	0.052	0.037	0.028	0.015	0.007	0.003	0.002	0.001	0.000			
8(−1)	1.25	0.311	0.231	0.172	0.125	0.086	0.065	0.045	0.032	0.022	0.014	0.010	0.004	0.002	0.001	0.000					
1	1.00	0.219	0.158	0.108	0.075	0.049	0.035	0.021	0.015	0.010	0.006	0.003	0.001	0.000							
2	5.00(−1)	4.89(−2)	2.84(−2)	1.48(−2)	0.78(−2)	0.43(−2)	0.21(−2)	0.10(−2)	0.04(−2)	0.02(−2)	0.01(−2)	0.00(−2)									
4	2.50(−1)	3.77(−3)	1.45(−3)	0.48(−3)	0.14(−3)	0.04(−3)	0.01(−3)	0.00(−3)													
6	1.66(−1)	3.60(−4)	0.87(−4)	0.19(−4)	0.04(−4)	0.00(−4)															
8	1.25(−1)	3.77(−5)	0.58(−5)	0.00(−5)																	

$W(r^2_r,u) = 0$

Table 11.b: *Values of Stallman's function $W(r^2_r,u)$ for bounded confined and unconfined aquifer (Kruseman et al., 1994)*

u	1/u	$r_r = 5.0$	5.5	6.0	7.0	8.0	9.0	10.0	15	20	25	30	35	40	45	50	55	60	70	80	90	100
1(−6)	1.00(6)	10.02	9.84	9.65	9.34	9.08	8.86	8.63	7.82	7.25	6.80	6.44	6.15	5.86	5.64	5.42	5.23	5.05	4.75	4.48	4.26	4.04
2(−6)	5.00(5)	9.32	9.14	8.96	8.65	8.37	8.16	7.94	7.13	6.55	6.10	5.74	5.44	5.17	4.93	4.73	4.54	4.36	4.06	3.78	3.57	3.35
4(−6)	2.50(5)	8.63	8.45	8.26	7.96	7.68	7.45	7.25	6.43	5.86	5.42	5.05	4.75	4.48	4.13	4.04	3.86	3.67	3.38	3.10	2.88	2.68
6(−6)	1.66(5)	8.23	8.05	7.86	7.55	7.28	7.05	6.84	6.03	5.46	5.01	4.65	4.34	4.08	3.86	3.64	3.46	3.28	2.97	2.72	2.50	2.29
8(−6)	1.25(5)	7.94	7.75	7.75	7.27	7.00	6.76	6.55	5.74	5.17	4.73	4.36	4.05	3.78	3.57	3.35	3.18	2.99	2.70	2.45	2.22	2.03
1(−5)	1.00(5)	7.72	7.53	7.35	7.04	6.78	6.55	6.33	5.52	4.95	4.50	4.14	3.86	3.57	3.35	3.14	2.96	2.78	2.49	2.23	2.03	1.82
2(−5)	5.00(4)	7.02	6.83	6.66	6.35	6.07	5.86	5.64	4.83	4.26	3.82	3.46	3.16	2.90	2.67	2.47	2.29	2.12	1.84	1.59	1.41	1.22
4(−5)	2.50(4)	6.331	6.149	5.960	5.665	5.378	5.155	4.948	4.142	3.574	3.136	2.783	2.487	2.235	1.909	1.823	1.659	1.494	1.243	1.014	0.847	0.702
6(−5)	1.66(4)	5.927	5.745	5.567	5.251	4.986	4.756	4.545	3.742	3.176	2.743	2.395	2.105	1.860	1.659	1.464	1.309	1.168	0.917	0.728	0.578	0.454
8(−5)	1.25(4)	5.639	5.457	5.269	4.973	4.706	4.465	4.259	3.458	2.896	2.468	2.125	1.841	1.589	1.409	1.223	1.076	0.931	0.719	0.548	0.411	0.311
1(−4)	1.00(4)	5.417	5.235	5.053	4.746	4.481	4.259	4.038	3.239	2.681	2.251	1.919	1.659	1.409	1.223	1.044	0.906	0.774	0.572	0.419	0.311	0.219
2(−4)	5.00(3)	4.726	4.536	4.363	4.058	3.778	3.574	3.355	2.568	2.027	1.624	1.309	1.060	0.858	0.694	0.560	0.450	0.360	0.227	0.135	0.086	0.048
4(−4)	2.50(3)	4.038	3.858	3.671	3.379	3.098	2.881	2.681	1.919	1.409	1.044	0.774	0.572	0.420	0.256	0.219	0.158	0.108	0.052	0.022	0.009	0.004
6(−4)	1.66(3)	3.637	3.458	3.283	2.975	2.717	2.497	2.295	1.556	1.076	0.746	0.514	0.349	0.235	0.158	0.100	0.065	0.039	0.015	0.004	0.001	0.000
8(−4)	1.25(3)	3.355	3.176	2.992	2.705	2.449	2.220	2.027	1.309	0.858	0.560	0.360	0.227	0.135	0.086	0.049	0.028	0.015	0.004	0.001	0.000	
1(−3)	1.00(3)	3.136	2.959	2.783	2.487	2.235	2.027	1.823	1.122	0.702	0.432	0.260	0.158	0.086	0.049	0.025	0.013	0.006	0.001	0.000		
2(−3)	5.00(2)	2.468	2.287	2.125	1.841	1.589	1.409	1.223	0.625	0.311	0.147	0.065	0.027	0.010	0.003	0.001	0.000					
4(−3)	2.50(2)	1.823	1.659	1.494	1.243	1.014	0.847	0.702	0.260	0.086	0.025	0.006	0.001	0.000								
6(−3)	1.66(2)	1.464	1.309	1.168	0.917	0.728	0.578	0.454	0.126	0.028	0.005	0.001	0.000									
8(−3)	1.25(2)	1.223	1.076	0.931	0.719	0.548	0.411	0.311	0.065	0.010	0.001	0.000										
1(−2)	1.00(2)	1.044	0.906	0.774	0.572	0.419	0.311	0.219	0.035	0.003	0.000											
2(−2)	5.00(1)	0.560	0.450	0.360	0.227	0.135	0.086	0.048	0.002	0.000												
4(−2)	2.50(1)	0.219	0.158	0.108	0.052	0.022	0.009	0.004	0.000													
6(−2)	1.66(1)	0.100	0.065	0.039	0.015	0.004	0.001	0.000														
8(−2)	1.25(1)	0.049	0.028	0.015	0.004	0.001	0.000															
1(−1)	1.00(1)	0.025	0.013	0.006	0.001	0.000																
2(−1)	5.00	0.001	0.000				$W(r_r^2,u) = 0$															
4(−1)	2.50	0.000																				

Appendix F: Tables of subsurface property values

Table 12: *Ranges of total and effective porosity values (Data from Enviro Wiki Contributors, 2019; table from* Woessner and Poeter*, 2020)*

Total and Effective Porosity		
	Total Porosity	**Effective Porosity**
Unconsolidated Material		
Gravel	0.25 - 0.44	0.13 - 0.44
Coarse Sand	0.31 - 0.46	0.18 - 0.43
Medium Sand		0.16 - 0.46
Fine Sand	0.25 - 0.53	0.01 - 0.46
Silt, loess	0.35 - 0.50	0.01 - 0.39
Clay	0.40 - 0.70	0.01 - 0.18
Sedimentary and Crystalline Rocks		
Karst and reef limestone	0.05 - 0.50	--
Limestone, dolomite	0.00 - 0.20	0.01 - 0.24
Sandstone	0.05 - 0.30	0.10 - 0.30
Siltstone	--	0.21 - 0.41
Basalt	0.05 - 0.50	--
Fractured crystalline rock	0.00 - 0.10	--
Weather granite	0.34 - 0.57	--
Unfractured crystalline rock	0.00 - 0.05	--

Table 13: *Summary of specific yield values of common earth materials compiled by Morris and Johnson (1967) with additional data from Rivera (2014), Freeze and Cherry (1979) and Domenico and Schwartz (1998). "NA" represents not available. (Table from* Woessner and Poeter*, 2020)*

Measurements of Specific Yield for Some Common Earth Materials (Percent)		
Material	**Number of Samples**	**Range of Specific Yield %**
Unconsolidated Sediments		
Clay	27	1 - 18
Silt	299	1 - 40
Loess	5	14 - 22
Eolian sand	14	32 - 47
Sand (fine)	287	1 - 46
Sand (medium)	297	16 - 46
Sand (coarse)	143	18 - 43
Gravel (fine)	33	13 - 40
Gravel (medium)	13	17 - 44
Gravel (coarse)	9	13 - 25
Consolidated Sediments		
Shale	NA	0.5 - 5
Siltstone	13	1 - 33
Sandstone (fine-grained)	47	2 - 40
Sandstone (medium-grained)	10	12 - 41
Limestone and dolomite	32	0 - 36
Karstic limestone	NA	2 - 15
Igneous and Metamorphic Rocks		
Fresh granite and gneiss	NA	<0.1
Weathered granite/gneiss	NA	0.5 - 5
Fractured basalt	NA	2 - 10
Vesicular basalt	NA	5 - 15
Tuff	90	2 - 47

Table 14: *Range of values of compressibility of earth materials and water (after Domenico and Mifflin,1965; Freeze and Cherry, 1979; table from* Woessner and Poeter*, 2020).*

Compressibility of Some Common Earth Materials	
Material	**Compressibility ($meter^2$/Newton)**
Geologic Type	**Range of Compressibility α**
Clay	$1x10^{-6}$ - $1x10^{-8}$
Sand	$1x10^{-7}$ - $1x10^{-9}$
Gravel	$1x10^{-8}$ - $1x10^{-10}$
Jointed Rock	$1x10^{-8}$ - $1x10^{-10}$
Sound Rock	$1x10^{-9}$ - $1x10^{-11}$
Fluid	**Compressibility β**
water	4.4×10^{-10}

Table 15: *Horizontal hydraulic conductivity for different soil types (Biron et al., 2004)*

Soil types	**Kh [m/d]**
Peat	0,3
Clay	0,005
Sandy clay	0,05
Extremely fine	0,5
Very fine	1
Fine sand	3
Medium fine sand	15
Medium coarse sand	40
Coarse sand	50
Very coarse sand	60
Extremely coarse sand	80
Fine gravel	100
Gravel	200

Appendix G: Pumping test results - Large figures

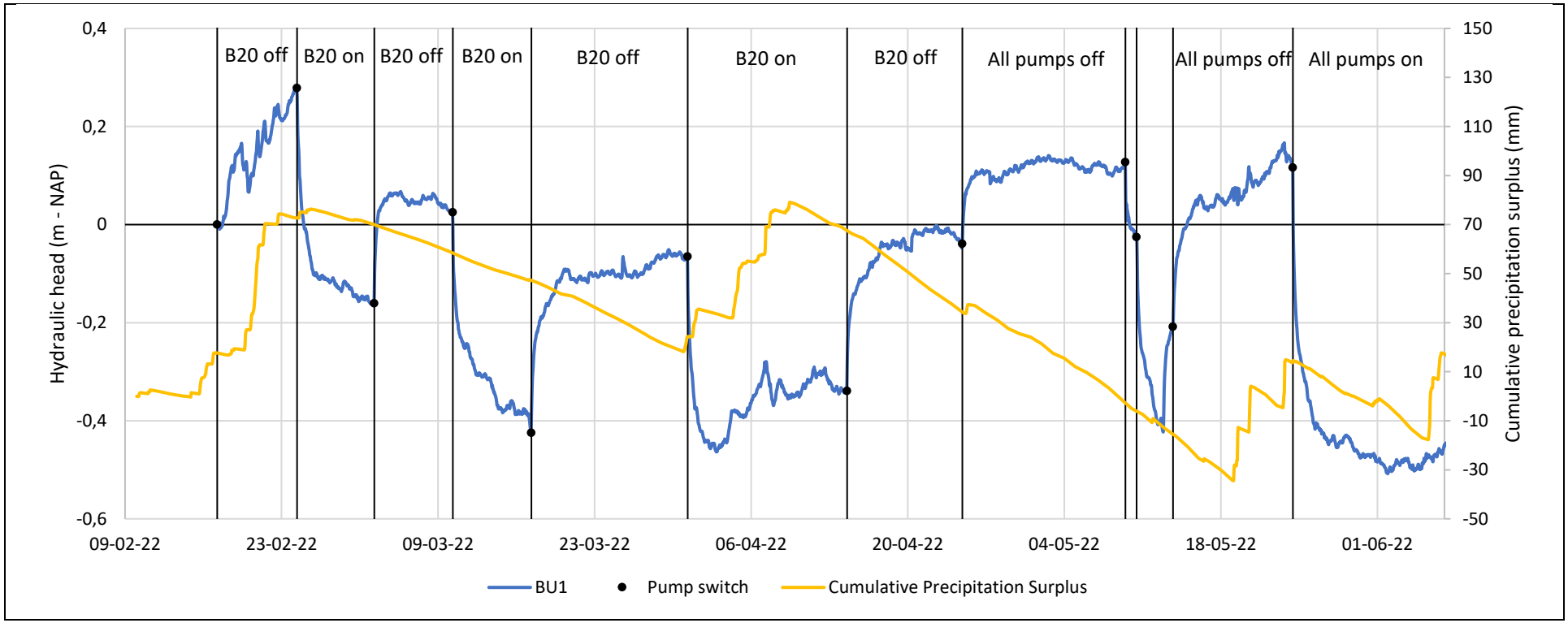

Figure 12.b: *Hydraulic head variations and cumulative precipitation surplus in the 1st aquifer of the Griftpark during the pumping test between February to June 2022.*

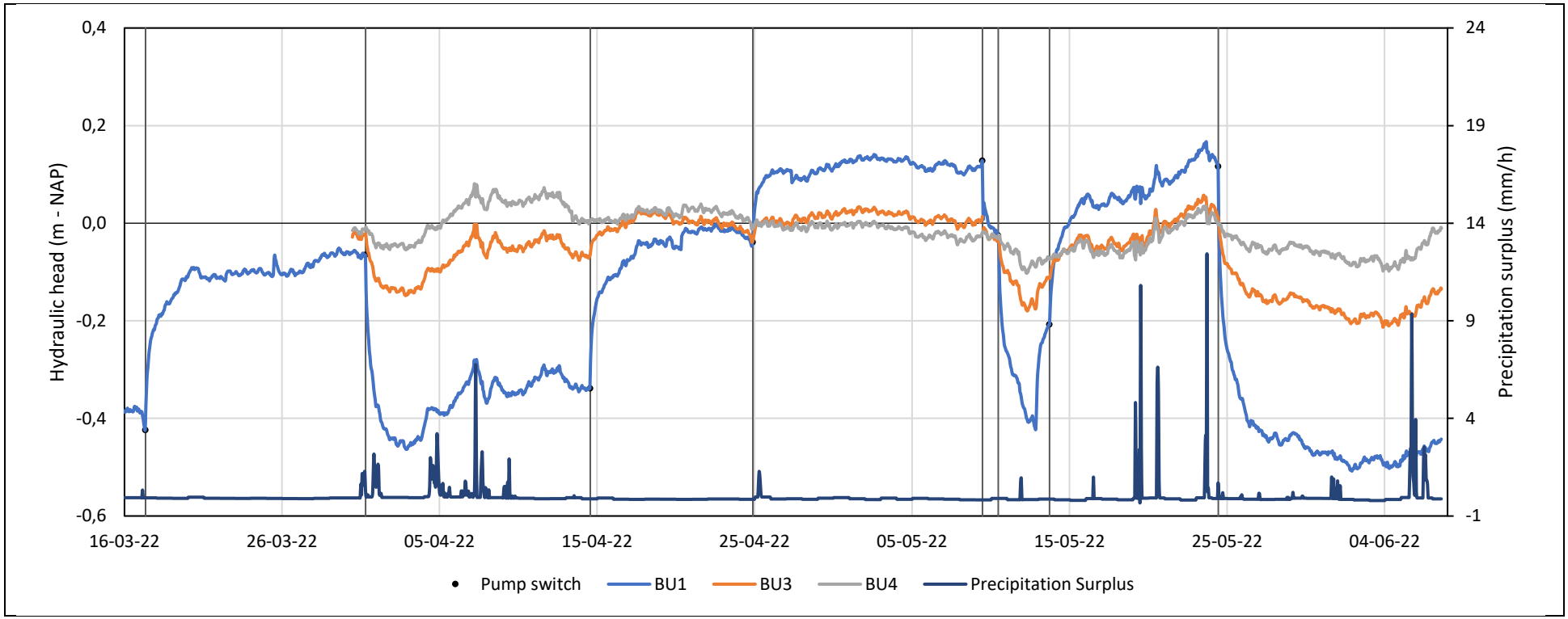

Figure 15.b: *Hydraulic head variations of the Griftpark 1st aquifer (BU1), aquitard (BU3), and 2nd aquifer (BU4) between April and June 2022.*

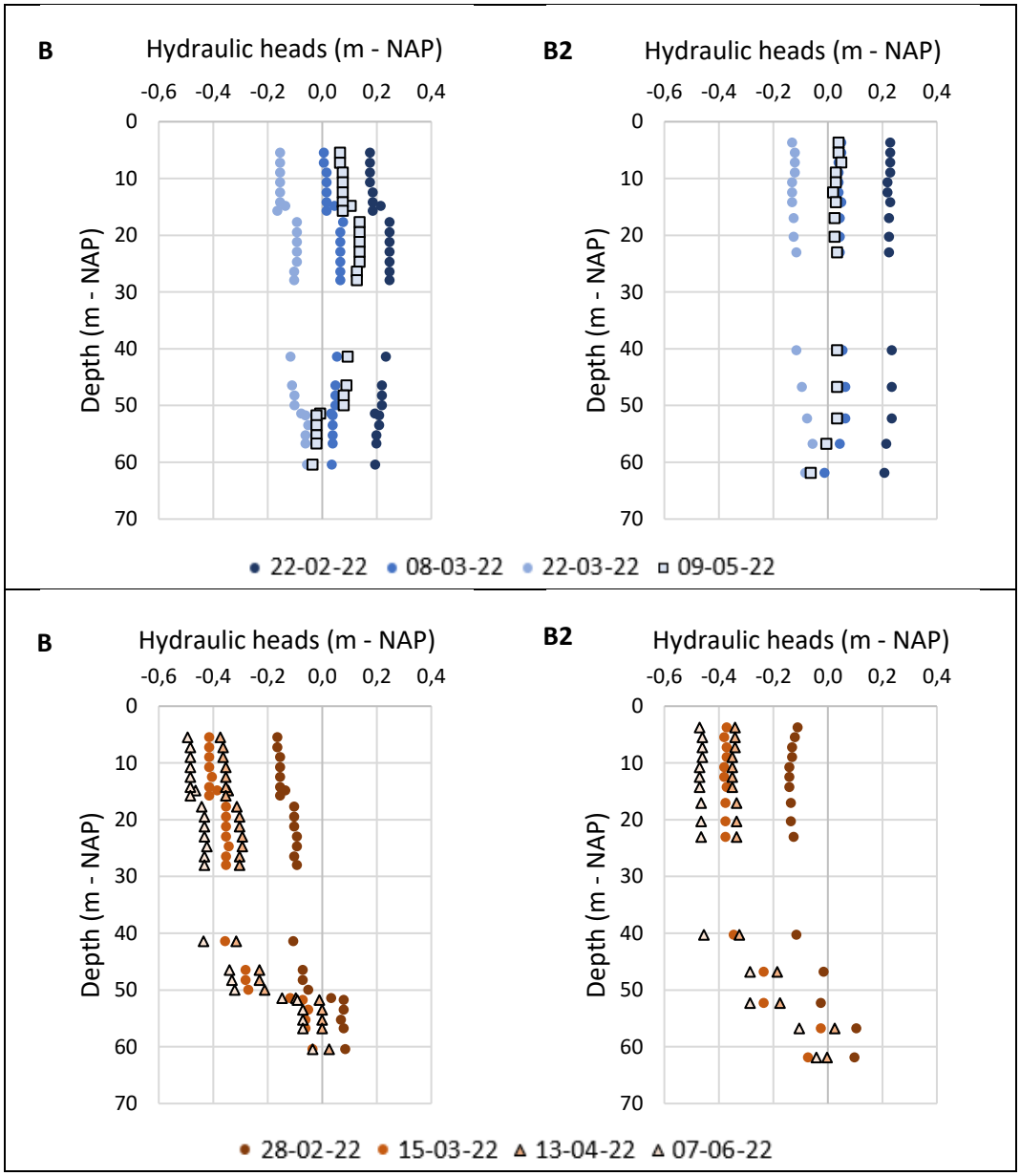

Figure 28: *Hydraulic head profiles of location B (left) and B2 (right).*

- • Measurements taken 5-6 days after pump B20 was switched off or on
- □ Measurements taken 13 days after all three pumps were switched off
- Δ Measurements taken 13 days after pump B20 was switched on

References

Biron, D.J., van de Ven, F.H.M, Brouwer, R., Horstmeier, T.H.W, & Hartjes, A.G (2004). Een verkennend onderzoek naar het bouw- en woonrijp maken in de Nederlandse praktijk en de problematiek rondom wateroverlast op de bouwplaats.

Bockelmann, A., Zamfirescu, D., Ptak, T., Grathwohl, P., & Teutsch, G. (2003). Quantification of mass fluxes and natural attenuation rates at an industrial site with a limited monitoring network: a case study. J. Contam. Hydrol. 60, 97–121.

Bösel, D., Herfort, M., Ptak, T., & Teutsch, G. (2000). Design, performance, evaluation and modeling of a natural gradient multitracer transport experiment in a contaminated heterogeneous porous aquifer. Tracers and Modelling in Hydrogeology, IAHS Publication No. 262, ISBN. 1-901502-21-X, pp. 45–51.

Burr, D.T., Sudicky, E.A., & Naff, R.L. (1994). Nonreactive and reactive solute transport in three-dimensional heterogeneous porous media: Mean displacement, plume spreading, and uncertainty. Water Resour. Res. 30(3), 791–815.

Cao, V., Schaffer, M., Taherdangkoo, R., & Licha, T. (2020). Solute Reactive Tracers for Hydrogeological Applications: A Short Review and Future Prospects. Water, 12, 653; doi:10.3390/w12030653

Chowdhury, M.F. (2020). Significance of Barometric efficiency and loading efficiency for confined aquifers.

Cohen, A., & Cherry, J. (1990). Conceptual and Visual Understanding of Hydraulic Head and Groundwater Flow. Groundwater Project, Guelph, Ontario, Canada.

Dagan, G., (1989). Flow and Transport in Porous Formations, Springer, Berlin.

de Moel, P.J., Verberk, J.Q.J.C., & van Dijk, JC. (2006). Drinking Water: Principles and Practices. World Scientifi, https://doi.org/10.1142/6135

Di Federico, V., & Neuman, S.P. (1998). Transport in multiscale log conductivity fields with truncated power variograms. Water Resour. Res. 34(5), 963–973.

DINOloket (2017). REGIS II v2.2 Hydrogeological model. https://www.dinoloket.nl/ondergrondmodellen

Divine, C.E., & McDonnell, J.J. (2005). The future of applied tracers in hydrogeology. Hydrogeol, 13, 255–258.

Eijkelkamp (2016). Product Manual: Diver. https://www.vanessen.com/manuals

Engineering ToolBox (2003, June 16). Water - Density, Specific Weight and Thermal Expansion Coefficients. https://www.engineeringtoolbox.com/water-density-specific-weight-d_595.html

Enviro Wiki contributors (2019), Advection and Groundwater Flow, Enviro Wiki, Page Version ID: 12554, www.enviro.wiki/index.php?title=Advection_and_Groundwater_Flow&oldid=12554 , accessed July 31, 2022.

Ferris, J.G., Knowless, D.B., Brown, R.H., & Stallman R.W. (1962). Theory of aquifer tests. U.S. Geological Survey, Water-Supply Paper 1536E, 174 pp.

Fetter, N., Boving, T., & Kreamer, D. (2018). Contaminant Hydrogeology. Waveland Press, Inc.

Finkel, M., Liedl, R., & Teutsch, G. (1997). Modelling coupled reactive transport of PAH and surfactants. In McDonald, A.D., McAleer, M. (Eds.), MODSIM97, International Congress on Modelling and Simulation, Proceedings, vol. 2., pp. 566–571.

Flury, M., & Wai, N.N. (2003). Dyes as tracers for vadose zone hydrology. Rev. Geophys., 41, 2.1–2.37.

Ge, S., & Gorelick, S.M. (2015). Hydrology, Floods, and Droughts: Groundwater and surface water. In G. North Editor, J. Pyle Editor & F. Zhang Editor (Eds), Encyclopedia of Atmospheric Sciences (2nd ed., pp. 209-216).

Gelhar, L.W. (1986). Stochastic subsurface hydrology from theory to applications. Water Resour. Res. 22(9), 135S–145S.

Gemeente Utrecht (2022, July 31). *« Bij het aanleggen van het Griftpark werd een flinke bodemverontreiniging ontdekt ».* https://web.archive.org/web/20170923050701/https:/www.utrecht.nl/wonen-en-leven/milieu/bodem/projecten/griftpark/

Gonthier, G.J. (2007). A Graphical Method for Estimation of Barometric Efficiency from Continuous Data—Concepts and Application to a Site in the Piedmont, Air Force Plant 6, Marietta, Georgia: U.S. Geological Survey Scientific Investigations Report 2007-5111, 29 p., Web-only publication available at http://pubs.usgs.gov/sir/2007/5111/.

Grathwohl, P., & Kleineidam, S.,(1995). Impact of heterogeneous aquifer materials on sorption capacities and sorption dynamics of organic contaminants, Groundwater Quality: Remediation and Protection, IAHS Publ. 225, pp. 79–86.

Grondmechanica Delft (1988). De geologie van het Griftpark te Utrecht, nummer CO-296920.

Heidemij adviesbureau (1990). Aanvullend verontreinigingsonderzoek Grifpark, projectnummer 633-13465

Herfort, M., & Ptak, T., (2002). Multitracer-Versuch im kontaminierten Grundwasser des Testfeldes Süd. Grundwasser 1(7), 31–40.

Internaitonal Agency for Research on Cancer (1992). Monographs on the evaluation of the carcinogenic risk of chemicals to man. Geneva: World Health Organization, International Agency for Research on Cancer, 54, 206.

Jaszczak, E., Polkowska, Z., Narkowisz, S., & Namiesnik, J. (2017). Cyanides in the environment: analysis, problems and challenges. *Environmental Science and Pollution Research*, 24, 15929-15948. DOI 10.1007/s11356-017-9081-7

Kabala, Z.J. (1993). The dipole flow test: a new singleborehole test for aquifer characterization. Water Resources Research, 29(1): 99-107.

Koninklijk Nederlands Meteorologisch Instituut (2022, July 31). "*Uurgegevens van het weer in Nederland". https://www.knmi.nl/nederland-nu/klimatologie/uurgegevens*

Kruseman, G.P., & de Ridder, N.A. (1994). Analysis and Evaluation of Pumping Test Data (2nd ed.). International Institute of Land Reclamation and Improvement, publication 47.

Luhmann, A.J., Covington, M.D., Alexander, S.C., Chai, S.Y., Schwartz, B.F., Groten, J.T., & Alexander, E.C., Jr. (2012). Comparing conservative and nonconservative tracers in karst and using them to estimate flow path geometry. J. Hydrol., 448–449, 201–211.

Mayer, A., & Hassanizadeh, M. (2005). Soil and groundwater contamination: Nonaqueous Phase Liquids. American Geophysical Union.

Miralles-Wilhelm, F., & Gelhar, L.W. (1996). Stochastic analysis of sorption macrokinetics in heterogeneous aquifers. Water Resour. Res. 32(6), 1541–1549.

Mitrov, G., & Chcrnozeniski, I. (1985). Nutrition and Cancer. *Medicina i Eizkullura*. Sotla, 67-9S.

Newell, C.J., Bowers, R.L., & Rifai, H.S. (1994). Impact of Non-Aqueous phase liquids (NAPLs) on groundwater remediation. Unpublished manuscript. Summer National AICHE Meeting.

Ptak, T., & Kleiner, K. (1998). Application of multilevel–multitracer transport experiments for the investigation of hydraulic and hydrogeochemical aquifer properties, Groundwater Quality: Remediation and Protection, IAHS Publication No. 250, ISSN 0144-7815, pp. 343–351.

Ptak, T., & Schmid, G. (1996). Dual-tracer transport experiments in a physically and chemically heterogeneous porous aquifer: Effective transport parameters and spatial variability. J. Hydrol. 183(1-2), 117–138.

Ptak, T., & Strobel, H. (1998). Sorption of fluorescent tracers in a physically and chemically heterogeneous aquifer material. In: Arehart, G.B., Hulston, J.R. (Eds.), Water–Rock Interaction, Balkema, Rotterdam, pp. 177–180.

Ptak, T., & Teutsch, G. (1994a). Forced and natural gradient tracer tests in a highly heterogeneous porous aquifer: Instrumentation and measurements. J. Hydrol. 159, 79–104.

Ptak, T., Piepenbrink, M., & Martc, E. (2004). Tracer tests for the investigation of heterogeneous porous media and stochastic modelling of flow and transport—a review of some recent developments. Journal of Hydrology, 294, 122-163.

Rijkswaterstaat, Ministry of Infrastructure and the Environment of the Netherlands (2014). Into Dutch Soils.

Roos, G., Thomson, N.R., Wilson, R.D. & Thornton, S.F (2008). The dipole flow and reactive tracer test for aquifer parameter estimation. AGU Fall Meeting Abstracts.

Royal Haskoning DHV (2014). Griftpark scopeverandering: Historisch onderzoek ten behoeve van nadar onderzoek grondwater.

Staykova, T., Ivanova, E., & Velcheva, I. (2005). Cytogenic effect of heavy metals and cyanide in contaminated waters from the regions of southwest Bulgaria. *Journal of Cell and Molecular biology,* 4, 41-41.

Sutton, D.J., Kabala, Z.J., Schaad, D.E., & Ruud, N.C. (2000). The dipole-flow test with a tracer: a new single-borehole tracer test for aquifer characterization. J. Contam. Hydrol. 44, 71–101.

Teutsch, G., Klingbeil, R., & Kleineidam, S. (1998). Groundwater Quality: Remediation and Protection. In: Herbert, M., Kovar, K. (Eds.), Numerical modelling of reactive transport using aquifer analogue data, IAHS Publ. 250, pp. 381–390.

Todd, D.K (1980). Groundwater Hydrology. 2d ed. New York: John Wiley& Sons.

VEWIN, Association of Dutch Water companies (2017). Dutch drinking water statistics 2017, From source to Tap.

Woessner, W.W., & Poeter, E.P. (2020). Hydrogeologic Properties of Earth Materials and Principles of Groundwater Flow. The Groundwater Project, Guelph, Ontario, Canada.

Zlotnik, V., Zurbuchen, B., Ptak,T., & Teutsch,G. (2000). Support volume and scale effect in hydraulic conductivity: Experimental aspects. Geological Society of America, Boulder, Colorado, Special Paper 348. In: Zhang, D., Winter, C.L. (Eds.), Theory, Modeling, and Field Investigation in Hydrogeology: A Special Volume in Honor of Shlomo P. Neuman's 60th Birthday, pp. 215–231.